Hydro-Mechanical Analysis of Unsaturated Collapsible Soils and their Stabilization

Dissertation

in fulfillment of the requirements for the degree of "Dr.-Ing."

of the Faculty of Mathematics and Natural Sciences

at Kiel University

Submitted by

Ahmed Al-Janabi

(University of Babylon)

2014

First referee: Prof. Dr.-Ing. habil. Frank Wuttke.

Second referee: Prof. Dr.-Ing. habil. Tom Schanz.

Date of the oral examination: 16.12.2014.

Approved for publication: 09.01.2015.

Prof. Dr. Wolfgang J. Duschl

Dean

Erklärung

Hiermit erklre ich, Ahmed Al-Janabi, da die vorgelegte Abhandlung, abgesehen von der Beratung durch meine akademischen Lehrer, nach Inhalt und Form meine Arbeit ist und ausschlielich unter Verwendung der angegebenen Hilfsmittel entstanden ist. Ferner erklre ich, da ich weder diese noch eine hnliche Arbeit an anderer Stelle im Rahmen eines Prfungsverfahrens vorgelegt habe.

Ahmed Al-Janabi
September / 2014

Acknowledgements

Praise be to God, the most gracious and the most merciful, for His help that enables me to finish this work. I would like to express my deep gratitude and sincere appreciation first and foremost to my supervisor, Prof. Dr.-Ing. habil. Frank Wuttke, Head of the Institute of Marine and Land Geomechanics and Geotechnics for his meticulous guidance and patience throughout my period of candidature. This doctoral research would undoubtedly not have been possible without his support.

I would like to acknowledge the financial support for my PhD research provided by the Deutscher Akademischer Austausch Dienst, DAAD (German Academic Exchange Service). Many thanks also go to Prof. Dr.-Ing. habil. Tom Schanz, Prof. Dr. R. Bousquet and Prof. Dr. Lorenz Kienle for their agreement to be reviewers of this dissertation.

I want to express my deep and sincere gratitude to Dr. Norman Wagner (MFPA institute in Weimar) for their useful discussions and help in my study.

My gratitude also is extended to my former colleagues from the Laboratory of Soil Mechanics at Bauhaus-Universitt Weimar, including the research and laboratory staff. Special thanks go to Ms. Gabriel Tscheschlok, Mr. Frank Hoppe (Alma), Mr. Kafle, Mr. Hailemariam, for their assistance in the experiments, discussion, and sharing of ideas. My deep thanks to my colleagues (research and laboratory staff) at Christian-Albrechts-University of Kiel. I would like pass on my gratefulness to everyone who indirectly assisted me during my stay in Weimar and Kiel.

Finally, and most importantly, I would like to express my deepest thank to my family, especially my parents, my wife Rafal, my son Zain Al-Abeeden and my daughter Fataim Alzahra for their help, support, and encouragement throughout my life.

Abstract

Collapsible soils are defined as soil that has a low dry density, low moisture content and high capacity for applying a large vertical stress with a small compression at dry state, but then experience much larger collapses after wetting. To solve this problem, fly ash (a by-product from the burning of coal in the electric power plants) is currently in use for soil stabilization in some countries like USA, Japan, Scandinavian countries, India, and some other countries and has several recommendations and regulations. In Germany, however, fly ash is a variable material with large amount and low cost and still is not used for soil-stabilization very common. The present study is an attempt how the use of fly ash to improve the geotechnical properties of unsaturated collapsible soil.

The experimental programs are consisting (i) physical and chemical properties tests (ii) hydro-mechanical properties tests (including oedometer test, unconfined compressive strength (qu), soil-water characteristic curve (SWCC) and suction control-collapse test), (iii) electromagnetic properties tests (including permittivity and conductivity test for non/fly ash stabilized soil at different cases and (iv) seismic wave tests level (including V_s and V_p wave velocity test for non-stabilized soil and ultrasonic V_s and V_p wave velocity testing as non-destructive method for the fly ash-stabilized soils.

The summary of the present study illustrated the following findings:

The addition of fly ash to the natural collapsible soil led to a reduction of the plasticity index, an increase in the optimum moisture content and a decrease in the maximum dry density. This is due to the ionic exchanging between the free Ca^{+2} in fly ash and Na^{+1} in clay minerals of soil which caused a reduction in size of diffused water layer, flocculation and agglomeration of the clay particles.

The collapse potential of undisturbed natural soils depend on the initial

hydro-mechanical properties in skeleton of soil (include initial water content, initial void ratio, SWCC shape, the air-entry value and the fabric water holding capacity), on the physic-chemical properties, double layer size and attraction and repulsive forces of pore fluid. The addition of fly ash to the tested soil up to cretin percent (15%) caused decreasing in collapse potential, increasing unconfined compressive strength (*qu*) increasing air-entry value, increasing the water holding capacity and change in the hydro-mechanical properties due to the increase in density as a result of new pozolanic products as well as to the ionic exchanging which led to decrease of double layer size.

In recent years, electromagnetic tests have been used in geotechnical applications to determine the water content (TDR technique) and suction (Tensiometer) based on the dielectric properties (permittivity and conductivity) of soil. In the present work, Non-invasive tests (include electromagnetic properties tests and seismic wave tests) are used as a new tool to investigate the change in the hydro-mechanical properties (include change in water content, void ratio, vertical stress and collapse potential and fly ash-stabilized content). The electromagnetic results noted that the electrical permittivity and conductivity of the soil is highly influenced by changes in the water content, soil porosity and the chemistry of pore water of soil. By this fact the experiments are the base for functional relation between the macro and micro hydro-mechanical behavior as well as the electromagnetic properties and the collapse phenomena. The results show it is possible to use the electromagnetic measurement to monitor the fabric change of soil which is directly related to the collapse potential. The outcome of this investigation give the engineering applications a new useful tool and suggestion equation for determining the collapse potential depending on the void ratio, water content, vertical stress and electromagnetic properties for the given soil.

Additionally, a very few studies have been carried out to monitor the setting, hardening and the changes in the electromagnetic properties during the cementation process as a liquid state. In the present work, Electromagnetic properties tests give a strong indication as to the change of chemical

properties during the fly ash stabilizing process (ion exchanges and pozzolanic reactions) of fly ash-stabilized soil. Therefore, in addition to basic chemical analyses, this new tool can be used in a trial with a small stabilized soil sample to evaluate the intensity of pozzolanic reaction before starting to stabilize the soil.

Zusammenfassung

Kollapsfähige Böden sind zum einen gekennzeichnet durch eine geringe Trockendichte und geringen Wassergehalt (oder vielleicht auch Wasserhaltekapazität). Zum anderen zeigen sie im trockenen Zustand oft eine relativ hohe Festigkeit gegenüber vertikaler Last, sehr im Gegensatz zum Zustand bei Wassersättigung, bei dem solche Böden auffällig versagen. Um den Boden tragbar, d.h. gebrauchsfähig zu machen, wird vielfach unter anderem Flugasche (ein Nebenprodukt bei der Kohleverfeuerung) zur Stabilisierung eingesetzt. Dies geschieht beispielsweise in Ländern wie den USA, Japan, Skandinavien, Indien und anderen Nationen. Das Verfahren unterliegt verschiedenen Empfehlungen und Vorschriften. In Deutschland, wo es in größeren Mengen vorhanden und günstig zu bekommen ist, ist Flugasche ein vielschichtiges Material; sie wird aber dennoch nicht oft im Sinne einer Bodenstabilisierung verwendet. Die vorliegende Studie stellt einen Versuch dar, die Verwendbarkeit von Flugasche für die geotechnische Verbesserung der Standfestigkeit empfindlicher ungesättigter Böden zu zeigen.

Das experimentelle Programm besteht aus (i) der Bestimmung grundlegender physikalischer und chemischer Eigenschaften, (ii) der Beschreibung hydromechanischer Eigenschaften (einschließlich Oedometertests, nicht-eingeschränkter Kompression (*qu*), Ermittlung der Boden-Wasser-Kennlinien (soil-water characteristic curve, SWCC) und kontrollierte Saugspannung-Versagenstests. Das Programm beinhaltet ferner (iii) Tests zur Bestimmung elektromagnetischer Eigenschaften (einschließlich Permitivität und Leitfähigkeitsuntersuchungen an Böden mit und ohne Flugasche als Stabilisator unter verschiedenen Bedingungen und (iv) die Untersuchung des Verlaufs seismischer Wellen (V_s und V_p Wellengeschwindigkeiten an nichtstabilisiertem Bodenmaterial sowie die Nutzung von Ultraschallwellen als zerstörungsfreie Prüfmethode für flugaschengestützte Böden. Die Zusammenfassung der vorliegenden Arbeit stellt die folgenden Beobachtungen heraus:

Die Zugabe von Flugasche führt zu einer Minderung des Plastizitätindexes eines solchen Bodens, setzt den optimalen

Wassergehalt herauf und die maximale Trockendichte herab. Dieses steht im Zusammenhang mit dem Ionenaustausch zwischen freiem Ca^{2+} in der Flugasche und Na^{1+} in den Tonmineralen des Bodens. Dieser Prozess verursacht eine Reduzierung der Dicke der diffus angelagerten Wasserschicht, Flockung und Agglomeration der Tonpartikel.

Das Versagenspotential ungestört gelagerter, natürlicher Böden hängt von den initialen hydromechanischen Eigenschaften des Bodenskeletts ab (einschließlich initialem Wassergehalts, der initialen Porenzahl, der SWCC-Form, den Luftzutrittsbedingungen und des intrinsischen Wasserhaltevermögens). In physiko-chemischer Hinsicht spielen die Stärke der Doppelschicht sowie die Anziehungs- und Abstoßungskräfte des Porenfluids eine Rolle dabei. Die Zugabe von bis zu 15% (in der Trockenmasse) an Flugasche führte zu einer Minderung des Versagenpotentials, einer Zunahme der Druckfestigkeit (*qu*), zu einem besseren Gasaustausch, einer Erhöhung des Wasserhaltekapazität und letztlich zu Veränderungen der hydromechanischen Eigenschaften. Die Zunahme der Dichte als Ergebnis der Verwendung neuer puzzolanischer Produkte wie auch die Ionenaustauschkapazität führen in diesem Zusammenhang zu einer Abnahme der Doppelschichtstärke.

In den letzten Jahren haben elektromagnetische Messverfahren in geotechnischen Anwendungen und Fragestellungen hinsichtlich der Bestimmung des Wassergehaltes (TDR Technik) und des Saugvermögens (Tensiometer) – basierend auf dielektrische Eigenschaften wie Permitivität und Leitfähigkeit- an Bedeutung gewonnen. Für die vorliegende Arbeit wurden nicht-invasive Tests durchgeführt (Bestimmung elektromagnetischer Eigenschaften und Untersuchung seismischer Wellen). Sie bieten neue Möglichkeiten, die Veränderungen hydromechanischer Eigenschaften aufzuzeichnen (Veränderungen des Wassergehaltes, Porenzahlbestimmung, Vertikalstress, ermöglichen Aussagen zu Versagenspotential und sinnvollem Flugascheanteil

Die Ergebnisse der elektromagnetischen Untersuchungen ergaben, dass die elektrische Permitivität und Leitfähigkeit des Bodens durch Veränderungen des Wassergehaltes, durch die Bodenporosität und den Chemismus des Bodenwassers in hohem Maße beeinflusst werden.

Dadurch bedingt bilden die Experimente die Basis für die Erkenntnisse der Beziehungen zwischen hydromechanischem Verhalten im Makro- und Mikromaßstab wie auch der elektromagnetischen Eigenschaften und des Versagens des Bodens an sich. Die Ergebnisse belegen, dass die Anwendung elektromagnetischer Messverfahren als Monitoring geeignet ist, qualitativ Gefügeänderungen im Boden zu zeigen. Diese Gefügeänderungen stehen in direkter Verbindung zum Versagenspotential.

Die Resultate dieser Untersuchungen bieten ein neues nützliche Werkzeug/eine neue nützliche Technik für ingenieurmäßige Anwendungen und stellen Gleichungen zur Bestimmung des Versagenspotentials vor, je nach Porenzahl, Wassergehalt, Vertikalspannung und elektromagnetischen Eigenschaften des gegebenen Bodens.

Nur sehr wenige Studien befassen sich bisher mit der Erfassung von Setzung, Aushärtung und den elektromagnetischen Eigenschaften während des Zementationsprozesses im ‚flüssigen' Zustand. In vorliegender Arbeit zeigen die elektromagnetischen Eigenschaften deutlich die veränderlichen chemischen Eigenschaften im Aggregat während des Einbindens der Flugasche (Ionenaustausch und puzzolanische Reaktionen) in den zu stabilisierenden Boden.

Vereint mit der chemischen Analyse kann das neue Verfahren, begleitet von kleinmaßstäbigen Laborversuchen an Testböden, genutzt werden, um die Intensität puzzolanischer Reaktionen abzuschätzen bevor großmaßstäbig Boden in situ stabilisiert wird.

Contents

List of Figures

List of Tables

Chapter 1

Introduction

1.1 Background and Motivations

Many problems in engineering occur with soils in unsaturated states because their voids contain both water and air. This type of material is very common in arid or semi-arid areas, where the water table level normally changes with climate change. In many constructed structures, the soil in natural and compacted fills such as those used as road subgrades, earth dams and embankments, is placed in an unsaturated state. Whenever unsaturated soil interacts with water, volume change may occur. Such water-soil interaction may cause a reduction in soil volume (collapse) or swell, depending on the initial condition of the soil. Moreover, soaking with water causes a reduction of the strength (softening). These behaviors of unsaturated soils in general appear to be relatively complex when compared with fully saturated soils. This is due to the larger number of physical and chemical phenomena involved in unsaturated soils. With decreasing and increasing water content, which is related to rises and falls in the water table and an increasing and decreasing in soil suction, the constitutive behavior of unsaturated soils changes significantly so that studying the effects of water content and suction in soil on the hydro-mechanical behavior becomes of major interest for solving the problems of geotechnical engineering [Fredlund, 1991].

Collapsible soil is one type of problematic soil which covers approximately 10 % of the world's landmass (see Figure 1.1) and can be defined as a soil that is susceptible to a large and sudden reduction in volume upon wetting. Collapsible soil usually has low

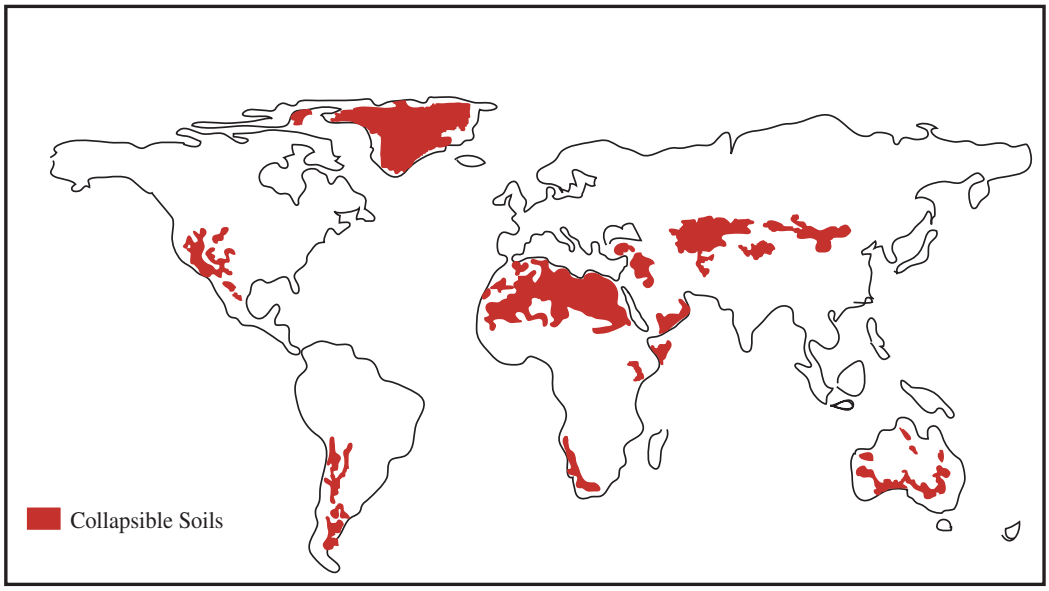

Figure 1.1: World distribution of collapsible soils, modified after [FAO, 1990].

dry density and low moisture content and can withstand large applied vertical stress with small compression when in a dry state, but then experience much larger collapses after wetting. However, the open structure that encourages strong root development makes the soil susceptible to collapse upon the application of load and/or water. In fact, the collapse potential of such open structures can cause a reduction in volume up to 30% [Waltham, 1988]. In compacted fills, many collapsible materials, such as loose or loosely compacted fills can undergo large deformations and volume change as the materials are wetted at relatively large stress, bringing about damage to the overlying structures. Future changes in climate could potentially cause significant changes in the soil moisture regime in many areas of the world [Barden et al., 1973].

Previous studies show that collapse potential occurs in several types of soil due to the breaking of bonds of soil structure when water content increases. This bond failure in collapsible soils is classified in the following way: (i) breaking of clay bonds, which occurs in natural loose soil material [Barden et al., 1973] (ii) removing the physical-chemical forces of clay plates, which happens in compacted collapsible soils when compacted on low dry relatively densities under certain conditions and where the largest factors influencing collapse potential are stress, initial unit weight, moisture content, type and the amount of clay [Victor et al., 1998] (iii) removing the cementation

material, which occurs in soil with a cementation material as a binder (for example, gypsum, salt). This cementation material will be dissolved during the wetting, causing the removal of the binding forces among the soil particles and subsequent collapse [Al-Mufty, 1997].

In addition to the physical phenomenon, collapse is also governed by the physical-chemical behavior of clay plates in soils. This behavior can be described in terms of the double layer theory, given that the forces of clay plates are mostly controlled by surface micro-chemical forces, due to their small size of the diffuse double layer which forms around the clay plates. As the moisture content decreases, the ionic concentration in the pore fluid will increase, which causes an increase in the attraction force between the clay plates and a decrease in the thickness of double layer size and so the particles become close to each other, causing an increase in the strength of the fabric. Upon wetting, the ionic concentration in the pore fluid decreases with the increase in water content and the reduced ionic concentration thickness leads to an increase in the size of the double layers thickness, an increase of repulsion forces and so clay particles disperse, leading to a removal of the strength of fabric and subsequent collapse of solid structure [Victor et al., 1998]. The physical-chemical forces between the clay plates can be investigated through the electromagnetic properties of the pore fluid which is affected by several parameters such as ion concentration, valence, pH-value, and permittivity in the space between the clays plates [Fang et al., 1992] and [Santamarina and Fam, 1995].

Electromagnetic properties of non-ferromagnetic unsaturated porous geo-materials are defined in terms of broadband electromagnetic transfer functions such as the complex effective relative to permittivity ($\varepsilon^*_{r,eff}$) or complex effective electrical conductivity (σ^*_{eff}) [Wagner et al., 2011]. Porous mineral materials consist mainly of four phases: solid particles (various mineral phases) pore air, pore fluid as well as a solid particle-pore fluid interface. The fractions of these phases vary both in space (due to composition, specific density and surface area) and time (due to changes of water content, porosity, pore water chemistry and temperature) [Kaatze, 2007b].

The electromagnetic properties are directly related to changes in soil structure and therefore to the collapse potential. However, for the development of robust approaches under consideration of highly concentrated salt solutions and a complex pore water chemistry as well as structural changes with hydration of clay minerals there is a lack

of systematic investigation by broadband dielectric spectroscopy of unsaturated and saturated porous media under controlled thermal, hydraulic, mechanical and chemical conditions [Wagner et al., 2011].
In addition to the high collapsibilty of these types of soils, a large reduction in shear stiffness occurs when saturation starts due to the removal of the cementation material. Initial shear stiffness (G_{max}) is an important parameter for unsaturated soil used in geotechnical design applications. The shear modulus is usually expressed as the secant modulus by the extreme points on the hysteresis loop. The slope in the origin point to the stress-strain curve corresponds to the shear modulus (G_{max}) or (G_0). The stress-strain relationship in very small strain is considered a line; therefore, (G_{max}) is the shear modulus in the small-strain range, usually assumed at values below the linear elastic threshold strain of about $5 * 10^{-3}$%. Initial shear stiffness (G_{max}) is a key parameter which is used to predict soil behavior or soil-structure interaction during change in hydro-mechanical properties of soil such as volume change, collapsed potential and swelling [Seed et al., 1984].
To solve the geotechnical problems in collapsible soils, soil stabilization is one of the methods employed to improve these soils. It can be defined as the treatment which is used to improve soil properties by reducing the susceptibility to the influence of water. The process produces a more stable soil and can be performed in the field or applied to the soil before applying the load or before construction begins.
[Das, 1984] showed that the improvement of soil is usually carried out to:

1. Reduce the settlement of structures.
2. Reduce the collapse potential, shrinkage and swelling characteristics of soils.
3. Increase the safety factor for possible slope failure of embankments and earth dams.
4. Improve the shear strength of soil and thus increase the bearing capacity of shallow foundation.

Several methods were used and performed in the field to avoid the problems of collapsible soils. The modification of soil properties may be carried out in a number of ways, as summarized by [Bowles, 1984]:

1. Mechanical method (compaction): This is usually the cheapest method of improving site soil.

2. Chemical stabilization by Admixtures: Admixtures are occasionally used to stabilize soils in the field- particularly fine grained soils. The most common of these admixtures are lime, fly ash, cement and asphalt.

In this work, fly ash is used as a stabilizing material to increase the strength of collapsible soils. Fly ash is one of the chemical stabilization processes and involves blending a binder into the soil to increase its strength. When the fly ash is mixed with the soil in the presence of water, a set of reactions occur that result in the dissociation of lime in the binders and the formation of cementations and pozzolanic gels (calcium silicate hydrate gel and calcium aluminate silicate hydrate gel). These reactions are referred to as cementation and/or pozzolanic reactions that result in the formation of cementation gels which cause a reduction in collapse potential and an increase in stiffness and shear strength [Rogers and Glendinning, 2000].
The reasons for using fly ash as a stabilized material in this work can summarized as following:

1. Fly ash is available material with large amounts and low cost comparison with cement and lime (is produced as a waste material from burning finely ground coal in electric power plant).

2. The previous studies noted the fly ash has high percentage of (SiO_2) and (Al_2O_3) (is called high-energy-based materials) when compared with cement and lime. These two compounds are responsible to create the pozzolanic productions (calcium silicate hydrate gel (CSH) and calcium aluminate silicate hydrate gel (CASH) which cause increasing in the strength [ASTMC618, 2003].

3. In Germany, fly ash is not used as common material for soil stabilization and there are no German standards and practical procedures for fly ash soil stabilization. Therefore, one of the reasons for using the fly ash is to find the guidelines and more date base about the fly ash-stabilization practical procedure methods.

1.2 Objectives and Scopes

Several studies of soil collapse potential have been in done in the past, however there are still fundamental questions regarding the phenomenon. The objective of this thesis is the study the understanding in micro-and meso-mechanical behavior of this soils in particular in unsaturated ranges and stabilization of this material by alternative hydraulic binder like fly ash in geotechnical applications. The present handle the collapse analysis and study on different collapsible soils. The analysis scopes are: physical behavior, hydro-mechanical behavior, electromagnetic properties and shear stiffness. The description of unsaturated soils are essential to understand the relationships of the hydro-mechanical properties as collapse curve, stiffness and shear strength behavior. Therefore the study of the hydraulic behavior covers the two constitutive relationships as the soil-water characteristic curves and suction control-collapse behavior in an extensive manner.

Previous studies show that although some collapse soils improved by compaction technique methods to increase the density (decreasing in void ratio), still there is volume changing (i.e. collapse and/or swelling potential) in these type of soil under saturated condition. The mechanism of collapse potential in compacted soil depends on two main roles: water content and the chemical reaction of the minerals in the soils [Victor et al., 1998]. Based on this fact, one of the main objectives in this study is how to improve the chemical properties of this type of soil by adding stabilized material (fly ash stabilized) to reduce the physical- chemical changing during the wetting condition.

In recent years, electromagnetic tests have been used more and more to detect hydraulic soil properties based on the dielectric properties (complex permittivity and conductivity) of soil for geotechnical applications, like the water content (TDR technique) [Wagner et al., 2011] and suction measurement (Tensiometer) [Ridley and Burland, 1999]. Electromagnetic properties in soils are affected by two main parameters: volumetric water content θ and porosity n. Based on this fact, one objective of this thesis is to use this method to develop a new prediction and analysis technique for collapsible soils. The based is the hydraulic and molecular microscopic change and the implication on electromagnetic soil properties during soil collapse.

The state of the art covers several collapse studies about the hydraulic-mechanical behavior of unsaturated collapsible soil in particular the soil-water characteristic curve under different conditions as moisture content, void ratio, suction state, influence of net stress, loading path directions and flow conditions or stress and overburden conditions. In the present thesis, a new condition in addition to already named, is to study of stabilization opportunities like fly ash and their influence on the hydro-mechanical behavior.

Based on the electromagnetic analysis a new research is carried out in the field of collapsible soils in relation to the physical-chemical soil forces and hydraulic soil properties. Only few studies have been performed to the electromagnetic properties during a the cementation process, [Santamarina and Fam, 1995]. The electromagnetic analysis was used to monitor the setting and hardening of cement, bentonite-cement slurries, and attapulgite-cement slurries as a liquid state. In particular the relation between shear-wave velocity and permittivity provides complementary micro-level information on the fundamental dependency between chemical reactions, physical changes, and rigidity in cementitious materials. A further objectives of the thesis is the study the setting and hardening of fly ash-soil stabilized soils - in short-term (ion exchange reaction) and in long-term (pozzolanic reaction) by use of electromagnetic and mechanical waves.

Finally, the studies and developments lead to a noninvasive techniques that provides the assessment of soil stabilized material-cement materials during the stabilizing proses.

The objectives can be summarized in following:

1. Study and understanding of soil collapse related to hydro-mechanical changes in soils (covers initial void ratio, initial water content, suction and vertical stress).

2. Development of collapsible soil stabilization under use of fly ash as a hydraulic and pozzolanic binder. Determination standards, guidelines and practical procedures for applying this stabilization.

3. Application and development of electromagnetic measurements and properties

in collapsible geomaterial. Determination the relationships between the soil collapse, collapse potential and change of hydraulic conditions and stress.

4. Identification of stabilized soil setting, hardening and pozzolanic time-dependent reactions/products of fly ash-soil-mixtures under use joint indicators by seismic and electromagnetic wave methods as non-destructive process monitoring.

1.3 Organization of the Dissertation

The dissertation consists of seven chapters. The first chapter describes the background, motivations and objectives of the work, as well as its organization. The second chapter summarizes the literature on definitions and mechanism of collapsible soil, unsaturated soils, main principles and phases of unsaturated soil. Definitions and physics for soil suctions, soil water characteristic curve (SWCC) are presented. The concepts of effective stress and the two independent stress variables, the features of volume change of unsaturated soil are described. Fly ash-stabilized material soil, the methods for preparing the fly ash stabilization material sample, definition of fly ash material stabilization and micro-mechanical of stabilization soil are discussed. Non-invasive experimental soil analysis methods are presented, including definitions of the methods of seismic measurements and definition of electromagnetic properties.
The third chapter presents experimental materials, equipments and testing procedures, which include the physical and chemical properties of the materials used. Additionally the program of experimental tests is presented, including unconfined compressive strength tests, collapse potential tests, soil water characteristic curve (SWCC) tests, suction controlled-oedometer program tests, electromagnetic properties tests and finally seismic measurements tests.
In the fourth chapter, hydro-mechanical behaviors of stabilization and non-stabilization soil results are discussed, including physical properties results, oedometer test results, unconfined compressive strength test results, soil water characteristics curves results (SWCCs) and suction-controlled oedometer test results.
The fifth chapter presents the results of wave based soil behavior of stabilization and non-stabilization soil, including shear stiffness results / Ultrasonic results and electromagnetic properties results.

In the sixth chapter, the methods of collapse assessment and recommendations for stabilization and non-stabilization soil are presented, including monitoring the collapse development based on electromagnetic properties and methods and recipes of soil stabilization.
Finally, chapter seven summarizes the main results and the related conclusions of this study and provides an outlook for further studies in this field.

Chapter 2

State of the art

2.1 Introduction

This chapter offers a review of the behavior of partly saturated collapsible soils, the experimental techniques required for testing them and soil stabilization analysis. It is aimed at presenting the necessary background for the subsequent content of the thesis. The chapter is divided into four parts. The first part is concerned with definitions, failure mechanism, experimental geotechnical testing and the assessment of collapsible soils and their geotechnical problems. Secondly, the main concept of unsaturated soils is dealt with, including a definition of soil suction, the soil-water characteristic curve and the techniques employed for testing partly saturated soils. Thirdly, the mechanism of stabilization methods for collapsible soil is investigated. The final section reviews the non-invasive experimental soil analysis methods, including definition, measuring of seismic measurements and electromagnetic properties and the shear stiffness behavior of partly saturated collapsible soil. The gaps in current knowledge will then be discussed.

2.2 State of the art-collapsible soils

2.2.1 Definitions of collapsible soils

Collapsing soils, which are defined as metastable soils, are unsaturated soils that undergo a large volume change upon saturation. This volume change may or may not be the result of the application of additional load. Many collapsing soils may be residual soils that are the products of parent rock weathering. The process of weathering produces soils with a large range of particle size distribution and these soils may contain soluble and colloidal materials which are leached out by weathering, resulting in large void ratios and thus unstable structures [Das, 1990].
[Clemence and Finbarr, 1981] defined collapsible soils as any unsaturated soil that goes through a radical rearrangement of particles and great loss of volume upon wetting, with or without additional loads. It was shown that upon wetting many collapsible soils lose the strength that is provided by a cementing agent such as gypsum, salt or calcium sulphate. The following section discusses the mechanism of collapse in natural, compacted and gypsum collapsible soils.

2.2.2 Mechanism of failure in collapsible soils

Collapse is a sudden reduction of soil volume of fill material or natural soil deposit upon inundation, with no change in applied stress. The inundation source may be downward infiltration of surface water, rising ground water table, the bursting of underground water supply lines or other means. The collapse potential (C_p) is determined by the equation:

$$C_p = \frac{\Delta e}{1+e_0} * 100\% = \frac{\Delta h}{h_0} * 100\% \tag{2.1}$$

where:

Δe = Change in void ratio in a oedometer test on inundation at a given stress.

e_0 = Initial void ratio of the oedometer test specimen before inundation.

Δh = Change in thickness due to inundation at the given stress.

h_0 = Initial height of the sample before inundation.

[Dudley, 1970], [Barden et al., 1973] and [Pereira and Fredlund, 2000] noted the following factors producing collapse in soils:

1. An open, partially unstable, unsaturated fabric.
2. High enough net total stress that will cause the structure to be metastable.
3. A bonding or cementing agent that stabilizes the soil in the unsaturated condition, which is reduced on addition of water causing the inter aggregate or inter granular contacts to fail in shear, resulting in a reduction in total volume of the soil mass.

[Jennings and Knight, 1975] has suggested criteria to assess the severity of the problem associated with collapse, based on values of collapse potential according to Table 2.1

Table 2.1: Collapse potential and severity of collapse [Jennings and Knight, 1975]

Collapse Potential C_p[%]	Severity of Collapse
0–1	No-Problem
1-5	Moderate Trouble
5-10	Trouble
10-20	Severe Trouble
>20	Very Severe Trouble

The types of bond failure in collapsible soils are classified into:

2.2.2.1 Bond breaking in loose collapsible soils

Collapse mechanisms in loose soils have been studied by several researchers [Jennings and Knight, 1957] ; [Holtz and Hilf, 1961]; [Burland, 1965]; [Dudley, 1970]; [Barden et al., 1973] and [Mitchell, 1993]). The collapse phenomenon is primarily related to the open structure of the soil. [Jennings and Knight, 1957] noted that a portion of the fine-grained fraction of the soil acts as bonding material for the larger grained particles and that these bonds undergo local compression in the small gaps between adjacent grains resulting in the development of strength. At natural moisture content, these soils compress slightly as a result of increasing overburden pressures due to the construction load. However, the structure remains noticeably unchanged. When the loaded soil is exposed to moisture, and a certain critical moisture content is exceeded, the fine silt or clay bridges that provide the cementation are removed, weakened and/or dissolved to some extent. Eventually, the binders reach a stage where they no longer

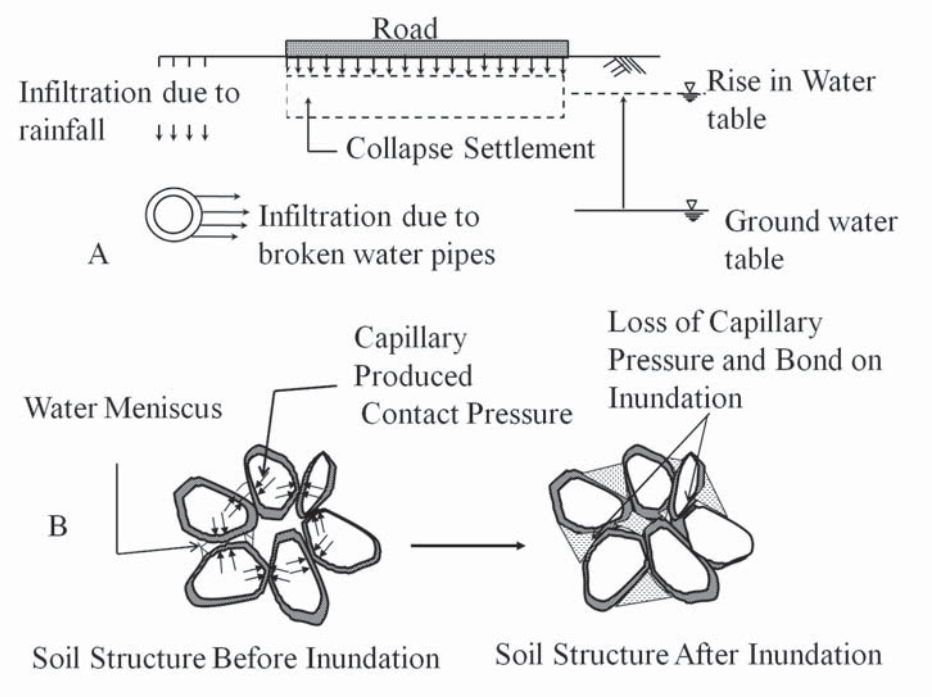

Figure 2.1: Mechanism of collapse, modified after [Barden et al., 1973], A) macroscopic effects and B) microscopic phenomenon during collapse.

resist deformation forces and the structure collapses as shown in Figure 2.1.
[Holtz and Hilf, 1961] described the collapse mechanism as the result of capillary pressures approaching zero and the degree of saturation increasing to 100 %. [Burland, 1965] described the collapse mechanism in terms of the stability at the inter-particle contact points. Due to wetting, the negative pore water pressure at the contact points decreases, causing grain slippage and distortion.

2.2.2.2 Change of physical-chemical forces at clay particles in compacted collapsible soils

The mechanism of collapse potential in compacted soils depends on two main roles: water content and the chemical reaction of the minerals in the soils. As the moisture content decreases, fine particles displace towards the menisci, the ionic concentration in the pore fluid increases, the thickness of double layers shrinks and van der Waals attraction prevails over double layer repulsion. This evolution of inter-particle electri-

cal forces is captured in Figure 2.2. These results were computed with soil parameters

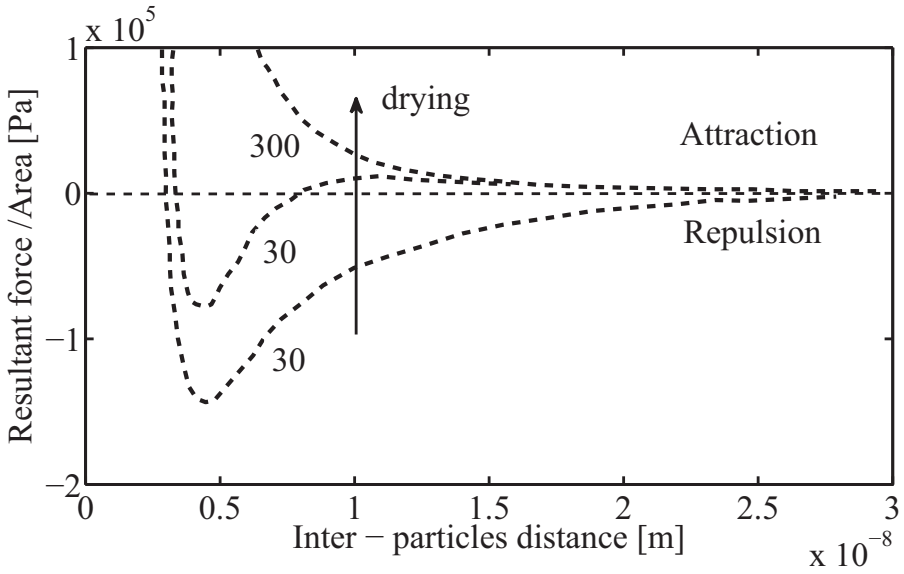

Figure 2.2: Increase in inter-particle attraction as the moisture content decreases and the ionic concentration of the electrolyte increases [Victor et al., 1998].

applicable to clays in compacted and platy particle geometry. As the inter-particle force-balance becomes attraction dominated, clay particle flocculation forms the clay bridges and buttresses at contact points. If the water content is even further reduced, hydrated cations in the double layer dehydrate and ionically link two contiguous clay particles. In the meantime, the concentration of salts reaches saturation and salts precipitate as crystals that strengthen the soil structure [Victor et al., 1998]. Upon wetting, most of the processes that contribute to strengthening the soil mass are reversed:

1. Soluble salt hydrates and softens.

2. The ionic concentration in the fluid continues to decrease with the increase in water content.

3. The lower the ionic concentration, the thicker the double layers that form around particles (this is aggravated by the low local confinement clay particles experienced in clay bridges and buttresses). The shear stiffness and strength of the clayey formations decreases as the thickness of the hydration layers increases.

Repulsion forces may become dominant and clay particles disperse [Victor et al., 1998].

2.2.2.3 The dissolving of chemical cementation bonds in collapsible gypsum soil

Collapsible gypsum soil is one of types the collapsible soils and is widespread in arid or semi-arid regions throughout the world. Gypsum soil refers to soils containing more than 2% of hydrated calcium sulphate ($CaSO_4.2H_2O$) which is called gypsum. Gypsum acts as a binder between soil particles, causing the soil to be very hard when it is dry. Upon wetting, it can be speculated that part of this binder will be dissolved, causing the soil to be soft and highly compressible, leading to severe foundation problems due to the collapse of soil structure [Alphen and Romero, 1971].
According to [Klein and Hurlbut, 1985], gypsum ($CaSO_4.2H_2O$) is the most important and abundant hydrous sulphate. As a result of the dehydration of gypsum, the first 1.5 molecules of water in gypsum are lost relatively continuously between (0^oC) and (65^oC), leading to bassanite ($CaSO_4.\frac{1}{2}H_2O$). At about 70^oC, the remaining ($\frac{1}{2}H_2O$) molecule in bassanite is still retained relatively strongly but at about (95^oC) it is lost and the structure transforms to that of anhydrite $CaSO_4$. [Freeze and Cherry, 1979] reported that the solubility of gypsum in pure water at (25^oC), a total pressure of 1 bar and at a pH value of 7, is 2.1 [kg/m^3]. Gypsum soils are usually stiff when they are dry especially because of the cementation of soil particles by gypsum, but great loss in strength and sudden increasing in compressibility occur when these soils are fully or partially saturated. The dissolution of the cementing gypsum causes great softening of the soil and the problem becomes more complicated when the ground water flows through the gypsum soil, causing leaching and movement of gypsum. In addition to softening, a loss in soil solids takes place. This causes a continuous collapse in the gypsum soil [Al-Mufty, 1997].

2.3 State of the art-concept and experimental analysis of collapsible soils

The soil near the ground surface, especially in arid or semi-arid regions, is mostly unsaturated, and compacting, excavating, and remolding soil processes are used in

several engineering constructions, such as earth dams, highways, embankments, and airport runways. In the following sections, the main concepts of unsaturated soils will be defined in more depth.

2.3.1 Phases in unsaturated soil

An unsaturated soil has a three-phases system compared with two-phases in saturated soils, namely the solid phase, the liquid phase and the gas phase (see Figure 2.3). The solid phase is defined as the soil grains. The solid phase may range from fine grained soils such as silts and clays to coarse grained soils such as sands and gravels, depending on the grain sizes (grain-size distribution curve). The liquid phase consists of any liquid or combination of two or more liquids (e.g. water, oil, etc.). Additionally, the liquid phase includes the contractile skin, which acts as a tension on the liquid surface. The assumption in this work is that the solid phase, the liquid phase and the gas phase of the unsaturated soil are the soil solids, water (with the contractile skin) and air, leading to a 3-phases system [Fredlund and Rahardjo, 1993].

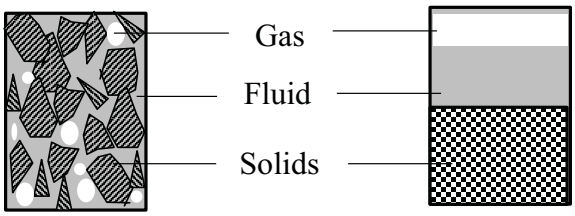

Figure 2.3: Three phases system of unsaturated soils [Fredlund and Rahardjo, 1993].

2.3.2 Definitions and physics for soil suction

The soils above the water table have a force to absorb the water above the groundwater table which either partially or fully fills in the space within the soil pores. This soil is normally under tension stress or negative pore water pressure. This tension stress, measured through a porous tip making an intimate contact with the soil water is known as ”suction”. It can be described as the potential of the soil for absorbing water. It is considered to be the key variable which governs the mechanical behavior of partly saturated soils [Fredlund, 1991].

Soil suction generally consists of two components: the matrix component and osmotic component. The sum of these two components (i.e., matrix suction, s, and osmotic suction, π is called total suction, S_t as equation 2.2, which can be defined as the stress required to change a water molecule from the soil into the vapor phase.

$$S_t = s + \pi \tag{2.2}$$

Matrix suction, s, is defined as the difference between pore-air pressure, u_a, and pore-water pressure, u_w, in the soil (the air-water interface or surface tension), giving rise to the capillary phenomenon as expressed by equation 2.3

$$s = u_a - u_w \tag{2.3}$$

Matrix suction is described by the two main physical phenomena, namely capillarity and surface adsorption. The capillarity phenomenon is directly related to the surface tension of water. This capillary force and thus the suction are defined also as the curvature of the water in a tube. The smaller the radius in a tube the greater the curvature, and the higher the water will rise within the tube. Similarly, the capillary rise above groundwater level within a soil depends on the pore size and distribution in the soil structure. In the same soil, fine textured soils normally have a higher capillary rise than coarse textured soils [Lu and Likos, 2004].
The surface adsorption is principally related to chemical minerals in clay and occurs as a result of the clay particles' negatively charged surfaces. This powerful electrical force around clay particles strongly attracts water molecules. The mineral types of clay also affect a very important role in the adsorption of water by clay surfaces. For example, soils with high activity clay minerals, such as montmorillonite, are able to retain a greater amount of water around their particles and remain saturated even at suctions as high as 10-20 MPa so that they have a tendency for greater collapse, shrinkage or expansion in volume during the drying or wetting cycles [Fredlund, 1991].
As shown by the equation 2.2, the total suction is the sum of the matrix suction, s, and the osmotic suction, π. The osmotic suction is a function of the concentration of dissolved salts within the soil water; any changes in the concentration of salts dissolved within soil water, or in the osmotic suction can lead to flow of water in a soil. The

moisture content of a soil in contact with the atmosphere is also determined by the total suction, which corresponds to the atmospheric humidity [Alonso et al., 1987].

2.3.3 Soil water characteristic curve (SWCC)

The Soil-Water Characteristic Curve (SWCC) is a function which describes the relationship between suction and the corresponding state of soil wetness. The state of wetness can be expressed in different terms, namely, degree of saturation S_r, gravimetric water content W or volumetric water content θ, which are all related by the equation 2.4

$$\frac{W * g_s}{1+e} = \frac{S_r * e}{1+e} \tag{2.4}$$

where (g_s) is the specific gravity of the soil and (e) the void ratio. A general description of the SWCC is shown in Figure 2.4 as a plot between volumetric water content (θ) and logarithmic suction. The sample is gradually dried from a fully saturated condition (S_r = 100%) and during the increases in suction, the sample remains fully saturated until air starts flowing through the largest pores at the de-saturation or air-entry point. The sample then continues de-saturating with increasing suction until the residual point is reached, after which the degree of saturation hardly changes with suction [Fredlund and Xing, 1994].

As shown in Figure 2.4, soil-water characteristic curves can be divided into three main zones, namely:

Saturated zone: The zone between soil suction ψ= 0 and the air-entry value ψ_{aev}. All voids are filled with water (assuming no vapor phase) with the liquid phase continuous and the gas phase non-continuous.

Transition zone: After increasing the suction of the air-entry value ψ_{aev}, the large voids of the soil begin to drain followed by small voids. The volumetric water content decreases until it reaches the residual water content θ_r. The zone between the air-entry value ψ_{aev} and the residual volumetric water content θ_r is termed the transition zone. In this zone, the pore water is retained mainly by capillary forces and the amount of water flow in the saturated zone and the transition zone mainly depends on the pore-grain size distribution. Both the liquid and the gas phases are continuous.

Residual zone: The residual zone follows after the transition zone and in this zone the pore water is retained in form of thin films on the soil grains caused by the specific

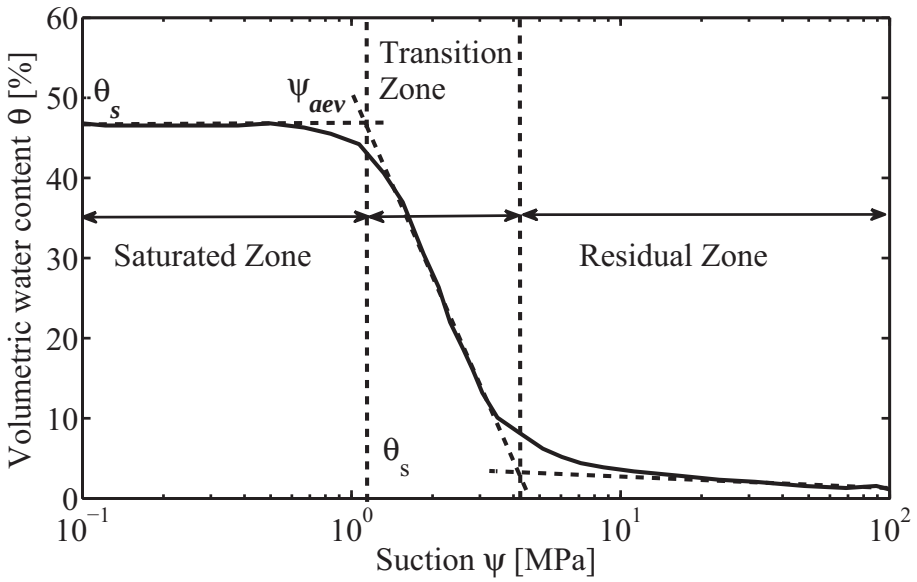

Figure 2.4: Parameters and zones of soil water characteristic curve [Fredlund and Xing, 1994].

surface properties and specific charge properties of the soil. Liquid is only transported by diffusion in the gas, and the liquid phase becomes non-continuous. The typical parameters of the soil-water characteristic curve can be estimated by following [Fredlund and Xing, 1994]:

Air-entry value ψ_{aev}: This is the suction value of soil where air starts to enter the largest voids of the soil during the drainage process.

Saturated volumetric water content θ_s: This is the water content of soil when suction ψ is 0, and in this water content all pores are filled with liquid.

Residual soil suction ψ_r and residual volumetric water content θ_r: The residual soil suction ψ_r and corresponding residual volumetric water content θ_r defined by [Sillers, 1997] as the point where water starts to be held in the soil by adsorption forces. The SWCC is considered to be the key for studying the behavior of unsaturated soils with regard to its hydraulic conductivity, volume changes, collapse potential and shear strength. These unsaturated soil properties vary as the soil suction changes and these changes can be related to the amount of water present in the soil pores. The SWCC can provide approximate estimates of the above mentioned properties. These approximations may be satisfactory for geotechnical engineering practice. Therefore, given

its importance, the soil-water characteristic curve should be considered as a standard test for unsaturated soils [Leong and Rahardjo, 1997].

2.3.4 Factors influence on the shape of (SWCC)

The shape of the soil-water characteristic curve (SWCC) is influenced by both structure and composition of a given soil. The factors are as follows:

Suction range: In the low-suction range (0-100 kPa), the SWCC is principally influenced by soil structure and amount of water retained depends mainly on the capillary effect and the pore-size. As the suction increases (100 kPa <suction), the surface adsorption plays a greater role in retaining water around soil particles. At higher suction, the water retention is affected less by the structure and more by the chemical composition and specific surface of the soil [Hillel, 1998].

Type of soil: For different types of soils (sand, silt and clay), the soil-water characteristic curves are differ from each other and depend upon the grain size distribution of the soil particles, pore-size distribution as well as the density. Figure 2.5 shows the SWCC for sand, silt and clay and it can be seen that the soil-water characteristic curve of the sand is located in a limit range of suction while the soil-water characteristic of clay is located in a large range of suction [Reeve et al., 1973; Richards and Weaver, 1944; Salter and Williams, 1965].

The pore size distribution: The shapes of SWCCs can also be considered as an indication of the pore size distribution of the soil. For the soils with a normal pore size distribution, the typical S-shape of SWCC is usually observed. However, if the soil is highly structured, its pore size distribution may be multi-level, resulting in the multimodal SWCC curves [Camapum et al., 2002]. Additionally, there are a number of factors affecting SWCC, including stress state, compaction effort, and stress history [Ng and Pang, 2000]. In general, when the soil is compacted with greater effort or an increase in the applied stress, the pore size would be expected to decrease, so that the result is a shift of the SWCC to higher suctions.

2.3.5 Experimental techniques to determine the suction

[Ridley and Wray] classified the suction measuring equipments into two types; those that measure directly and others that measure indirectly. With direct measurement, the

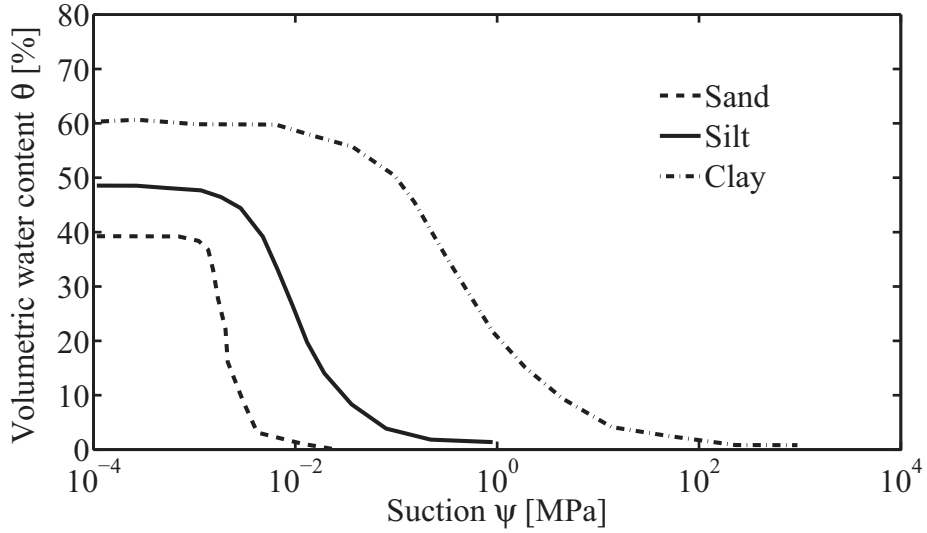

Figure 2.5: Soil-water characteristic curves for different type of soils [Reeve et al., 1973].

relevant quantity under scrutiny is determined, namely the energy of pore water or tensile stress. Meanwhile, indirect measurements are ones that measure other parameters: relative humidity, resistivity, conductivity or moisture content, which are related to suction through calibration relationships. In both cases, it is important for the research to know whether total or matrix suction is being measured. In general, if no contact between the measuring equipment and the soil water is made, the total suction in the soil is measured in the relative humidity of the ambient air within the soil. If it is assumed that the dissolved salts concentration is the same everywhere, the matrix suction is measured. In case of soil at low degrees of saturation, the soil water might drop into the finer pores and become discontinuous, in which case it is difficult to produce full contact and therefore matrix suction is measured. The following review presents the techniques which are used in current research, namely the Imperial College tensiometer and the filter paper method. For other techniques, the reader is referred to [Ridley and Wray] for a more complete review.

2.3.5.1 Imperial College Tensiometer

A tensiometer is defined as the device that directly measures the absolute negative pore water pressure in the soil water at atmospheric pore air pressure. It consists of a saturated porous ceramic filter, a reservoir of water, and the pressure measuring device. The porous ceramics filter should be in good contact with the soil water so that the water will flow between the soil and reservoir through the filter, until equilibrium between the soil water and the reservoir water is reached. A negative pressure is a suction value. The soil suction, thus transferred to the reservoir, is subsequently measured by a manometer, gauge, or electronic transducer. Matrix suction is measured by the device as long as good contact is between the tensiometer and the soil water is established. The main limitation of the conventional tensiometer is that bubble formation normally occurs when suction reaches between 60 to 100 kPa, and subsequently the suction will no longer be transmitted efficiently to the measuring device. To avoid this problem, the axis-translation technique is used. By raising the ambient air pressure, the pressure of pore water is also raised by an equal amount and becomes measurable [Hilf, 1956]. However, the disadvantage of this technique is that it is not practicable for measuring suction in the field. [Ridley and Wray] also noted that caution should be exercised in making use of this technique in the laboratory because changing the absolute water pressure may affect air coming into or out of solution, especially when the experiments involve wetting and drying processes.

The suction probe or Imperial College tensiometer was introduced by [Ridley, 1993] to avoid the problem of bubble formation, or cavitation, associated with conventional tensiometers. The suction probe can measure suctions in excess of 100 kPa for relatively long periods (e.g. $>$ 1 month). Since its initial development, the suction probe has undergone further improvements [Ridley and Burland, 1999]. To design the suction probe, some considerations should be taken into account to include the optimization of various components, namely (a) the type and the location of pressure sensor, (b) the volume of the fluid reservoir, (c) the material used to construct the tensiometer and (d) the porosity of the ceramic filter.

[Ridley and Burland, 1999] in their final design, the probe is constructed entirely from stainless steel and fitted with a high air entry (1500 kPa) ceramic filter. The very small volume of the water reservoir was designed to inhibit cavitation. If the probe has

been preconditioned carefully, the maximum suction that can be measured is normally around 1500 kPa, corresponding to the air entry value of the filter. The measurement can be finished in several weeks and the suction should not exceed around 75% of the measured air entry value of the filter. The procedure for suction probe preparation has been described by [Ridley and Burland, 1999] and should be followed carefully so that a reliable measurement can be made. The calibration of the probe is carried out in the positive pressure range and thus extrapolation is needed for the usual operation in the negative range. [Ridley, 1993] and [Tarantino and Mongiovi, 2003] showed the justification for this extrapolation experimentally.

2.3.5.2 Filter paper technique

The filter paper technique method was first used in the field of agricultural science and has since undergone subsequent improvements in testing procedures. [Ridley, 1993] provides an extensive review of these developments. In the laboratory at Imperial College, this technique is used extensively with Whatman No.42 filter papers. This technique includes placing filter papers in contact with a soil sample in an air-tight container for a period (normally around 7 days) in order that equilibrium is attained between the suctions in the papers and the sample. Then the water content of the filter papers is measured which reflects the suction using its soil-water retention relationship, i.e. the relationship between the suction and water content of the papers.
When other porous media are used, the relationship between suction and water content of the filter paper is affected by the hysteresis and direction of flow of the water. In this respect, [Ridley and Burland, 1995] noted that it different calibration curves should be used for the initially wet and initially dry filter papers. This technique is affected by the type of contact between the paper and the sample which can determine whether total or matrix suction is being measured because the technique relies on the transfer of moisture between the soil sample and the filter paper. In general, matrix suction is believed to be measured when good contact is made between the paper and the sample. When contact is not made, it is the total suction which is being measured. However, there is a transition region where it is not certain which suction is being measured, especially when the soil has a low degree of saturation and soil water retreats into the finer pores. [Ridley and Burland, 1995] noted that careful observation of the condition

of the filter paper when it is removed from the sample can give an indication of the change from matrix suction to total suction measurement because even when a contact is made, there is no guarantee that matrix suction is being measured.
[Ridley et al., 2003] also studied the effect of salt present in the soil on the equilibrium water content in the filter papers when making in-contact measurements. They noted that the equilibrium of water content between the soil and filter paper is reduced when salt is present in the soil sample. Regarding total suction measurement, since no contact between the soil and the papers is made, the transfer of moisture is only made through the vapor phase. The vapor transfer process normally takes place over a relatively long period and consequently the equilibrium time is of great importance in determining the calibration relationship.
Other factors that can affect the calibration relationship of the filter paper include the gap distance between the soil and the filter paper for non-contact measurement, and the temperature fluctuation in the laboratory. [Ridley and Burland, 1995] suggested that when using the filter paper method, it is very important to perform the calibration under conditions as near as is reasonable to expect to the conditions likely to be encountered during the subsequent tests.

2.3.6 Concept of stress state in unsaturated soil

The state of stress in the soil used to describe the mechanical behavior of a soil, e.g. volume change, collapse potential or shear strength. Two concepts have been proposed to classify the state of stress in unsaturated soil:

2.3.6.1 Single effective stress

Several studies have been carried out to find relationship between total stress, pore air pressure, and pore water pressure in order to investigate the stress of saturated and unsaturated soil within a single effective stress variable. For all types of soil (e.g. sand, silt, clay), the effective stress is used to described the mechanical behavior of soil because it is independent of the soil properties. Fundamental principles and the concept of effective stress for saturated soil (two phases: water and solids) is different compared with unsaturated soil (three phases: water, air and solids). Terzaghi [1943] suggested that in saturated soils the effective stress σ' is defined as the difference

between the total stress, σ, and the pore water pressure, u_w. The effective stress is located exclusively in the solid skeleton of the soil and is given by:

$$\sigma' = \sigma - u_w \tag{2.5}$$

In unsaturated soils the stress acts in the air phase as pore air pressure as well as matrix suction, which is defined as the difference between air pressure and water pressure. The most widely used relationship for the effective stress, σ', in unsaturated soil is as follows;

$$\sigma' = (\sigma - u_a) + \chi(u_a - u_w) \tag{2.6}$$

Where σ is the total stress, and χ is a function of degree of saturation, S_r , varying from (0-1) for (0 to 100%) of S_r, respectively. The value of χ is estimated from shearing tests, by assuming the validity of the principle of effective stress [Bishop, 1959].

2.3.6.2 Two independent stress state

Because of the limitation of the principle of single effective stress for partly saturated soils, many of the experimental results and modelling were carried out in terms of separate stress variables, namely the net stress$(\sigma - u_a)$ and the matrix suction $(u_a - u_w)$ [Bishop and Blight, 1963; Coleman, 1962]. [Fredlund and Morgenstern, 1977] noted a theoretical basis for this approach based on multiphase continuum mechanics and proposed the state of stress in unsaturated soils to be described in terms of two independent (two independent stress variables), $(\sigma - u_a)$, at the macroscopic scale and $(u_a - u_w)$ at the pore scale, to avoid the introduction of a material parameter in the effective stress equation. The variables $(\sigma - u_a)$ and the matrix suction $(u_a - u_w)$ have been by far the most widely used in the interpretation of experimental results and constitutive modeling [Wheeler and Karube, 1996]. The stress state variables are related to equilibrium conditions in the unsaturated soil and combination of the net normal stress $(\sigma - u_a)$ and matrix suction $(u_a - u_w)$ is commonly used in engineering practice. [Datcheva and Schanz, 2003] used the net stress and suction stress variables for development of a constitutive model describing the behavior of unsaturated cohesion less soils under complex loading conditions and loading history.

2.3.7 Volumetric strain of unsaturated soil

Many attempts have previously been made to describe the volume strain behavior of unsaturated soil because the classical one-dimensional theory used in saturated soils to determine the consolidation and the change in volume due to the change in effective stress with respect to pore-water pressure does not play an important role for unsaturated soils [Fredlund and Rahardjo, 1993].
[Coleman, 1962] and [Bishop and Blight, 1963] defined volumetric behavior of unsaturated soils as a function of separate stress variables, net stress, and matrix suction. [Matyas and Radhakrishna, 1968] carried out the isotropic and K_o compression tests on a silt-clay mixture and described the volumetric behavior of unsaturated soils as the state surface curve, which relates void ratio, and degree of saturation to net stress and suction. The studies of volumetric change can be divided into two parts: the first studies dealt with the volume change-stress-suction relationships for unsaturated soil [Fredlund and Pham, 2007; Ho, 1988; Khalili and Blight, 2004; Wheeler and Sivakumar, 1995].
Other studies dealt with particular topics of volume change of unsaturated soils, such as the collapsibility of soil [Jennings and Knight, 1957; Kanazawa et al., 2009; Lawton et al., 1991]. According to the state of stress, the description of the volume change behavior for unsaturated soils is classified into two approaches: the effective stress approach [Bishop, 1959] and the two independent stress state variables approach [Fredlund and Morgenstern, 1977].

2.3.7.1 Volume strain - single effective stress behavior:

Many studies have been carried out to investigate the volume strain behavior of unsaturated soil by using the single effective stress concept. The relationship between the effective stress parameter, (χ) and the degree of saturation, S_r, has been determined [Aitchison and Donald, 1956; Bishop and Blight, 1963; Bishop, 1959; Croney and Coleman, 1961; Jennings, 1962].
The studies of unsaturated soil show the effective stress parameter (χ) classified into three classes according to the state of the soil: i) fully dried state, (χ)=0; termed class 1 models, ii) saturated state, (χ) which is a function of matrix suction; termed class 2 models and iii) unsaturated condition, (χ) which is a function of the degree of satura-

tion, S_r, and suction, s, termed class 3 models. The formulations of class 2 and class 3 may be defined to satisfy the definition of the effective stress in unsaturated soils. Class 3 formulations (χ) is a function of S_r [Karube and Kawai, 2001]. [Aitchison, 1960] showed that, by making use of an idealized model of an unsaturated soil, the parameter, (χ) is given by the expression:

$$\chi = \frac{\sigma'}{s} = S_r + \frac{1}{s}\sum_{0}^{s} 0.3 * s * \Delta S_r \tag{2.7}$$

[Jennings, 1962] determined, χ by using the equation 2.6. They found that at the same void ratio of unsaturated condition, the parameter χ is equal to the ratio of net normal stress to the effective stress on the normal consolidation line (NCL) as shown in Figure 2.6.

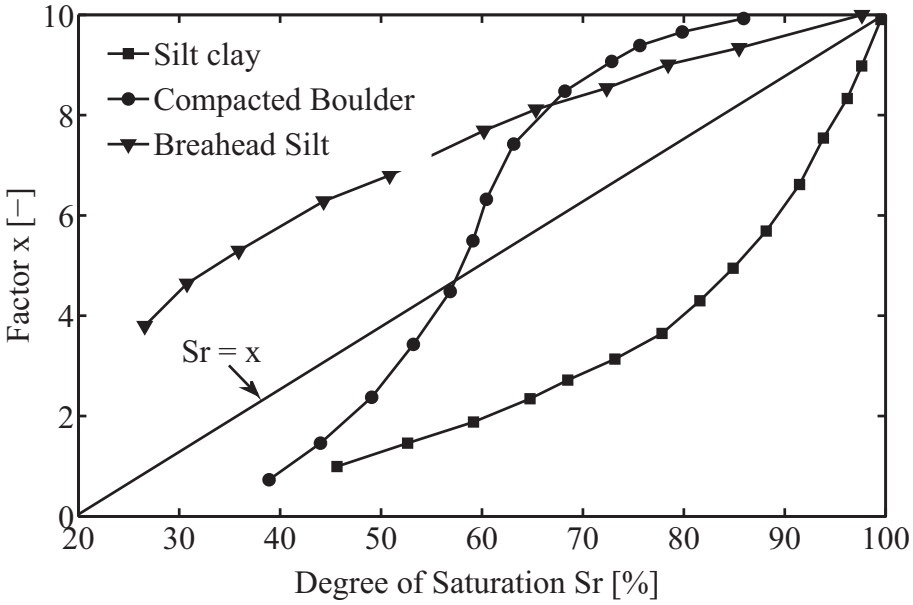

Figure 2.6: Curves of effective stress parameter and degree of saturation for various soils [Jennings, 1962].

Other studies describe volumetric strain, such as collapse within an effective stress framework by defining the state surface as a function of suction [Bolzon et al., 1996; Khalili and Blight, 2004; Khalili and Khabbaz, 1998]. [Khalili and Blight, 2004] showed that even in saturated soils, the collapse phenomenon cannot be explained

in terms of effective stress alone. [Kohgo et al., 1993] studied the micro-macro mechanical behavior of unsaturated soils. They used the suction effects to described the overall mechanical behavior of unsaturated soils and these effects were classified into two categories. Firstly, an increase in suction induces an increase in effective stresses and secondly, an increase in suction induces an increase in both yield stress and the stiffness of the soil skeleton. The effect of suction can be estimated by formulating the relationship between suction and shear strength. According to the experimental results, they found the relationship between shear strength and suction is postulated as a hyperbolic function, so the (χ) will be:

$$\chi = \begin{cases} 1 & \text{if } s \leq s_e \\ a_e(s_c - s_e)/(s^* + a_e)^2 & \text{if } s > s_e \end{cases}$$

Where s = suction; s^* = the effective suction stress (which represents the excess suction over the air-entry value); s_e= the air-entry suction; s_c= the critical suction; a_e= material parameter.

[Gallipoli et al., 2003] studied the mechanical effects in the unsaturated soil. They investigated two effects: the first effect acts on the soil skeleton and the bulk water of the soil, while the second effect is due to the stabilizing action exerted at the inter-particle contacts of the soil, provided by the water menisci. These two mechanical effects directly influence the distribution of soil water. [Khalili and Khabbaz, 1998] conducted a relationship between the effective stress parameter, χ and the suction ratio $(u_a - u_w)/(u_a - u_w)_b$, as shown in Figure 2.7. The term $(u_a - u_w)/(u_a - u_w)_b$ represents the air-entry value of soil, S_{aev}.

The equation 2.6 was used to calculate the effective stress parameter, χ and the best-fit value of the exponent γ = -0.55 is appropriate to represent the behavior of different soil types. The parameter γ can therefore be considered as a material-independent constant. The air-entry value, s_{aev} depends on the soil type and on the void ratio, though in the original formulation it was considered, for simplicity, as void ratio independent constant.

$$\chi = \begin{cases} 1 & \text{if } s < s_{aev} \\ (s/(s_{aev})^{\gamma} & \text{if } s \geq s_{aev} \end{cases}$$

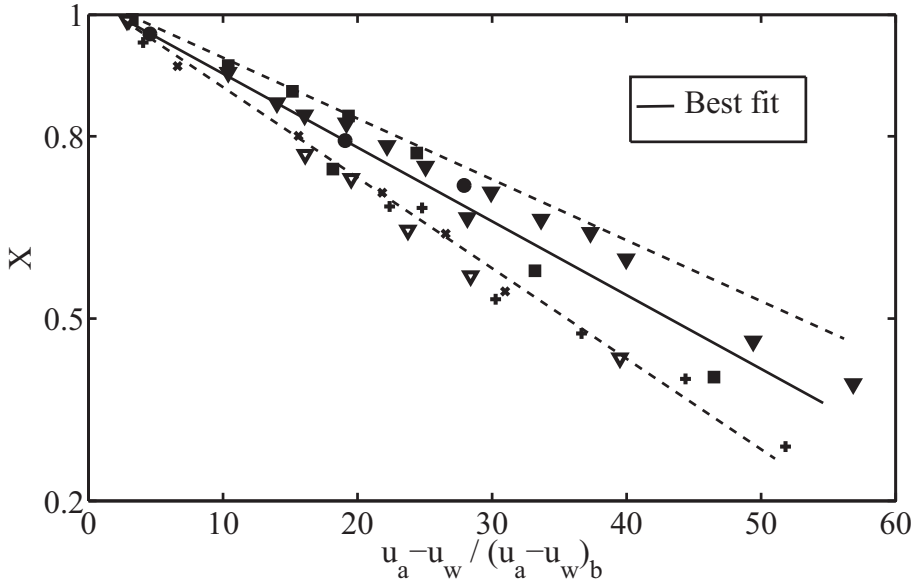

Figure 2.7: Relationship between the effective stress parameter and the suction ratio $(u_a - u_w)/(u_a - u_w)_b$ [Khalili and Khabbaz, 1998].

2.3.7.2 Volume strain - two independent stress behavior:

Volume change is commonly used to describe the deformation state variables associated with the soil structure and the water phase. The change in soil structure is represented by using the change in void ratio or porosity as a deformation. On the other hand, changes in water content can be considered as the deformation state variable for the water phase [Fredlund and Morgenstern, 1977]. The mechanical behavior of unsaturated soils is controlled by the same stress variables which control the equilibrium of the representation value of the soil and the effective stress equation 2.6, containing material parameter (the effective stress parameter, χ). Depending on this variables, the description of a stress should be independent of the material properties.
Several studies have been presented on the volume strain-stress-suction relationship using the two independent stress variables approach for unsaturated soil.
[Alonso et al., 1990] found a constitutive model in the Barcelona Basic cell test, one of the essential models for unsaturated soils, for describing the stress-strain behavior of unsaturated soils. It was noticed that the volumetric response of unsaturated soils depends not only on the initial and final stress and suction values but also on the par-

ticular path followed from the initial to the final state. For isotropic stress conditions, the model is characterized for each initial condition by two yield curves (LC; loading-collapse and SI, after suction-increase).

2.4 State of the art-stabilization of soil

The soil in its natural state at a construction site may not always be totally suitable for supporting the load of structures such as bridges, building, high ways and dams. These types of soils (e.g. collapsible soil, swelling soil and gypsum soil) are unsatisfactory in their initial condition state and can be altered by proper compaction or by the use of additives, thus making them more suitable for the structure load. Therefore, soil stabilization can be defined as any treatment used to improve the properties of soil by reducing the susceptibility to the water effect. The process produces a more stable soil and can be performed in the field or applied to the soil before applying the load or prior to construction.
[Das, 1984] showed that the purpose of improving soil is usually the following:

1. To reduce the settlement of structures.
2. To reduce the collapse potential, shrinkage and swelling characteristics of soils.
3. To increase the safety factor against possible slope failure of embankments and earth dams.
4. To improve the shear strength of soil and thus increase the bearing capacity of shallow foundations.

2.4.1 Common methods of Soil Stabilization

Several methods were used and performed in the field to control the problems of soils. The modification of soil properties may be done in number of ways as summarized by [Bowles, 1984]:

1. Mechanical method (compaction): This is usually the cheapest method of improving site soil.

2. Precompression method: This method is primarily employed to reduce future settlement but may also be used to increase shear strength.

3. Drainage using sand blankets and drains: This is used to speed up settlements under preloading but may also increase shear strength.

4. Densification using vibratory equipment: This is particularly used in sand, silty sand and gravelly sand deposits.

5. Foundation grouting: Grouting is a technique of inserting some kinds of stabilizing agents into the soil mass under pressure.

6. Soil reinforcement by the usage of geotextiles.

7. Soil stabilization by Admixtures: Admixtures are occasionally used to stabilize soils in the field particularly fine grained soils. The most common of these admixtures are cement lime, fly ash, and asphalt.

In the following sections, cement, lime and fly ash stabilize are discussed in more detail.

2.4.2 Cement stabilized

There are specifically three stabilization techniques that are more sophisticated than the rest. These are cement, lime and bituminous stabilization. Out of these three, cement stabilization is by far the most common cement stabilization is used widely for road construction. A major use of cement stabilization on secondary roads in the United States is for the salvaging of old pavements and gravel surfaces. This technique is often applied also in street or sub-foundation constructions where curb lines are firmly established and there is a need for strengthening the pavement without the addition of excessive amount of pavement, which might destroy drainage to the curb and gutter section [Yoder and Witczak, 1975]. Soil cement also has properties that are valuable for other applications such as the building of water retaining structures. This takes advantage of the effect the cement treatment has on the soils permeability. These are a few of the uses for cement stabilization. Uses that take full advantage of the effects the added cement has on soils.

Cement stabilization can be used on all soil types, except organic soils, to increase the soil strength and bearing capacity increase durability to wet/dry cycles and decrease the soils permeability by bonding soil particles together. The addition of even small quantities of cement, up to 2 percent, will modify the properties of the soil; whereas large amounts will radically alter the properties clean gravel with 5 to 10 percent of cement will behave almost like concrete [Ingles and Metcalf, 1973].

[Al-Rawasa et al., 2005], studied Al-Khod (town in northern Oman) expansive soil was stabilized using lime, cement, combinations of lime and cement, Sarooj (artificial pozzolan) and heat treatment. Initially, the chemical and physical properties of the untreated soil were determined. Then the soil was mixed with lime, cement and Sarooj (produced from Bilad Seet, a town in northern Oman) at 3%, 6% and 9% by dry weight of soil. Fixed percentages of lime (3% and 5%), plus different percentages of cement were also mixed with the soil. The physical results of the treated samples were determined. The untreated soil values were used as control points for comparison purposes. It was found that with the addition of 6% lime, both the swell percent and swell pressure reduced to zero. Heat treatment reduced swelling potential to zero. The use of lime showed superior results when compared with the other stabilizers.

[Khaled and Mehedy, 2003] studied the mechanical behavior of a soil-cement-fly ash composite, reinforced with recycled plastic strips (high-density polyethylene) that were obtained from postconsumer milk and water containers. The specific objectives of the study were to evaluate the compressive, split tensile and flexural strength characteristics of the material, and to determine the effectiveness of recycled plastic strips in enhancing the toughness characteristics of the composite. Experimental data show that the soil-cement matrix stabilized with 4% to 10% by weight of fly ash and reinforced with 0.25% to 0.5% (by weight) plastic strips (with lengths of 19 mm or 38 mm) can achieve a maximum compressive strength of 7000 kPa, a split tensile strength of 1000 kPa, and a flexural strength of 1200 kPa. These ranges in strength values are suitable for a high-quality stabilized base course for a highway pavement.

[Osinubi et al., 2011] studied the improvement of Black Cotton Soil with Ordinary Portland Cement - Locust Bean Waste Ash Blend (LBWA). This group of soils is usually very poor for engineering use. Ordinary Portland cement (OPC) / locust bean waste ash (LBWA) blend in stepped concentration of 0, 2, 4, 6 and 8% each by dry weight of soil, was used to treat the soil. Compaction was carried out using British

Standard light (BSL) energy and the three criteria for the evaluation of strength (i.e., UCS, CBR and Durability) were considered. The UCS values of specimens treated with 6% OPC / 6% LBWA increased from 178, 381 and 760 $[kN/m^2]$ for the natural soil to 986, 1326 and 1348 $[kN/m^2]$ when cured for 7, 14 and 28 days, respectively. The CBR value of 5% of the natural soil increased and peaked at 42% for 6% OPC / 6% LBWA treatment, while the durability in terms of resistance to loss in strength increased from 13% for natural soil to 58%. The strength and durability values also increased with curing ages, thus indicating that the blend has potential for a time dependent increase in strength that will reduce the quantity of cement needed for the construction of low volume roads over the expansive soil.

A laboratory study was carried out by [Gerald and Shahriar, 2000] to evaluate the effect of cement kiln dust (CKD) as a soil stabilizer. The study revealed that increases in the unconfined compressive strength (UCS) of soil occurred with the addition of CKD. Increases in UCS were inversely proportional to the plasticity index (PI) of the untreated soil. Significant PI reductions occurred with CKD treatment, particularly for high PI soils. Measurements indicate that the change in pH of soil as a function of CKD content is related to the PI of the untreated soil, and good correlation between pH response and performance of CKD treated soil was observed.

[Bahar et al., 2004] investigated a stabilized soil by either mechanical means such as compaction and vibration and/or chemical stabilization by cement. The soil used was characterized by its grading curve and chemical composition. Compaction was either applied statically or dynamically by a drop weight method. Sand was mixed with different quantities of cement. The effect of each method of stabilization on shrinkage, compressive strength, splitting tensile strength and water resistance are briefly reported. The experimental results showed that the best method of stabilization of the soil investigated, which gives a good compressive strength and a better durability at a reasonable cost, could be a combination of a mechanical compaction and chemical stabilisation by cement or sand and cement up to a certain level.

[Karim, 2008] studied the effect of adding cement with (1, 2, 3%) on the properties of collapsible gypsum soil with a gypsum content of about 32%. He found that increasing the cement percentage causes a significant decrease in collapse potential because of the increases in connection between the particles and decrease in void ratio in soil structure as summarized in Table 2.2.

Table 2.2: Result of collapsible gypsum soil before and after additional cement [Karim, 2008]

Soil types	Cc	e_0 [-]	Collapse potential C_p [%]
Natural soil with gypsum	0.28	0.60	30
Natural soil with 1% Cement	0.26	0.56	20
Natural soil with 2% Cement	0.24	0.54	15
Natural soil with 3% Cement	0.22	0.52	15

[Sreekrishnavilasam et al., 2007] evaluated two fresh and one landfilled cement kiln dusts (CKD) for soil treatment. Only one fresh CKD (with free lime in the 2-5% range) was found to be sufficiently reactive and showed potential for use in soil stabilization. The results for the other fresh and the landfilled (both with only traces of free lime) suggest that these materials may be used for treating wet subgrades or waterlogged areas. In presence of 10-20% (by dry mass of the soil) of these, it became possible to compact soils outside their normal compaction range, and the further addition of 1% Portland cement produced mixtures of considerable strength. The results obtained highlight the importance of knowing the chemical composition of each batch collected and suggest that changes in plastic limit and pH may provide insights into the suitability of a particular CKD for soil stabilization.

[Suat and Seracettin, 2010] investigated the effects of four different additives, such as cement, lime, fly ash and silica fume on the CEC, pH, zeta potential, and swelling pressure of three expansive soils, which were researched experimentally under laboratory conditions. The test results indicated that the additives lime, fly ash, and silica fume reduced the cation exchange capacity of the expansive soils, whereas cement slightly increased the cation exchange capacity for all the samples. On the other hand, the values of the zeta potential changed slightly for all the samples with the additives. The pH values of the samples increased with increases in the percentage of cement and lime additives. However, the addition of fly ash and silica fume slightly reduced the pH values with increasing percentages of the additives in expansive soils. It could be explained from the test results that the swelling pressures were decreased by increasing the additive contents given the decreasing CEC values of all the samples, except cement.

[Al-Zoubi, 2008] investigated the influence of cement addition on the behavior of an expansive soil from Jordan. A wide range of cement content varying from 0 to 25%

by dry weight of soil was used. The study shows that the liquid limit of the treated soil decreases drastically for cement content of up to 6%, then sharply increases for cement content in the range of 6 to 10%, after which the liquid limit becomes practically constant. The study showed also that the swell potential of the treated soil decreases drastically for cement content of up to 4%, then sharply increases for cement content in the range of 4 to 6%, after which the swell potential may decrease or may become constant depending on the initial water content. The undrained shear strength was generally observed to increase with the increase of cement content from 0 to 20%; however, the maximum rate of this increase was observed to be in the range of cement content from 6 to 10%. The results are interpreted in terms of cation exchange, flocculation and pozzolanic reactions that are associated with cement addition to soil.

2.4.3 Lime stabilized

Stabilization of soils with hydrated lime is broadly similar to cement stabilization in that similar criteria and testing and construction techniques are employed. It differs, however, in two important respects: first, it is applicable to far heavier, clayey soils, and is less suitable for granular materials; and second, it is used more widely as a construction expedient, that is, to prepare a soil for further treatment or to render a sufficient improvement to support construction traffic. As was mentioned for cement stabilization, lime is commonly used to modify clay soil in preparation for cement stabilization, although, this is not always the case. Lime by itself is a very good soil stabilizer. It is most effective, and may be more effective than cement, in clayey gravels, and is particularly suited to the stabilization of heavy clay soils [Ingles and Metcalf, 1973]. Unless of course the soil is highly organic, in which case lime stabilization is rendered fairly ineffective. Also, lime does not work very well in clean sands or gravels. It is important that the type of lime to be used is clearly defined. It is unfortunate that the term lime is used to describe calcium carbonate (agriculture lime), calcium hydroxide (slaked or hydrated lime) and calcium oxide (quicklime). In general engineering practice, the term lime means hydrated lime. Lime modification of soil has been used for three main purposes: to reduce the plasticity of an otherwise acceptable mechanically stable material, to improve the workability of a soil and its resistance to deflocculating and erosion, and to produce a rapid increase in strength in wet clay soils as a con-

struction expedient [Ingles and Metcalf, 1973]. These changes are the result of several reactions. The first of these reactions is alteration of the water film surrounding the clay minerals. The strength of the linkage between two clay minerals is dependent on the charge, size, and hydration of attracted ions. The calcium ion (lime) is divalent and serves to bind the soil particles close together. This in turn decreases plasticity and results in a more open and granular structure. The second process by which the lime changes a soil is that of flocculation of the soil particles. The amount of lime ordinarily used in construction (5 to 10 percent) results in a concentration of calcium ion greater than that actually needed. The third process by which the lime affects soil is reaction of lime with soil components to form new chemicals [Yoder and Witczak, 1975].
Application of lime is similar to that for cement. The soil will be scarified and pulverized, the lime will be applied to the soil, and then the two will be mixed. After the mixture, water will be added. The amount of water required is dictated by compaction. The lime-soil mixture is then compacted. To obtain satisfactory soil-lime mixtures adequate pulverization and mixing must be achieved. For heavy clay soils two stage pulverization and mixing may be required while for other soils one stage mixing and pulverization may be satisfactory. This difference is due primarily to the fact that the heavy clays are more difficult to break down [Broms and Boman, 1987].
Several studies were carried out to know the behavior and the mechanical properties when added a lime as a stabilized material.
[AL-Obaydi, 2003], investigated the effect of lime stabilization of the properties of gypseous soils. He found that decrease of the coefficient of permeability (k) with increase of lime percent and increase in compressive strength (qu).
[Al-Janabi, 1997], studied the compressibility of gypseous soils stabilized with lime in north Iraq (Samara and Al-Nibaee city). He found that:

1. Increase (qu) with increase in lime content to a max. (qu) at optimum lime content then decrease.

2. Increase (k) then decrease with optimum lime content.

3. Diminished of (C_p) by lime stabilization.

[Jagadish and Pradip, 2010], studied the effects of lime-stabilized soil cushion on the strength behavior of expansive soil. Unconfined compression tests and CBR tests

were conducted on both expansive soil alone and expansive soil cushioned with lime-stabilized non-expansive cohesive soil. Lime contents of 2, 4, 6, 8 and 10% by dry weight of cohesive non-swelling soil was used in the stabilized soil cushion. Both expansive soil and lime stabilized soil cushion were compacted to Standard Proctors optimum condition with thickness ratio 2:1. Tests on cushioned expansive soils were conducted at different curing and soaking periods i.e., 7, 14, 28 and 56 days. The test results revealed that maximum increase in strength was achieved after 14 days of curing or soaking period with 8% of lime content.

[Bell, 1996] analyzed clay soil stabilized by the addition of small percentages by weight of lime, thereby enhancing many of the engineering properties of the soil and producing an improved construction material. Three types of minerals in clay, kaolinite, montmorillonite and quartz, were subjected to a series of tests. As lime stabilization is most often used in relation to road construction, the tests were chosen with this in mind. Till and laminated clay were treated in similar fashion. The results showed that with the addition of lime, the plasticity of montmorillonite was reduced whilst that of kaolinite and quartz was increased somewhat. The addition of lime to the till had little influence on its plasticity but a significant reduction occurred in that of the laminated clay. All materials experienced an increase in their optimum moisture content and a decrease in their maximum dry density, as well as enhanced California bearing ratio, on the addition of lime. Some notable increases in strength and Youngs Modulus occurred in these materials when they were treated with lime. The length of curing time and the temperature at which curing took place had an important influence on the amount of strength developed.

[Zhang and Xing, 2002] studied the effects of lime and fly ash on the geotechnical characteristics of expansive soil. Lime and fly ash were added to the expansive soil at 4% - 6% and 40% - 50% by dry weight of soil, respectively. Testing specimens were determined and examined in chemical composition, grain size distribution, consistency limits, compaction, CBR, free swell and swell capacity. The effect of lime and fly ash addition on reducing the swelling potential of an expansive soil is presented. It is revealed that a change of expansive soil texture takes place when lime and fly ash are mixed with expansive soil. The plastic limit increases by mixing lime and the liquid limit decreases by mixing fly ash, which decreases the plasticity index. As the amount of lime and fly ash is increased, there is an apparent reduction in maximum dry density,

free swell and swelling capacity under 50 kPa pressure, and a corresponding increase in the percentage of coarse particles, optimum moisture content and CBR value. Based on the results, it can be concluded that the expansive soil can be successfully stabilized by lime and fly ash.

[Khattab and AL-Taie, 2006] studied the behavior of the soil water characteristic curve SWCC for three expansive soils. The effect of lime treatment was also studied on SWCC. Three types of expansive soils from Mosul city in Iraq (termed D, W and H) were selected with different swelling pressure. Soil type D had the highest swelling pressure. SWCCs were determined with range 0-1000000 kPa. The effect of lime 2, 4, 6%, compaction and curing time (up to 150 days) were studied on statically compacted soil samples. A computer package was prepared using Fortran Station based on the Fredlund Xing modeling equation [Fredlund and Xing, 1994]. The program calculated the best equation parameters (i.e. a, m, n). It was found that the water holding capacity increases with lime addition of 0 to 6%. They explained that higher lime percentages would cause more pozzolanic products and air-entry values and residual suction would increase with greater lime percentages. The boundary effect stage was also expanded as summarized in Table 2.3. Usually, lime addition causes a needle-like interlocking metalline structure, but the crystallization of pozzolanic products would block this opened structure [Litte, 1995].

Table 2.3: SWCC parameters [Khattab and AL-Taie, 2006]

Lime [%]	Air-Entry value (θ_a)	Residual suction (ψ_r)
0	40.470	18000
2	40.409	24000
4	42.563	25000
6	43.35	40000

[Yucel et al., 2007] investigated the impact of cyclic wetting and drying on the swelling behavior of lime-stabilized clayey soils. Swelling potential and swelling pressure tests were carried out on soil mixtures with various amounts of kaolinite, bentonite clays, and on a high plasticity clayey soil sample. The tests were repeated after the addition of lime to the lime-treated samples in different preparation. In each cycle the tested samples were allowed to air dry to their initial water content thus shrinking to their initial height, which is called the partial shrinkage method. The results showed that

the initial beneficial effect of lime stabilization was lost after the first cycle and the swelling potential increased in the subsequent cycles. On the other hand, the swelling potential and the swelling pressure of the untreated soil samples started decreasing after the first cycle and they reached equilibrium after the fourth cycle.

An attempt have been made by [Rajasekaran and Narasimha, 2002] to investigate the lime induced permeability changes in the permeability and engineering behavior of different lime column treated soil systems. Lime column treated marine clay shows an increase in permeability up to a maximum value of 15-18 times that of untreated soil with time. The shear strength of the treated soil systems show an increment of up to 8-10 times that of untreated soil within a period of 30-45 days curing. In the case of lime injection systems, the permeability has been increased up to 10-15 times that of untreated soil, whereas the strength of the soil has been higher by 8-10 times that of untreated soil. Furthermore, consolidation tests show a reduction in the compressibility of up to 1/2- 1/3 of the original values. The test results revealed that both lime column and injection techniques could be used to improve the behavior of underwater marine clay deposits.

[Al-Khashab and Al-Hayalee, 2008] studied the possibility of the stabilization of expansive clayey soil pre-treated by lime, with an emulsified asphalt addition. Soil from Mosul was chosen, which is classified as medium to high expansiveness in its natural state. The pre-treated soil was treated with lime addition (0.5, 1.0, and 1.5% by weight). After a short period, emulsified asphalt was added with different percentages namely (2, 4, 6 and 8%) by weight, for optimum percentages of an emulsified asphalt to give the most useful stabilization results. The test result of lime addition alone showed that there was a considerable reduction in soil plasticity, 1.5% of lime addition converted the clayey soil towards non-plastic types. The addition of emulsified asphalt to the mixture caused a slight increase in plasticity but their values on the whole remained below the value of the natural soil. The specific gravity decreased with the emulsified asphalt addition along with a general reduction, compatible with the increase in the optimum moisture contents. The absorption values of the treated soil with the emulsified asphalt showed consequent reduction compared with the original one. A significant reduction in swelling pressure and swelling percent were obtained, as well as an improvement in some values of the unconfined compressive strength which were realized at low percentages of emulsified asphalt addition, compatible with reduction

in values of high percent additions.

2.4.4 Fly ash stabilized

Fly ash is one of the many types of solid waste product which it is created by the firing of coal. It is expelled from the boiler by flue gases and extracted by electrostatic precipitators or cyclone separators and filter bags. Its appearance is generally that of a light to dark-gray powder of predominantly silt size [Chu and Kao, 1993].
Fly ash is created in large amounts in Germany (around than 65 million metric tons per year) as a waste product of burning coal in electric power plants. The benefit for using fly ash as stabilization material in soil has increased significantly in many countries due to the increased availability and the introduction of new environmental regulation that encourage the use of fly ash in geotechnical applications since it is environmentally safe [Ferguson, 1993].
Fly ash has been called a high-energy-based material. [ASTMC618, 2003] classified fly as in two classes: Class F and Class C fly ash. Class F fly ash is normally produced from burning anthracite or bituminous coal and contains small amounts of lime. This fly ash has pozzolanic properties and by itself possesses little or no cementitious value, but in the presence of moisture, reacts chemically with lime at ordinary temperatures to form cementitious compounds. Class C fly ash is normally produced from burning sub bituminous or lignite coal; and usually contains a significant amount of lime along with pozzolanic materials. This type of fly ash may show both pozzolanic and cementitious properties. In general, it can be referred to in these two classes, depending on the amount of lime, as low-lime (Class F) and high-lime (Class C) fly ash. Fly ash with a high lime content is usually recycled as an engineering material to take advantage of its pozzolanic characteristics. This type of fly ash provides application opportunities where no other activators would be required and thus offers more economical alternatives for a wide range of stabilization applications. High-lime fly ashes have been used in earthwork applications to improve the mechanical properties of soils for more than 20 years. Fly ash particles are generally spherical in shape and range in size from 0.5 μm to 100 μm. They consist mostly of silicon dioxide (SiO_2), which is present in two forms: amorphous, which is rounded and smooth, and crystalline, which is sharp,

pointed and hazardous; aluminum oxide (Al_2O_3) and iron oxide (Fe_2O_3). Fly ashes are generally highly heterogeneous, consisting of a mixture of glassy particles with various identifiable crystalline phases such as quartz, mullite, and various iron oxides [Inan and Sezer, 2003].

2.4.5 Chemical reaction of fly ash stabilization

Stabilization of soils using fly ash has been in practice for a considerable time. When added to reactive soil, two main reaction types occur:

1. Short term reaction which include cation exchange, flocculation, agglomeration and carbonation.

2. Long term reaction includes pozzolanic reaction.

The hydration of fly ash releases calcium ions, which in turn replaces original cations (most commonly sodium ions) in clay particles. This process is known as *cationexchange*. The free calcium of fly ash exchanges with the adsorbed cations of the clay mineral, which results in a reduction in the size of the diffused water layer surrounding the clay particles. This reduction in the diffused water layer allows the clay particles to come closer to one another, causing flocculation and agglomeration of the clay particles. Flocculation also causes a decrease in soil plasticity characteristics. Overall the flocculation and agglomeration of fly ash stabilization results in a soil that is more readily workable and mixable. Practically all fine grained soils display cation exchange and flocculationagglomeration reactions when treated with fly ash in the presence of water. The reactions occur quite rapidly when fly ash is added to soil. Depending on the availability of various types of cations in the pore fluid, cation replacement can take place as shown in Figure 2.8.
The cations are arranged in the order of their replacing power according to Lyotropic series $Li^{+1} < Na^{+1} < H^{+1} < K^{+1} < NH^{+4} < Mg^{+2} < Ca^{+2} < Al^{+3}$. In general, higher valency cations replace those of lower valency, and any cation will tend to replace the left of it. When fly ash carbonation reactions occur in soil mixture, fly ash reacts with carbon dioxide to form calcium carbonate in an undesirable reaction instead of forming cementations CAHs and CSHs. The reactions between fly ash, water, soil silica, and

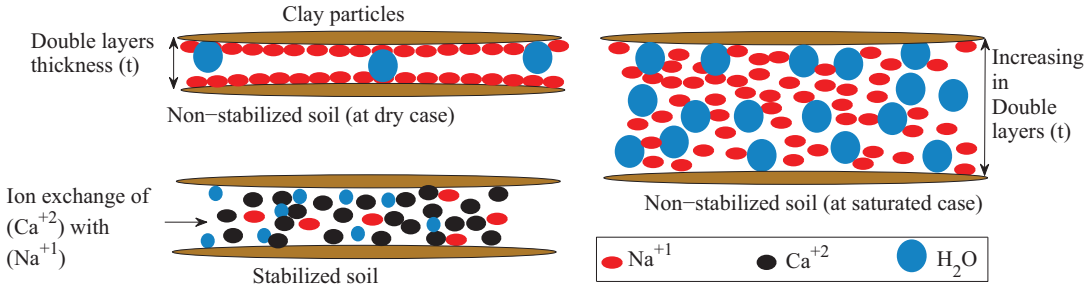

Figure 2.8: Formation of a diffused water layer around clay particle, modified after [Little, 1987].

alumina that form various cementing type materials are referred to as pozzolanic reactions. The cementing products are calcium-silicate-hydrates and calcium-aluminate-hydrates. The basic pozzolanic reaction is given by:

$$\mathrm{Ca(OH)_2} \rightarrow Ca^{++} + 2(OH)^{-}$$
$$Ca^{++} + OH^{-} + SiO_2 \text{ (soluble clay silica)} \rightarrow \text{calcium-silicate-hydrate (CSH)}$$
$$Ca^{++} + OH^{-} + Al_2O_3 \text{ (soluble clay alumina)} \rightarrow \text{calcium-aluminate-hydrate(CAH)}$$

Possible sources of silica and alumina in typical fine-grained soils include clay minerals, quartz, feldspars, micas, and other similar silicate or alumino-silicate minerals, either crystalline or amorphous in nature. Strength gain in soils using fly ash as stabilization occurs through the same type of pozzolanic reactions found when using cement stabilization. Both fly ash and cement contain calcium required for the pozzolanic reactions to occur. Similar to fly ash stabilization, carbonation can also occur when using cement stabilization when cement is exposed to air. The cement will react with carbon dioxide from the atmosphere to produce a relatively insoluble calcium carbonate [Rogers and Glendinning, 2000].

2.4.6 Stabilization of collapsible soil

Collapsible soils are widely distributed in many regions in world and are recognized as one of the problematic soils. Therefore, during recent years, many studies have been carried out to improve these soil characteristics. The following explains some of these studies.

[Ferguson, 1993] examined soil stabilization in a racetrack with Class C fly ash without

any other activator, which showed encouraging results. Improved engineering properties of fly-ash-stabilized soil were reported by [Kaniraj and Havanagi, 1999] conducting research on fly-ash-stabilized sub-base along with nine other stabilization alternatives, such as those using a sub-base layer consisting of foundry sand, foundry slag and bottom ash or geosynthetics reinforcement. The performance of Class C fly-ash stabilized sub-base seemed to be equal to or better than other stabilization alternatives. [Alper et al., 2004] studied the effect of using fly ash with very high lime content on properties of a soft clay sub-grade in a military zone in Izmir, Turkey. The soil was replaced with 0%, 5%, 10%, 15% and 20% of this fly ash. The samples were prepared by mixing fly ash with soil at optimum water content determined by a standard proctor test. The unconfined compressive strength and shear strength parameters, cohesion and internal friction angle, were determined after 1, 7, 28 and 90 days. They found that the addition of fly ash improved the properties of the soil and these improvements, enhanced with increasing fly-ash content, were attributed to the pozzolanic reaction and pore refinement effect of fly ash as well as its high free-lime content.
[Kolias et al., 2004] investigated the use of high calcium fly ash and cement in stabilizing fine-grained clayey soils. The percent of fly ash used was 5%, 10% and 20% by mass of the dry soil, and of cement (combined with fly ash) 2% and 4%. Some additional mixes are prepared with only cement for comparative purposes although it was anticipated that the results would be poor due to lack of homogeneity, which is inevitable when mixing plastic fine-grained soils with cement. These results show that the clayey soils could potentially benefit from stabilization with high calcium fly ash, but the properties of the stabilized soil depends on the amount of stabilizing agent, the type of soil and the curing time. Furthermore, use of a significant amount of fly ash leads to a denser and more stable structure of the soils and this is due to the formation of hydraulic products during the curing of clay containing high calcium fly ash as a stabilizing agent, as well as the addition of cement, which provides better setting and hardening. The combination of these two binders can increase the early and the final strength of the stabilized material. The free (CaO) of fly ash reacts with the clay constituents (SiO_2) and the other aluminum silicates leading to the formation of tobermorites and calcium aluminum silicate hydrates as well.
[Shenbaga and Vasant, 1999] studied the unconfined compressive strength of cement stabilized fly ash-soil mixtures. The fly ash collected from an electrostatic precipitator

of the Rajghat thermal power station in New Delhi, India, and German fly ash from a chemical manufacturing industry, Baumineral (near Bochum, Germany) were used. They were mixed with the locally available silt soils and ordinary Portland cement in different proportions (3-9%). The samples were prepared as cylindrical and cured for different period. It was found that:

1. The modulus and unconfined compressive strength increase as cement and fly ash content increases.

2. The water content of a fly ash-soil mixture depends on the curing time and cement content. The water content decreases as curing time and cement content increase. The influence of cement content is more pronounced than that of the curing time.

[Durand et al., 2012] investigated the soil-water characteristic curve (SWCC) of collapsing silty clay with and without the addition of cement and fly ash from coal combustion. The material analyzed is a mixture of sand (30%), silt (32%), and clay (38%) collected from the Guadalquivir basin in the province of Seville (Spain). Class F fly ash and cement were used to improve the properties of the soils. Three types of soil named IN untreated 100% initial mixture, IN-CEM Treated with cement 98% Initial Mixture + 2% cement and IN-ASH Treated with fly ash 98% initial mixture + 2% fly ash. SWCC curves of drying and wetting paths for samples type IN, IN-CEM and IN-ASH were conducted in accordance with equation by [Fredlund and Xing, 1994]. They showed that in the drying paths, the two treated samples display very similar behavior and they reduce saturation humidity, increase the air entry value, reduce residual moisture, and do not generate a uniform distribution of pore size. In the wetting paths, cement and fly ash treatments reduce the soil saturation humidity, with cement leading to an even greater loss of moisture in the hydration and setting processes. The air entry value of the samples IN-CEM is much greater than that of samples IN-ASH. The behavior of this sample differs very little from the behavior of the sample without treatment. For both wetting and drying paths, treatment with cement has proven to provide the greatest reduction in the size and number of free pores, a fact that is borne out by the increase in the air entry value in the sample IN-CEM when compared with samples IN and IN-ASH.
[Edil et al., 2002] conducted a field evaluation with fly ash of several alternatives

for construction over soft sub-grade soils. By-products such as fly ash, bottom ash, foundry slag, and foundry sand were used. A class C fly ash was used for one test section. Soil stiffness gauge (SSG) and a dynamic cone penetrometer (DCP) were tested in the field. The results were determined before and after fly ash placement by testing undisturbed samples in the laboratory. The results showed that 10% fly ash (on the basis of dry weight) was sufficient to provide the unconfined compression strength necessary for construction on the sub-grade. Unconfined compressive strength, soil stiffness, and dynamic cone penetration of native soil before fly ash placement ranged between 100 - 150 kPa, 4 - 8 MPa and 30 - 90 mm/blow, respectively. After fly ash addition, the unconfined compressive strength reached as high as 540 kPa, the stiffness ranged from 10 to 18 MPa, and the Dynamic Penetration Index (DPI) was less variable and ranged between 10 and 20 mm/blow. CBR of 32% was reported for the stabilized sub-grade, which is rated as good for sub-base highway construction. CBR of the untreated sub-grade was 3%, which is rated as very poor.

[Acosta, 2002] evaluate the properties of a sub-grade stabilizer with the self-cementing fly ashes for Wisconsin soils. Laboratory testing was carried out to evaluate the estimated properties of fly ash alone as well as to evaluate how different fly ashes can improve the engineering properties of a range of soft sub-grade soil from different parts of Wisconsin. Seven soils and four fly ashes were considered for the study. Soil samples were prepared with 0, 10, 18, and 30% fly ash content and compacted at different soil water content (optimum water content, 7% wet of optimum water content approximate natural water content of the soil, and a very wet conditions 9 to 18% wet of optimum water content). California bearing ratio tests, resilient modulus tests, and unconfined compressive strength tests were carried out. The soils selected represented poor sub-grade conditions with CBR ranging between 0 and 5 in their natural condition. A substantial increase in the CBR was achieved when soils were mixed with fly ash. The results show the specimens with 18% fly ash content and compacted at the optimum water content provided the best improvement, with CBR ranging from 20 to 56. The specimens with 18% fly ash which compacted at 7% wet of optimum water content produced a significant improvement compared to the untreated soils, with CBR ranging from 15 to 31 (approximately an average CBR gain of 8 times). On the other hand, the specimens prepared with 18% fly ash and compacted in very wet condition generated less improvement (CBR ranging from 8 to 15). Soil-fly ash mixtures pre-

pared with 18% fly ash content and compacted at 7% wet of optimum water content had similar or higher modulus than untreated specimens compacted at optimum water content. Resilient modulus of specimens compacted in significantly wet conditions, in general, had lower modulus compared to the specimen compacted at optimum water content. The resilient modulus increased with increasing curing time. The resilient modulus of specimens prepared at 18% fly ash content and compacted at 7% wet of optimum water content was 10 to 40% higher after 28 days of curing, relative to that of 14 days curing. Unconfined compressive strength of the soil-fly ash mixtures increased with increasing fly ash content. Soil-fly ash specimens prepared with 10 and 18% fly ash content and compacted 7% wet of optimum water content had unconfined compressive strength that were 3 and 4 times higher than the original untreated soil specimen compacted at 7% wet of optimum water content. CBR and resilient modulus data was used for a flexible pavement design. Data developed from stabilized soils showed that a reduction of approximately 40% in the base thickness could be achieved when 18% fly ash is used to stabilize a soft sub-grade.

[Senol et al., 2002] studied the use of self-cementing class C fly ash for the stabilization of soft sub-grade of a city street in Cross Plains, Wisconsin, USA. Both strength and modulus based approaches were applied to estimate the optimum mix design and to determine the thickness of the stabilized layer. Stabilized soil samples were prepared by mixing fly ash at three different contents (12, 16, and 20%) with varying water contents. Unconfined compression tests after 7 days of curing were used to measure water content strength relationship. The results proved that the mechanical properties, such as unconfined compressive strength, CBR, and resilient modulus increase substantially after fly ash stabilization. The stabilization process is construction sensitive and requires strict control of moisture content. The impact of compaction delay that commonly occurs in field construction, was evaluated, one set of the samples was compacted just after mixing with water, while the other set after two hours. The results showed that the loss of strength due to the compaction delay is significant and, therefore, must be considered in design and construction. CBR and resilient modulus tests were conducted and used to determine the thickness of the stabilized layer in pavement design.

[Thomas and White, 2003] investigated the self-cementing fly ashes (from eight different fly ash sources) to treat and stabilize five different soil types (ranging from ML to

CH) in Iowa for road construction applications. They determine various geotechnical properties (under different curing conditions) such as compaction, qu-value, wet/dry and freeze/thaw durability, curing time effect, and others. They noted that Iowa self-cementing fly ashes can be an effective means of stabilizing Iowa soil. Unconfined compressive strength, strength gain, and CBR-value of stabilized soils increased especially with curing time. Soil-fly ash mixtures cured under freezing condition and soaked in water slaked and were unable to be tested for strength. They also noticed that stabilized paleosol exhibited an increase in the freeze/thaw durability when tested according to [ASTMC593, 2001], but stabilized Turin loess failed the test.

2.5 State of the art-Non-invasive experimental soil analysis methods

2.5.1 Seismic measurements

2.5.1.1 Definition of Small-Strain shear stiffness G_{max}

Shear modulus is usually defined as the secant modulus by the extreme points on the hysteresis loop. The shear modulus depends on the strain value for which the hysteresis loop is determined and at a low strain value the shear modulus is high and decreases as the strain value increases. The shear modulus must be determined as a function of the strain changing in a soil specimen or soil deposit [Seed et al., 1984]. The slope line between the origin point to this curve corresponds to the *maximum shear modulus* G_{max} or G_0, which is also called *initial shear modulus* or *small-strain shear stiffness*. The stress-strain relationship in the small-strain is considered a line, therefore G_{max} is the shear modulus in the small-strain range.

The shear modulus begins to drop to a lower value after the strain amplitude exceeds a certain threshold until it reaches a significantly smaller value at large strains. The modulus ratio G/G_{max}, or *modulus reduction curve* is defined as the variation of shear modulus with strain (see Figure 2.9). This threshold is called the *linear elastic threshold strain* and represents a boundary between two types of soil behavior. The soil characteristics are changed according to shear strain amplitude. When it is smaller than the *l*inear elastic threshold strain, the particles are not displaced with respect to

each other and thus there is essentially no permanent microstructural change, residual cyclic pore water pressure essentially does not develop even for saturated undrained cases as well as the no volume change during strain. When shear strain value is higher than the *l*inear elastic threshold strain, particles are permanently displaced with respect to each other and thus the microstructure and the soil stiffness are changed. The value of this threshold varies according to plasticity and other factors, and ranges between 10^{-3}% and 10^{-2}% [Hsu and Vucetic, 2004; Ishihara, 1996; Vucetic, 1995]. Figure 2.9 shows the reduction of stiffness with increment of strain [Atkinson and Sallfors, 1991; Mair, 1993].

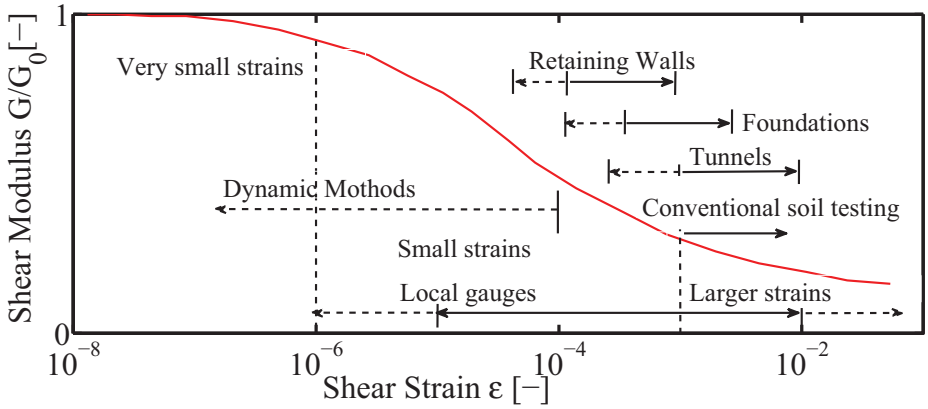

Figure 2.9: Modulus reduction curve of soil with typical strain ranges for laboratory tests and structures [Atkinson and Sallfors, 1991; Mair, 1993].

In general, it is expected that G_{max} does not change in the small-strain range. The figure also illustrates typical strain ranges for structures and typical laboratory tests to measure different strains. Vibrations caused by seismic in situ tests, traffic, construction works, weak earthquakes or even blasting usually have shear strain amplitudes below $5 * 10^{-3}$%.

2.5.1.2 Factors effect on Small-Strain Shear Stiffness G_{max}

There are many factors affecting the Small-Strain Shear Stiffness G_{max}, summarized as follows:

Effective confining pressure σ': Effective confining pressure σ' is probably the most important factor that has a significant influence on G_{max}. This was realized a

long time ago. An exponential relationship of the form $G_{max} \propto (\sigma^{'})^{n}$ was proposed by [Hardin and Richart, 1963]. This relation is still very commonly used. Several studies have been carried out to defined the exponent n for different types of soil. The exponent (n) is typically around 0.5 as proposed by [Hardin and Richart, 1963]. Many recent studies use (n) values in the range of 0.40 to 0.55 [Hoque and Tatsuoka, 2004; Kuwano and Jardine, 2002; Tika et al., 2003].

Type of material: [Fioravante, 2000] determined small-strain stiffness of two sands with different geological origin via laboratory seismic tests performed in a triaxial cell. Dry triaxial reconstituted specimens of Ticino river silica sand and of Kenya carbonatic sand were subjected to isotropic and anisotropic states of effective stress; then both shear and constrained compression waves were propagated in vertical, horizontal and oblique directions by means of five couples of piezoelectric transducers especially arranged in the specimens. The propagated shear waves allow the assessment of the shear modulus G_{max}. A relationship was found between G_{max} and e as equation 2.9 and $x = 0.8$ for sand.

$$G_{max} \propto e^{-x} \tag{2.9}$$

[Presti et al., 1993] studied the shear modulus of freshly deposited specimens of two different sands. This modulus was measured in a resonant column and torsional shear apparatus. The soil specimens studied included a calcareous, crushable, well-graded, coarse-to-medium sand containing about 2% fines and a silica, uniform, coarse-to-medium sand without fines (Ticino sand). They found $x = 1.3$ for cemented sand and fine-grained soils. While [Biarez and Hicher, 1994] found $x = 1$ for sand and clay. [LoPresti and Jamiolkowski, 1998] proposed the range 1.1-1.5 for x for various clays. Monotonic torsional shear tests, resonant column tests, compression triaxial tests and bender elements were performed in an oedometer apparatus or a triaxial apparatus. The tested material was six different Italian clays with different void ratios.

Void Ratio: [Hardin and Richart, 1963] measured shear wave velocity on various types of sand using resonant column method. It was found that velocity at 100% relative density may be quite different for two sands; however, their velocity were essentially the same when they were at the same void ratio. Accordingly, they proposed

the following relation between G_{max} and void ratio was proposed:

$$G_{max} \propto \frac{(2.17-e)^2}{1+e} \tag{2.10}$$

for round-grained sands $e < 0.80$ and

$$G_{max} \propto \frac{(2.97-e)^2}{1+e} \tag{2.11}$$

for angular-grained sands $e > 0.60$

Strain Rate $\dot{\gamma}$: [Dobry and Vucetic, 1987] found experimental evidence showing that the G_{max} and G go up when there is a significant several-fold increase in the strain rate $\dot{\gamma}$ or in the frequency of the cyclic loading, and thus concluded that G_{max} increases as $\dot{\gamma}$ increases.

[Clayton, 2011] verified the significance of using in practical applications by running a numerical experiment for estimating the ground deformations around a singly propped retaining wall. Sensitivity analysis of predicting displacements and bending moments were also carried out with different stiffness parameters. A propped cantilever wall was modelled using linear and nonlinear elasticity, and horizontal wall displacements, vertical displacements at original ground level, vertical displacements at excavation level, bending moments, and prop loads were calculated for different soil models. It was shown that stiffness at very small strain and the change of stiffness parameters with increasing strain had significant effects on computed displacements and wall bending moments. Predicted displacement patterns were sensitive to most parameters, including small-strain stiffness and rate of stiffness degradation. He concluded that small-strain stiffness can be used to establish the stiffness profile, which has a great influence on displacement patterns around new and existing infrastructure. [Atkinson, 2000] discussed in detail the influence of non linearity of soil stiffness on routine geotechnical design. He analyzed the influence of non linearity on foundation behavior and on the choice of design stiffness. He concluded that soil stiffness parameters back-calculated from Absorbed settlements of full-scale and model foundations are nonlinear and decay with settlements in the same way that stiffness decays with strain.

2.5.1.3 Measuring Small-Strain Shear Stiffness G_{max}

A variety of testing methods are available for measuring dynamic soil properties in the laboratory techniques. Each of these methods has its own advantages and disadvantages. Choosing the right method needs careful attention and extensive understanding of dynamic behavior which depends on the type of problem. This understanding is necessary to recognize the uncertainty in measured data. Uncertainty can be originated by sampling disturbance, anisotropy, variability of soil, limitations of field or laboratory equipment, testing errors, or interpretation errors [Kramer, 1996]. Therefore, efforts must be made to avoid these sources of uncertainty or at least minimize them. In this section, methods used to determine damping and stiffness in the small-strain range are explained. The methods in the laboratory techniques to determine large-strain dynamic properties of soil are summarized as follows, but can be found in details in [Kramer, 1996].

Local deformation transducers

In a triaxial testing device, displacement is usually measured between the top cap and the base pedestal, using a global transducer. The accuracy of such transducers is not enough to measure small strain. Furthermore, the sample may have no parallel and smooth ends; the top cap therefore probably has no perfect full instant contact at the small-strain range. The restraints at the ends of the sample cause non-uniform displacements over the height. Local deformation transducers (LDTs) avoid such problems of imperfect bedding. They are typically installed in a triaxial cell. Local deformation transducers can measure deformations axially or radially. They can measure stiffness at strain as small as 10^{-6} [Goto et al., 1991; Tatsuoka et al., 1999]. Several transducers may be used simultaneously in order to Absorb the loss of homogeneity of the strain field in the specimen. Local deformation transducers are convenient up to a specific strain limit, after which they could be destroyed. They can disturb the specimen (especially porous rock) due to the penetration of glue inside the pores. They measure displacements between two specific points to deduce strain in the specimen, assuming that deformations in the specimen are homogeneous. refer to tatsuoka regarding dynamic and static stiffness.

Resonant column

The resonant column test is a well-known technique to determine the dynamic shear

modulus, dynamic elasticity modulus and damping ratio. First proposed in the 1930s, and then further developed in the 1970s, it is mainly applied to strain levels of $10^{-4} - 10^{-2}\%$. In a triaxial cell a soil sample is installed and excited torsionally or axially at its top end. The excitation is most commonly harmonic, in a range between 30 and 300 Hz, but random noise or pulses have also been used. Devices for cylindrical samples and for hollow-cylindrical samples are available, the latter minimize the variation of shear strain amplitudes across the sample in the case of torsional excitation. With a built-in accelerometer, the acceleration at the top of the sample can be measured.

Bender elements

The bender element method is a simple technique to obtain the very small-strain elastic shear modulus of soil G_{max} by measuring the velocity of shear wave propagation through a sample by means of piezoelectric elements. The history of *piezoelectricity* dates back to 1880 when Pierre and Jacques Curie first discovered the piezoelectric effect in various substances including Rochelle salt and quartz. Piezoelectric materials can generate an electric charge with the application of pressure; conversely, they can change physical dimensions with the application of an electric field (converse piezoelectricity). The word Piezoelectricity comes from Greek; Piezo means Pressure in Greek, so the term (Piezoelectricity) means (electricity by pressure). In a material which has piezoelectric properties, ions can be moved more easily along some crystal axes than others. Pressure in certain directions results in a displacement of ions such that opposite faces of the crystal assume opposite charges. When pressure is released, the ions return to original positions.

The first practical application for piezoelectric devices was sonar, first developed during World War I. The use of piezoelectricity in sonar created intense interest in developing piezoelectric devices. Over the next few decades, new piezoelectric materials and new applications for those materials were explored and developed. [Shirley, 1978] first developed bender element transducers to measure shear waves in laboratory, using two ceramic piezoelectric elements fixed diametrically in a cylindrical sample. [Shirley and Hampton, 1978] achieved further technical improvement using a transducer including two piezoceramic plates rigidly bonded along their length. [Schultheiss, 1981] and [Dyvik and Madshus, 1985] initiated their use in conventional geotechnical apparatuses (e.g. triaxial, direct simple shear and oedometer devices). They introduced the experimental procedures and theoretical interpretations in detail to carry out a test. In

the 1990s, the test got more attention, with the result that error sources were sought and the problem of signal interpretation arose [Jovicic et al., 1996; Viggiani and Atkinson, 1995]. These problems are addressed and discussed comprehensively later in this thesis.

The technique was used to investigate the dependency of G_{max} and shear wave velocity V_s on many parameters and factors such as grain size [Wichtmann and Triantafyllidis, 2009], confining pressure [Asslan and Wuttke, 2010; Kuwano and Jardine, 2002; Wuttke et al., 2012], stress path [Lee and Huang, 2007], time effect [Chang et al., 2006], cementation [Pestana and Salvati, 2006] and unsaturated conditions [Cho and Santamarina, 2001; Sawangsuriya et al., 2008; Takkabutr, 2006]. The technique has been getting more interest from researchers due to its wide range of applicability. What makes it attractive is that the computation of G_{max} is more direct than other methods like the resonant column test or in-situ tests. Besides, bender elements are easy to install into most soil testing apparatus (e.g. triaxial tests, shear tests, resonant column tests and oedometer tests). The bender elements themselves are cheap, small and lightweight. Furthermore, they are non-destructive.

However, this method assumes a one-dimensional wave propagation, where a plane wave is assumed to be propagated in the medium. In reality, three-dimensional wave propagation from a not perfect point source causing the near-field effects are the norm. Furthermore, the specimen has its boundaries; therefore, there is reflection and wave interference. Another hypothetical assumption concerns the material isotropic, uniform and continuum, which disregards travel path and dispersion. There should be sufficient contact between the bender elements and the surrounding soil in order to transmit the mechanical wave from the elements to the soil. If this is not the case, the received signal can be unclear and difficult to analyze, especially for soils with large particles. That is why it is better to have minimum penetration in the soil according to particle diameter. These disadvantages can be overcome by using advanced signal processing methods, applying appropriate theoretical models and sophisticated laboratory equipment as discussed later.

2.5.1.4 Collapse potential and small-strain shear stiffness behavior

A few studies have been carried out into the relationship between collapse and small-strain shear stiffness behavior. While the previous studies were done to describe G_{max} in the dry case, no consistent model was established for unsaturated soil. Most studies in the literature are not concerned with small-strain range. For this range, very few models have been proposed to quantify G_{max} in unsaturated soil. These models rely on limited experimental data. In this section, experimental and theoretical investigations on small-strain shear stiffness in unsaturated soils are presented and discussed.

[Victor et al., 1998] studied the characterization of wave velocity in collapsible soils. Small-strain V_p and V_s velocities were measured in a loess specimen during water infiltration to gain further insight into the behavior of loess during collapse. The test started with the specimen at its natural moisture content; the applied isotropic load was 50 kPa. Results are shown in Figure 2.10. They found that collapse takes place within few minutes. The shear wave velocity decreases from V_s = 256 m/s to 152 m/s. The longitudinal wave velocity decreases from V_p = 405 m/s to V_p = 260 m/s; this indicates that the material is not saturated even after collapse (V_p = 1550 m/s for water). The sample continues deforming after collapse, yet, wave velocities remain constant.

Isotropic tests were performed in a triaxial cell modified with bender elements. Specimens were trimmed from an undisturbed block sample recovered at a depth of 1.5 m. Two specimens were tested. One was air-dry (w = 3%). The other specimen was saturated while confined at 30 kPa (w = 25%). Back pressure was not used, yet full saturation is not required to reduce soil suction to very low values. Confinement was increased in stages. For each load increment, the deformation of the specimen was monitored with a vertical LVDT, and measurements of wave velocity were repeated until constant values were obtained. Velocity was found to be much lower for the saturated specimen than for the air-dry specimen, at the same confinement, and more sensitive to changes in confinement, particularly at higher confining pressure.

[Razouki and Al-Azawi, 2003] studied resilient modulus behavior during long-term soaking of compacted Iraqi gypsiferous soil containing about 34% gypsum. Two samples each were soaked for periods of 0, 4, 7, 15, 30, 60, 120 and 180 days with 178 N surcharge load. Each sample was subjected to a compressive wave as well as to a shear wave using the ultrasonic pulse velocity technique. The ultrasonic pulse veloc-

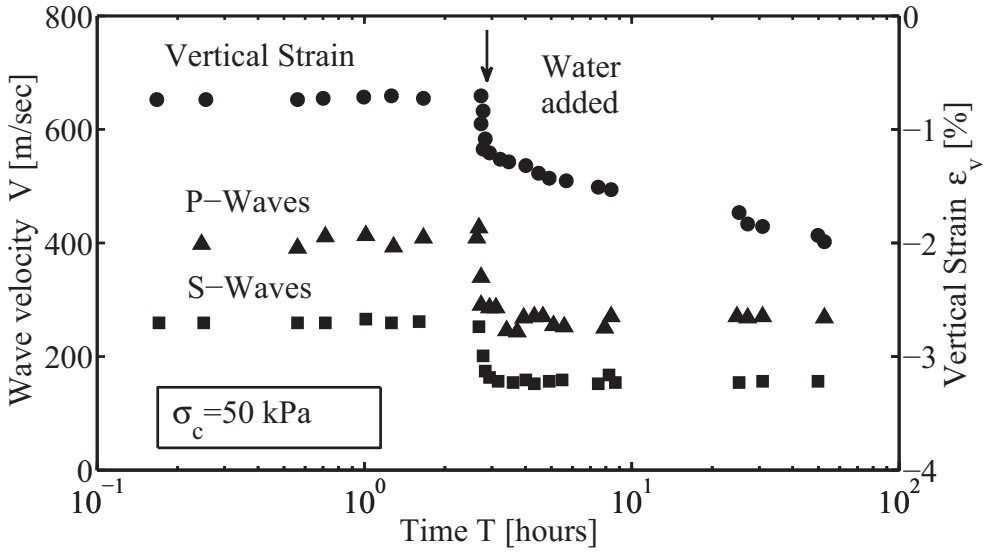

Figure 2.10: Undisturbed looses soil subjected to constant confining pressure σ_o =50 kPa [Victor et al., 1998].

ity technique was used to estimate the resilient modulus of the gypsiferous soil before and after soaking. The new Sonicviewer (Model - 5217 A) testing instrument used in this work consisted of the main device with a CRT display and two pairs of ultrasonic probes (transducers), one pair for V_c waves and the other for V_s [Das, 1984]. According to [Das, 1984], the longitudinal wave velocity of a soil sample confined in a mould is related to its elastic parameters as follows:-

$$V_c = \sqrt{\frac{E(1-\mu)}{\rho(1+\mu)(1-2\mu)}} \tag{2.12}$$

$$\mu = \frac{1-0.5\left(\frac{V_c}{V_s}\right)^2}{1-\left(\frac{V_c}{V_s}\right)^2} \tag{2.13}$$

Where : V_c = compression wave velocity, V_s = shear wave velocity, E = Young modulus of elasticity, ρ=mass density and μ = Poissons ratio.

As summarized in Table 2.4, they found that the compression wave velocity increased while the shear wave velocity decreased due to 4 days soaking. The Poissons ratio

also increased due to soaking as the soil approaches full saturation, while the resilient modulus decreased due to the dissolution of gypsum. Figure 2.11 shows the decrease in the resilient modulus with increasing soaking period.

Table 2.4: Resilient modulus before and after soaking [Razouki and Al-Azawi, 2003]

Condition of CBR sample	Before soaking	After 4 days soaking
$V_c[m/sec]$	399.14	428.38
$V_s[m/sec]$	188.13	176.26
μ	0.366	0.3981
Resilient modulus MR [MPa]	179.76	174.95

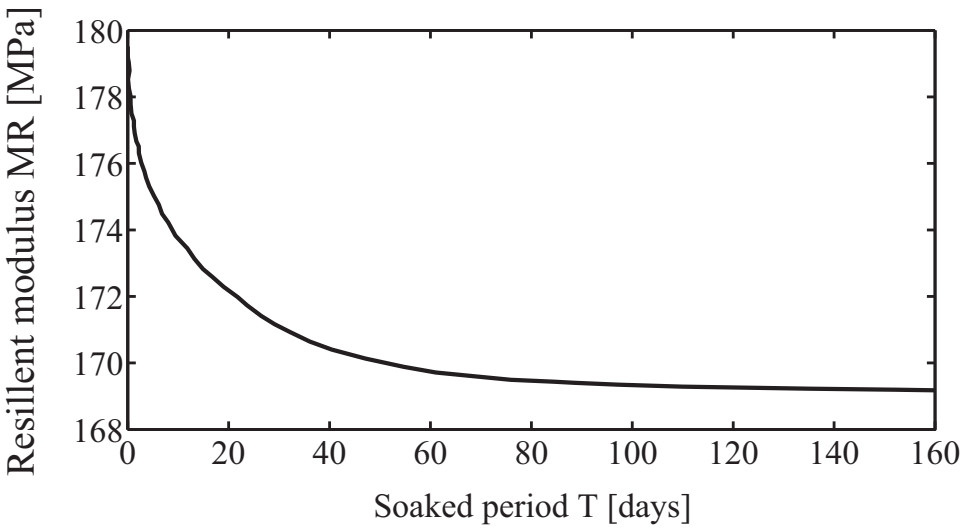

Figure 2.11: Effect of long term soaking on resilient modulus of gypsiferous soil tested [Razouki and Al-Azawi, 2003].

2.5.2 Electromagnetic material properties

2.5.2.1 Basic concept

Electromagnetic properties of non-ferromagnetic unsaturated porous geo-materials are defined in terms of broadband electromagnetic transfer functions such as the complex effective relative permittivity ($\varepsilon^*_{r,eff}$) or complex effective electrical conductivity

(σ^*_{eff}):

$$\varepsilon^*_{r,eff} = \varepsilon^{'}_{r,eff} - j\varepsilon^{''}_{r,eff} \tag{2.14}$$

$$\sigma^*_{eff} = j\omega\varepsilon_0\varepsilon^*_{r,eff} = \sigma^{'}_{eff} + \sigma^{''}_{eff} \tag{2.15}$$

Where $j = \sqrt{-1}$, angular frequency $\omega = 2\pi f$ and permittivity of free space ε_0 (Wagner et al. [2011]). Porous mineral materials consist mainly of four phases: solid particles (various mineral phases), pore air, pore fluid as well as the solid particle - pore fluid interface (see Figure 2.12).
The fractions of these phases vary both in space (due to composition, specific density and surface area) and time (due to changes of water content, porosity, pore water chemistry and temperature). The electromagnetic properties of the solid particles can be assumed to be frequency independent in the considered temperature-pressure-frequency range. Real relative permittivity of inorganic dielectric mineral materials varies from 3 to 15 [Robinson and Friedman, 2003]. The pore fluid as well as the interface fluid is assumed to be an aqueous solution with a temperature T, pressure p and frequency $\omega = 2\pi f$ dependent relative complex permittivity $\varepsilon^*_w(\omega$,T,p) according to the modified Debye model [Kaatze, 2007b]:

$$\varepsilon^*_w(\omega, T, p) - \varepsilon_\infty(T, p) = \frac{\varepsilon_s(T, p) - \varepsilon_\infty(T, p)}{1 + j\omega\tau(T, p)} - j\frac{\sigma_{Dc}(T, p)}{\omega\varepsilon_0} \tag{2.16}$$

With the high frequency limit of permittivity $\varepsilon_\infty(T, p)$, static permittivity $\varepsilon_s(T, p)$, relaxation time $\tau(T, p)$, direct current conductivity contribution $\sigma_{Dc}(T, p)$, and permittivity of free space $\varepsilon_s(T, p)$. In the case of concentrated aqueous salt solutions, the concentration and ion speciation dependence of the Debye-parameter in equation 2.16 has to be considered further [Kaatze, 2007a]. Hence, the effective electromagnetic transfer function of the porous mineral material in terms of effective complex relative permittivity, $\varepsilon^*_{r,eff}$ is a function of volumetric water content θ , porosity n, ion spe-

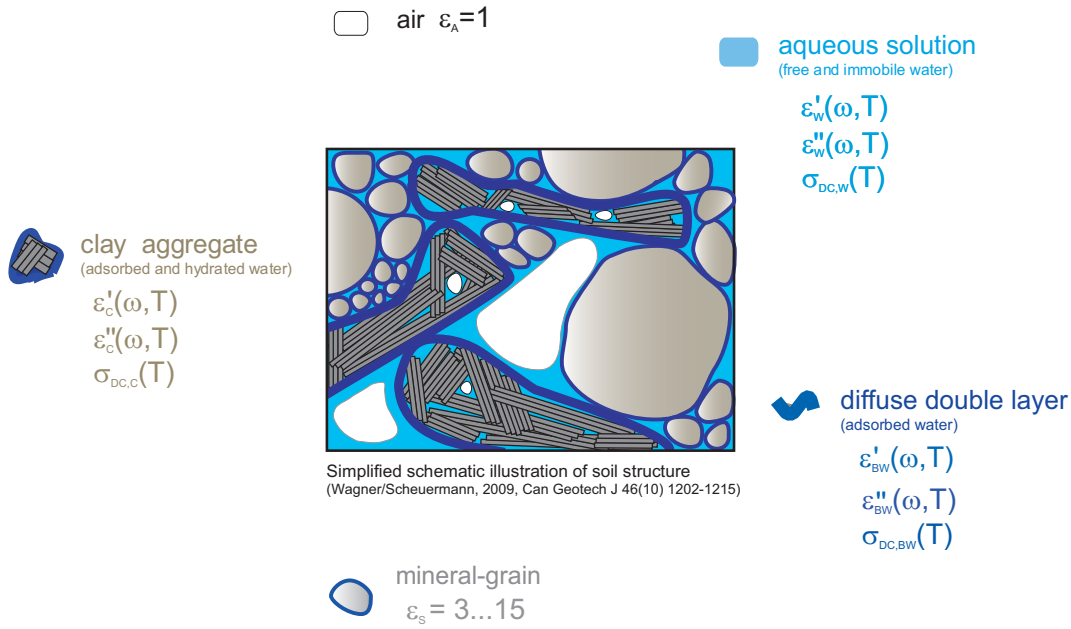

Figure 2.12: Simplified schematic illustration of the organic free soil structure. Indicated are the contribution of the single components to the dielectric material properties (' and " refer to the real and imaginary parts of complex relative permittivity, respectively) [Wagner and Scheuermann, 2009].

ciation and concentration c_i, frequency $\omega = 2\pi f$, temperature T and pressure p. In [Wagner et al., 2011], several broadband approaches were discussed to model $\varepsilon^*_{r,eff}$. The authors concluded that the class of power law models based on the Lichtenecker and Rother type mixture equation provide a useful approach in practical applications:

$$\varepsilon_{r,eff}^{*a(\theta,n)}(,\theta,n,c_i,\omega,T,p) = \Omega(c_i,\omega,T,p) + (1-n)\varepsilon_G^{a(\theta,n)} + (n-\theta) \qquad (2.17)$$

The parameter $0 \leq a \leq 1$ contains structural information regarding free and interface water and the term $\Omega(c_i,\omega,T,p)$ represents the contribution of relaxation processes. Hence, electromagnetic properties are directly related to changes in soil structure and therefore to collapse potential. However, for the development of robust approaches to

highly concentrated salt solutions as well as complex pore water chemistry, and structural changes with the hydration of clay minerals, there is a lack of systematic investigation using broadband dielectric spectroscopy of unsaturated and saturated porous media under controlled thermal, hydraulic, mechanical and chemical conditions.

2.5.2.2 Electromagnetic properties of unsaturated soil

The response of a material to a traveling electromagnetic wave is characterized as dielectric permittivity. Soil can be viewed as a dielectric with the electromagnetic properties, effective magnetic permeability, effective permittivity and effective conductivity [Lin and Cerato, 2013]. Since most naturally occurring soils are non-ferromagnetic, permittivity and effective conductivity are fully able to describe the dielectric responses of soil in an electromagnetic field. These two properties have been used to predict soil moisture, porosity and the presence of contaminants [Arulanandan, 2003], [Selig and Mansukhani, 1975] and [Thevanayagam, 1993]. As is the case in clay minerals, collapsible soils show variations in the permittivity and effective conductivity with changes in frequency, the phenomenon of which is called dielectric dispersion or relaxation. This is attributed primarily to certain polarization mechanisms, and the corresponding curves are known as dielectric spectra [Arulanandan, 2003].
Permittivity is a complex parameter, equation 2.15, where the real component ($\varepsilon^{''}_{r,d}$) reflects the stored energy in the soil when it is exposed to time harmonic electromagnetic field with angular frequency $\omega = 2\pi f$, [Wagner and Lauer, 2012], while the imaginary part, $\varepsilon^{''}_{r,eff} = \sigma_{Dc}/(\omega\varepsilon_0)+\varepsilon^{''}_{r,eff}(\omega)$, characterizes the Ohmic and polarization losses, respectively (see [Wagner et al., 2011],[Hasted, 1973]). Here $\sigma_{Dc}/(\omega\varepsilon_0)$ is the conductive losses and ε_0 is the permittivity of free space, [Topp et al., 1980] and [Robinson and Friedman, 2003]. The permittivity at different GHz frequencies represents the amount of free water in the soil. Furthermore, the complex permittivity at lower frequencies gives information about the absorbed water, [Santamarina and Fam, 1995]. Generally, the polarization of the material (in other words permittivity) increases monotonically from high to low frequencies.

High frequency electromagnetic (HF-EM) measurement techniques such as capacitance methods,[Evett et al., 2009], ground penetrating radar (GPR), [Jol, 2009] or time domain reflectometry (TDR), [Robinson and Friedman, 2003] work on the basis of de-

tecting changes in spatial and temporal variations of the HF-EM properties at or near the subsurface [Wagner and Lauer, 2012]. At lower frequency ranges from 1 MHz to 200 MHz capacitance methods are commonly used to determine complex permittivity. This method requires the removal of soil fractions of a size greater than 2 mm and hence the undisturbed nature of the soil cannot be maintained. In the frequency range from 1 MHz to 10 GHz time or frequency domain reflectometry techniques, [Behari, 2005] and [Wagner et al., 2011] are usually employed.
Classical TDR [Robinson and Friedman, 2003] measures the travel time of an HF-EM pulse running along a bifurcated short probe of known length, which is inserted into the soil. The apparent relative dielectric permittivity (ε_a) is obtained as:

$$\varepsilon_a = \left\{ \frac{c * t}{2 * l} \right\}^2 \tag{2.18}$$

Where c is the velocity of light ($c = 3 * 10^8 m/s$); t is the travel time of the electromagnetic wave and l is the length of the probe. Although measurement of electromagnetic properties using TDR with rod probes has some limitations, such as the dependence of the measured electromagnetic properties on the type of probe design and type of material soil investigated, relatively accurate results with little calibration effort and less measurement time can be obtained.
According to [Topp et al., 1980], the real apparent relative permittivity (ε_a) of soil can be obtained based on the volumetric water content $\theta(m^3 m^{-3})$ of the soil with the following empirical equation:

$$\varepsilon_a = 3.03 + 9.3 * \theta + 146 * \theta^2 - 76.7 * \theta^3 \tag{2.19}$$

Similarly, the frequency and temperature dependent mixing rule known as advanced Lichtenecker and Rother Model (ALRM), equation 2.20, as suggested by [Wagner et al., 2011] which was used to verify the experimental results. The model parameters were modified to obtain a best fit with the electromagnetic behavior of collapsible soils.

$$\varepsilon_{r,eff}^{*a(\theta,n)} = \theta \varepsilon_w^{*a(\theta,n)} + (1-n)\varepsilon_G^{a(\theta,n)} + (n-\theta) \tag{2.20}$$

Where, ε_G is the relative real permittivity of the solid grain particles. The equation suggested by [Dobson, 1985], equation 2.21, was used to obtain the relative real permittivity of the solid grain particles of the collapsible soil.

$$\varepsilon_G = 1.01 + 0.44 * {\rho_G}^2 - 0.062 \tag{2.21}$$

The term ρ_G in equation 2.21 represents the specific density of solid particles. The term (a) in equation 2.22 is dependent on the current states of gravimetric water content and porosity of the soil. The expression given in equation 2.22 with temperature independent constants A1, B1 and C1, [Hayashi, 2004], were used to get the values of a for soil at different values of porosity and gravimetric water content. The values of the temperature independent constants used in this paper were chosen so as to fit the behavior of the selected collapsible soil.

$$a(\theta, n) = A_1 + B_1 n^2 + C_1 \left\{ \frac{\theta}{n} \right\}^2 \tag{2.22}$$

Chapter 3

Used Materials, Equipments and Testing Procedures

3.1 Introduction

This chapter presents the experimental Materials, equipments and testing procedures in this study. The focus of the experimental program is to study the mechanical behavior of unsaturated collapsible soil and to analyze the fly ash stabilization materials to mitigate their geotechnical problems. Two types of soil, (i) undisturbed and (ii) disturbed samples were taken from collapsed soil areas. Some disturbed samples were prepared and compacted in their natural state and others were mixed and compacted with different percentages of fly ash material. This chapter summarizes the preparation of specimens, the devices, experimental techniques and procedures used in the determination of the volume change of saturated and unsaturated states as macro-physical behavior, micro-chemical behavior, suction-control behavior and electromagnetic properties behavior. The experimental program was carried out to measure the results of physical and chemical tests, unconfined compressive test, collapse potential value (single and double odometer test), soil water characteristic curve (by pressure plats tests and salt solution methods) and collapse-suction changes behavior (Barcelona-cell tests), collapse-electromagnetic proprieties changes and shear stiffness behaviors (bender element tests) of all samples used. All of these test are presented in the following sections.

3.2 Soil used

Two types of problematic collapsible soils, undisturbed and disturbed sample packets, were taken from 1-2 [m] depth from Baku in Azerbaijan (see Figure 3.1). This type of soil usually has a low dry density and low moisture content and it can withstand large applied vertical stress with small compression when in a dry state, but then experience much larger collapses after wetting. The soil studied showed low moisture content and low values of dry unit mass, with consequently low levels of saturation. Table 3.1 and Table 3.2 summarizes the physical and chemical properties respectively of soil used in this study. The investigation methods of physical and chemical properties are presented in Appendix A.

Table 3.1: Physical properties of soils used

Physical properties	Values
Specific gravity ρ_s $[g/cm^3]$	2.72
Initial moisture content w [%]	10-5
Max. dry density ρ_d $[g/cm^3]$	1.787
Optimum Moisture Content O.M.C [%]	16
Liquid limit (L.L. [%])	36.3
Plastic limit (P.L. [%])	17.8
Plastic Index (P.I. [%])	18.5
Clay (<0.002 mm) [%]	34 - 33
Silt (0.002-0.063 mm) [%]	42 41
Sand (0.063-2 mm) [%]	21 - 20
Gravel (>2 mm) [%]	3 - 6
Classification	Silty clay
Total surface area $[m^2/g]$	22.95
Total Sulphate % by mass	0.88
Exchange Sodium Percentage (ESP [%])	9 - 19
Sodium Adsorption Ratio ([SAR] [%])	7 - 16
Electric Conductivity	628 μs/cm
pH-value	8.8

Table 3.2: Mineral properties of soils used

Mineral analysis	by weight [%]
Mica	25
Tecosilicates	7
Kaoline	3
Chlorite	5
Silicates	44
Carbonates	12
Gypsum	1
Goethit	2
Organic	1

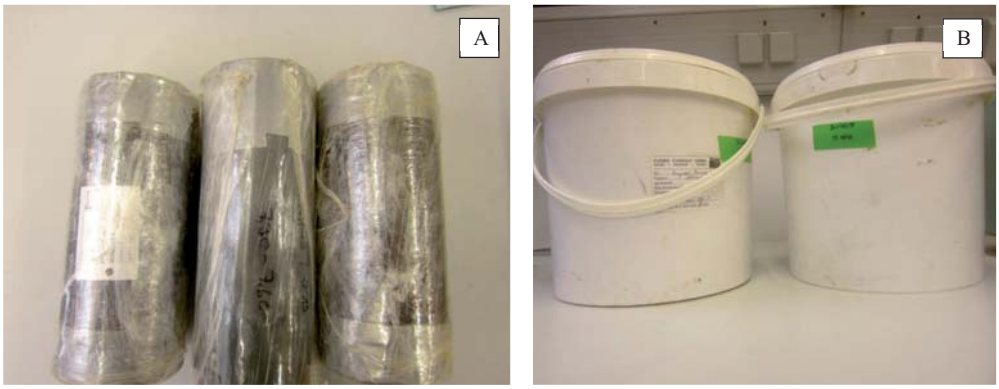

Figure 3.1: [A] Undisturbed samples and [B] disturbed sample packets.

3.3 Fly ash material used

The fly ash used in the present study (labelled Steament H-4) is from a local electric power plant at Herne, Block IV, a city east of Essen, Germany (see Figure 3.2). The fly ash has a powdery texture and is light grey in color, which indicates a high calcium oxide content. The chemical properties of the (Steament H-4) fly ash are summarized in Table 3.3 along with the chemical properties of class C and class F fly ashes. The chemical composition of fly ash is one of the most important indicators of material quality for various applications. Based on the chemical properties results, the fly ash used is close to typical F. As shown in Figure 3.3, grain size analysis of fly ash was

carried out through a combination of dry sieving and sedimentation analysis [Meyers et al., 1976].

Figure 3.2: Steament H-4 fly ash.

Table 3.3: Chemical properties of (Steament H-4) fly ash used

Chemical elements [%]	(Steament H-4) fly ash	Typical class C	Typical class F
SiO_2	53.6	39.9	54.9
Al_2O_3	24.9	16.7	25.8
Fe_2O_3	7.6	5.8	6.9
CaO	2.9	24.3	8.7
MgO	1.8	4.6	1.8
SO_3	0.4	3.3	0.6
$L.O.I$	8.8	6	6

3.4 Experimental testing procedures

The experimental testing procedures was carried out to investigate and determine the hydro-mechanical properties of unsaturated collapsible soils and analyze the effect of fly ash stabilizer material on their geotechnical properties. Therefore, different tests

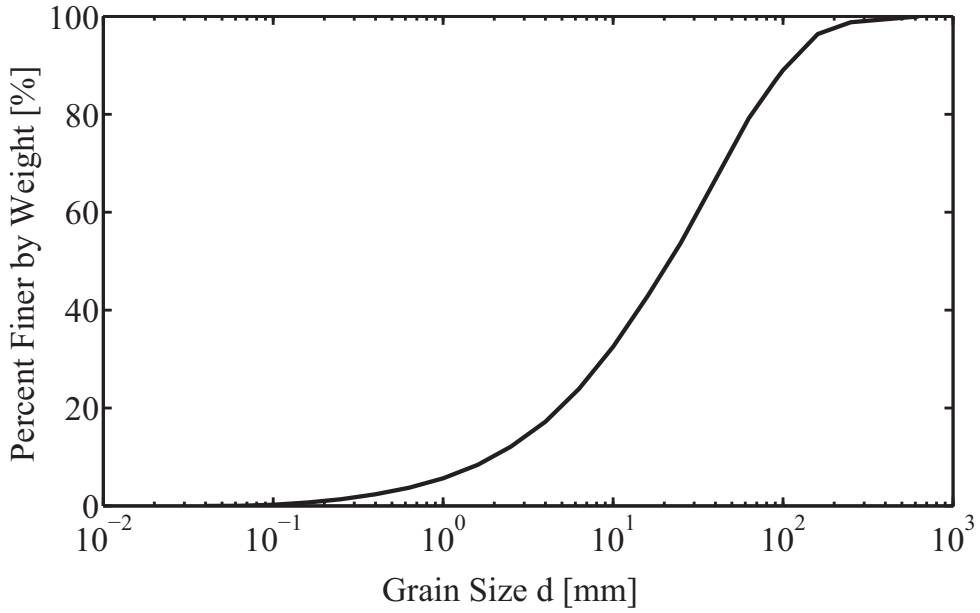

Figure 3.3: Grain size distribution for (Steament H-4) fly ash.

were performed on disturbed and undisturbed samples in natural and fly ash mixed states. The experimental programs consisted of (i) unconfined compressive strength tests (ii) collapse potential tests for unsaturated collapsible soils (iii) SWCC tests (v) suction control-oedometer tests (vi) electromagnetic properties-collapse tests and (vii) small shear strain-stress change behavior. Moreover, in the experimental program two cells were made to perform the experimental program.

3.4.1 Collapse potential testing procedures

Single and double oedometer tests were performed to investigate the stress-strain curve and determine the collapse potential value (C_p) at different initial conditions (different initial void ratio, different initial water content and different fly ash mixed content at different curing periods) for both saturated and unsaturated states. Several soils were prepared with different symbols, shown in Table 3.4. The preparation of samples and techniques used for the oedometer test are presented in Appendix A. The initial conditions of natural soil and soil mixed with 5, 15, 25% fly ash are summarized in Appendix B, Table B.1.

Table 3.4: The symbols of specimens collapse potential test

Symbol	Material content
UNS	100% Undisturbed Natural Soil
UCS	100% Undisturbed Compacted Soil
DS	100% Disturbed Soil
D5FA	95% Disturbed Soil+5%Fly Ash
D15FA	85% Disturbed Soil+15% Fly Ash
D25FA	75% Disturbed Soil+25% Fly Ash

3.4.2 Unconfined compressive strength testing procedures

3.4.2.1 Samples preparation Techniques used for unconfined compressive strength tests

A photograph of a soil specimen subjected to unconfined compression is shown in Figure 3.4. Unconfined compressive strength for natural soil and for fly ash - stabilized soils are determined by using a computerized triaxial instrument without application of cell pressure. The dimensions of the tested specimens are 150 [mm] height and 100 [mm] diameter. The unconfined compressive strength (qu-value) of the tested specimens is measured at the failure of the specimen. The speed of deformation (strain rate) is 0.01 [mm/min]. After compaction, the specimens were extruded, sealed in polyethylene bags, and stored in 98% relative humidity at 25^oC for 1, 3, 7, 14 up to 20 days of curing time (for soil-fly ash mixtures) in a computerized temperature-humidity chamber.

3.4.3 Soil water characteristic curve (SWCC) testing procedures

The soil-water characteristic curve describes the relationship between suction and the corresponding state of wetness of the soil. The state of wetness can be expressed in the degree of saturation, S_r [%] ; gravimetric water content, w [%] ; or volumetric water content, θ [%]. Laboratory determination of the soil water characteristic curve is generally performed by either increasing or decreasing the soil suction and measuring the resulting soil water content, w after equilibrium is reached. Soil suction can be determined either by direct or indirect methods. Direct methods include pressure plates, suction plates, pressure membranes and tensiometers. Indirect methods

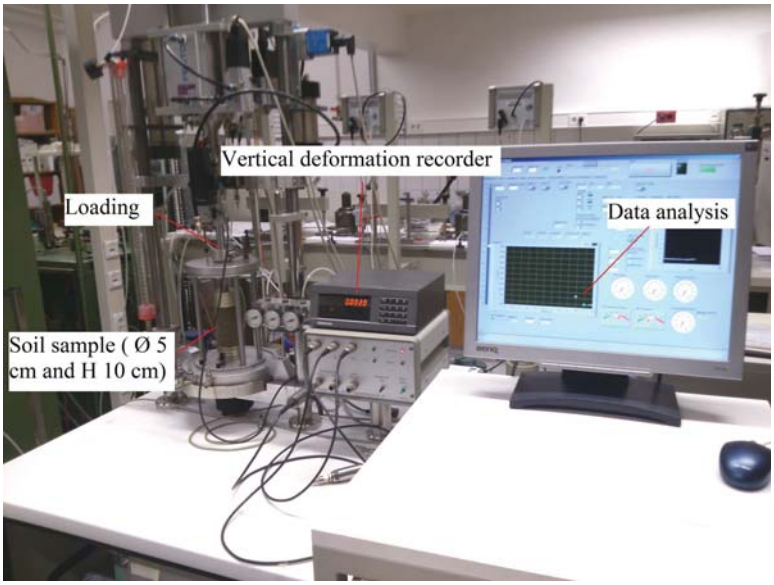

Figure 3.4: Unconfined compressive strength test.

include filter paper, salt solution method, moisture blocks, heat dissipation sensors and phychrometers [Fredlund and Xing, 1994]. Soil-water characteristic curves SWCC (studied ranged from 0-4000 kPa) were carried out with two methods: The pressure plate method was used to establish a relationship between volumetric water content and matrix suction (Su<1500 kPa) while the salt solution method was used to apply suction (Su>1500kPa). Table B.2 in Appendix A summarizes the initial condition of the SWCCs specimens. With the salt solution method, four desiccators with several aqueous of alt solutions were used to induce total suction to the specimen by changing the relative humidity vapor space in the desiccator. Appendix B, Table B.3, shows the type, properties and suction value of the salt solutions used in this method. The preparation of samples and techniques used for soil water characteristic curve (SWCC) test are presented in more details in Appendix A.

3.4.4 Suction controlled-oedometer testing procedures

Suction controlled oedometer tests were performed using the axis translating technique in a UPC-Barcelona cell. This test is carried out to study the hydro-volume change behavior of unsaturated soil with and without cementation material at changing suction values while stress is constant. In this program three stresses 50, 200 and 400 kPa were

used. For more details of this testing procedures and initial conditions of the samples see Appendix A and Table B.4 in Appendix B.

3.4.5 Electromagnetic testing procedures

Collapsible soils have to be considered as strong electrical loss and dispersive dielectric material with characteristic frequency dependent electromagnetic properties. Broadband electromagnetic measurements were performed at frequencies from 1 MHz to 10 GHz at room temperature (see [Wagner et al., 2011] and [Wagner and Lauer, 2012] for details).
The electromagnetic tests is carried out to investigate the change in electromagnetic properties of collapsible soils with and without cementation material during changes of vertical stress, degrees of saturation as well as the changes in the chemical reactions of fly ash soil stabilization. The program of electromagnetic properties tests was performed with two parts as follows:

3.4.5.1 Electromagnetic properties-without loading testing procedure

This test was carried out to investigate the electromagnetic properties of natural soil and soil mixed with different percentages of fly ash at different curing periods without loading. Natural soil and soil mixed with 5, 10, 15, 20, 25 % fly ash were used. Big cylinder samples (10 mm diameter and 15mm height) of the natural soil were prepared with known initial properties. The cylinder samples of soil mixed with fly ash were prepared with optimum moisture content and maximum dry density. From each big cylinder sample, a small sample (38.8 [mm] outer diameter, 15 [mm] inner diameter and 50 [mm] height) was taken to measure the electromagnetic properties. The electromagnetic samples of were analyzed under different conditions as following:

- The natural soil samples are tested at air-dry case and then at saturated case for 7 days by using ceramic stone plates until near saturation.
- Remolded samples of collapsible soil with varying porosity and gravimetric water content were used for the electromagnetic tests. The first set of tests were

performed on samples with initial void ratio of e_0 = 0.83 (natural loose condition) and varying water content. The second set comprised of samples with initial void ratio of e_0 = 0.43 (lab compacted condition) and with varying water contents. To identify the effects of changes in both porosity and water content on the electromagnetic properties at the same time, a third set of samples with varying void ratios and water content were used.

- Natural collapsible soil was mixed with (5, 10, 15, 20% and 25) of fly ash. The soils mixed were kept one hour in closed boxes with constant humidity (98% and constant temperature 25^oC for curing and to make a homogeneous. From each soil mixed, two cylinder samples (10 [mm] diameter and 10 [mm] height) were prepared with maximum dry density and optimum moisture content based on the proctor test as shown in Table 3.5. From one of cylinder sample, two small samples (38.8 [mm] outer diameter, 15 [mm] inner diameter and 50 [mm] height) and were cut to measure the electromagnetic properties for the soil-fly mixed as a bulk soil. From the other cylinder sample, a small amount of soil mixed were taken. By use centrifuge device, the water of these samples was extracted to electromagnetic properties of pore water only for the soil mixed. The electromagnetic properties test was measured at 1, 3, 7, 9, 14 and 23 days after preparation to monitor the ionic exchange and pozzolanic reaction with time curing. For measuring the permittivity spectra of disturbed soil samples, a two-port coaxial transmission line cell was designed, as depicted in Figure 3.5 (a, b) (see [Wagner and Lauer, 2012] for details).

3.4.5.2 Electromagnetic and shear stiffness - stress change testing

This test was carried out to investigate the change in dielectric properties (electromagnetic properties) and shear stiffness of the soil during the change in vertical stress behavior, change in degree of saturation, change in fly ash percentage and change in collapse values. The dielectric properties which were measured include the real and imaginary part of complex effective relative permittivity ($\varepsilon^*_{r,eff}$) or the real and imaginary part of complex effective electrical conductivity (σ^*_{eff}), while the shear stiffness test included shear (V_s) and longitude (V_p) wave velocities. The electromagnetic properties and shear stiffness of all types of soils used are determined at five stages; at

Table 3.5: The properties of initial condition and after near saturation are used to investigate the real and imaginary part of complex effective relative permittivity ($\varepsilon^*_{r,eff}$) and the real and imaginary part of complex effective electrical conductivity (σ^*_{eff}).

Initial properties of Natural soil				
Soil	Case	$e_0[-]$	W [%]	n [%]
NS	dry	0.534	4.6	34.8
NS	saturated	0.665	20.7	39.9
Initial properties of Natural soil mixed with fly ash				
fly ash [%]	O.M.C [%]	Max.dry density [g/cm^3]		
5	17	1.751		
10	18	1.72		
15	19	1.70		
20	20	1.68		
25	20.9	1.658		

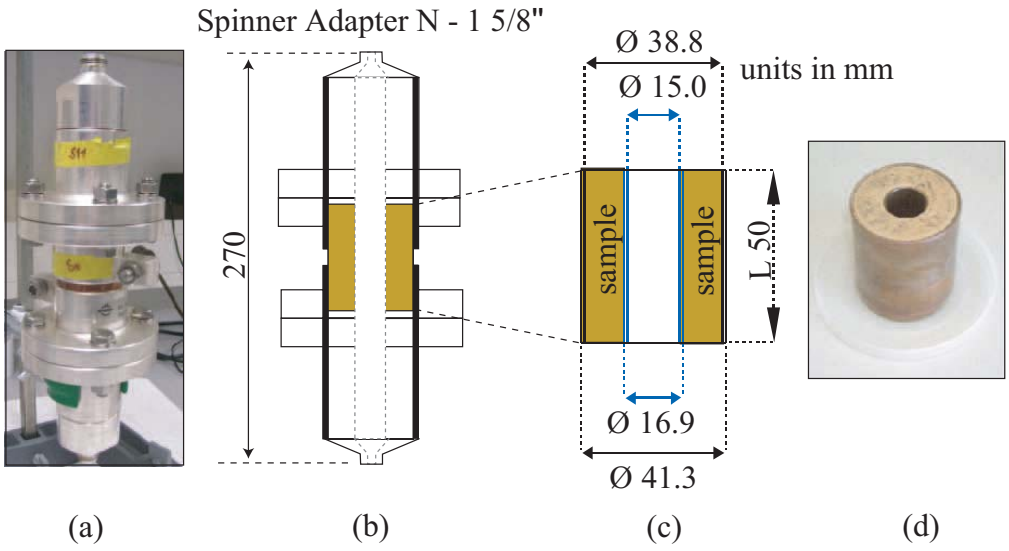

Figure 3.5: Two-port coaxial transmission line cell and sampling device. (a) Photograph of the measuring cell fixed in coupling elements used. (b) and (c) Schematic assembly (length L, 50 mm; inner conductor, 16.9 mm external diameter, 15 mm internal diameter; outer conductor, 41.3 mm external diameter, 38.8 mm internal diameter). (d) Photograph of the measuring cell filled with soil [Wagner et al., 2011].

Table 3.6: The program of electromagnetic properties and shear stiffness -stress change test

Soils	Vertical stress	Electromagnetic properties	Stage
All soils		Real and imaginary part	Air-dry
(NS)	50 [kPa]	of permittivity ($\varepsilon^*_{r,eff}$)	During loading
(NS5FA)	200 [kPa]		Constant loading
(NS15FA)	400 [kPa]	Real part	During saturated
and (NS25FA)		of electrical conductivity(σ^*_{eff})	Full saturated

initial property, during loading at certain vertical stresses (50, 200 and 400 kPa), constant loading before saturation, during the de-saturating process and at full saturation, as summarized in Table 3.6.

3.4.5.3 Techniques used to investigate the electromagnetic properties-collapse testing

This test was carried out to investigate the change in dielectric properties (electromagnetic properties) of the soil pores during the change in vertical stress / strain behavior, changes in the degree of saturation, cementation material and change in collapse values. The dielectric properties measured include the real and imaginary part of complex effective relative permittivity ($\varepsilon^*_{r,eff}$) or the real and imaginary part of complex effective electrical conductivity (σ^*_{eff}). A cylindrical specimen of soil with 11 [cm] diameter and 15 [cm] height was used. Five types of sample were prepared: soil with natural material and soil with natural material mixed with various cementation materials . Each sample loaded with three stresses 50, 200 and 400 kPa by using a mechanical machine. After applying the respective stress, the electromagnetic properties were determined by using a TDR device ([Wagner et al., 2011]) (see Figure 3.6) at five stages: at initial property, during loading at certain vertical stress, constant loading before saturation, during the saturation and at full saturation. The electromagnetic properties were investigated by inserting a coaxial line in the middle of sample depth as shown in Figure 3.6.

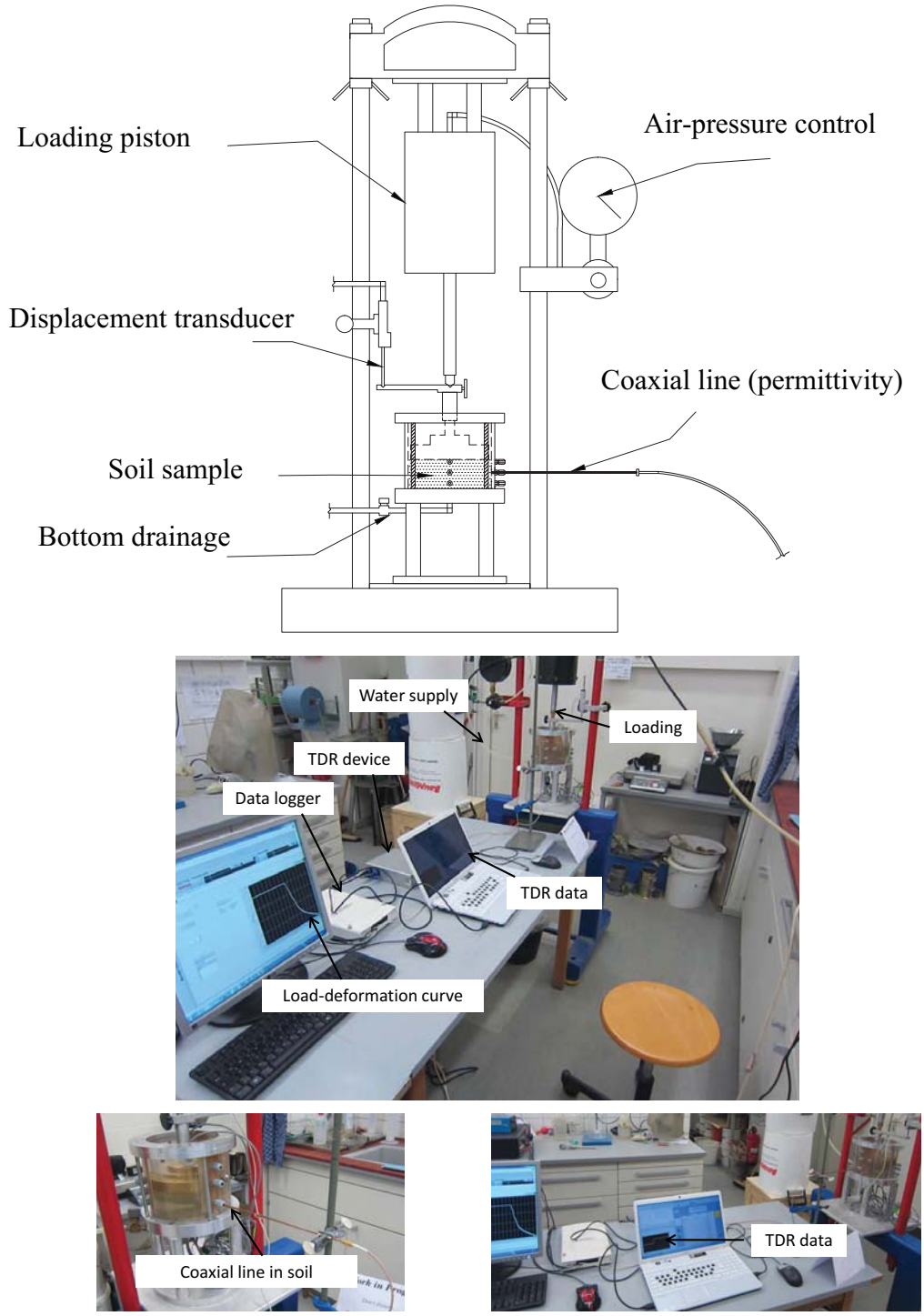

Figure 3.6: Techniques used to investigate the Electromagnetic properties-collapse test.

3.4.5.4 Preparation of sample

An ultrasonic test was carried out to measure shear (V_s) and longitude (V_p) wave velocities. To study the development of shear stiffness over time, natural soil was mixed with (5, 10, 15, 20 and 25%) of fly ash. From each soil-fly ash mixture, a cylindrical sample of 10 [cm] diameter and 10 [cm] height was prepared with optimum moisture content and maximum dry density based on the proctor test. The initial properties of the samples are summarized in Table 3.5. The samples were kept in place with constant humidity 98% and temperature 25 ^0C.

3.4.5.5 Techniques used for Ultrasonic test

Shear (V_s) and longitude (V_p) wave velocities were measured using ultrasonic measurement. The measurement system consisted of (V_s) and (V_p) transducers and S and P-wave receivers. One of the wave transducer is for transmitting waveforms, while the other is for receiving waveforms. The S and P-wave velocities of the samples were determined using the bender element method with the transmitting transducer placed on one end of the sample and the receiving transducer placed on the opposite end of the sample (see Figure 3.7).
The (V_s) and (V_p) were obtained as the quotient of the travel pass through the height of the specimen (l) and the travel time of the waves (t) (velocity V = l/t) [Yesiller et al., 2001]. The travel time was obtained from the bender elements transmitter which is excited by the LabVIEW program. It is defined as the first arrival time of the waves at the receiving transducer. The first arrival time of the wave velocity is indicated on the waveform. This process is carried out using the LabVIEW program, and the data logger. The program was developed in the laboratory of Soil Mechanics in Bauhaus-Universitt Weimar. For all waveforms and frequencies, input and output time histories are saved on the computer for the purpose of digital signal processing [Wuttke et al., 2012]. To study the development of shear stiffness over time, natural soil was mixed with (5, 10, 15, 20 and 25%) of fly ash. From each soil-fly ash mixture, a cylindrical sample with 10 [cm] diameter and 10 [cm] height was prepared with optimum moisture content and maximum dry density based on the proctor test. The samples were kept in place with constant humidity 98% and temperature 25 ^oC as shown in Figure 3.8.

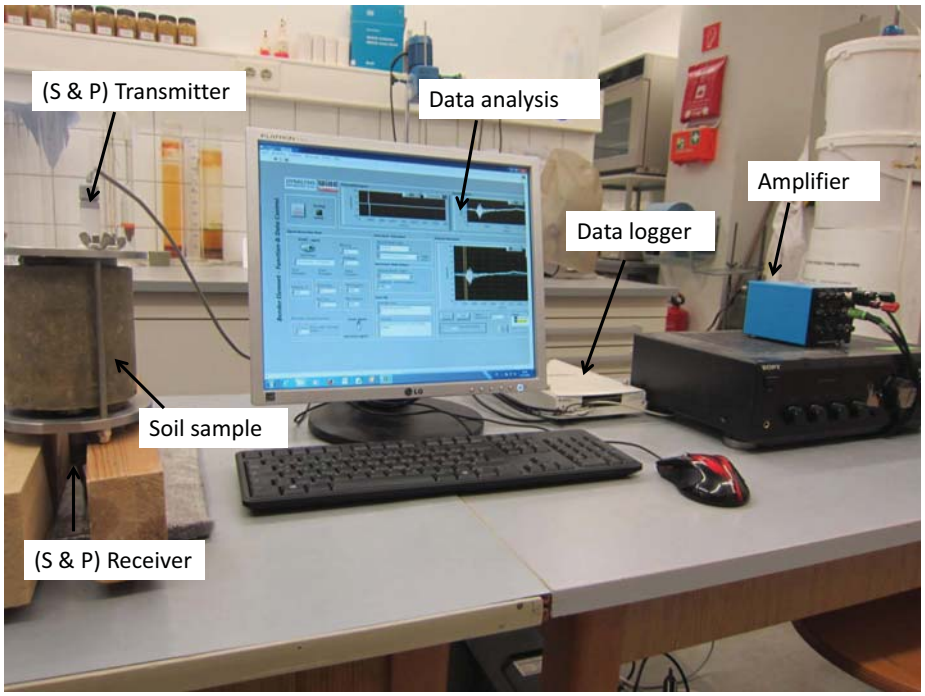

Figure 3.7: Techniques of ultrasonic measurement

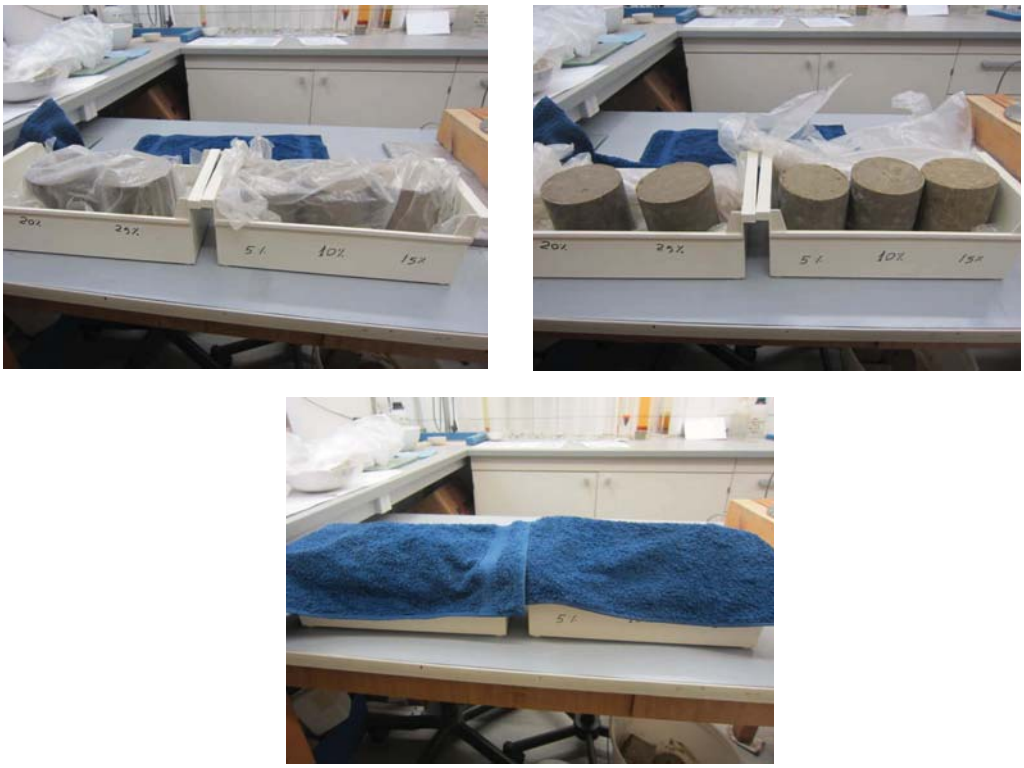

Figure 3.8: The curing of soil samples in ultrasonic measurement.

The velocity of (V_s) and (V_p) were measured two time per day up 20 days. By determining shear wave velocity (V_s) and longitude wave velocity (V_p), small-stain shear stiffness G_{max} and E-Modules E_0 were calculated by [Victor et al., 1998] as equations 3.1 and 3.2:

$$G_{max} = {V_s}^2 * \rho \tag{3.1}$$

$$E_0 = {V_p}^2 * \rho \tag{3.2}$$

Where :

G_{max} : Small-stain shear stiffness [MPa].

E_0 : E-Modules [MPa].

V_s : Shear wave velocity [m/sec].

V_p : Longitude wave velocity [m/sec].
ρ: Density [g/cm^3].

3.5 Summary

To study the hydro-mechanical properties, electromagnetic properties and seismic measurements of the natural soil (non-stabilized soil) and fly ash-stabilized soil, several short and long tests with large and small equipment are carried out. The rationale behind these tests is summarized as follows:

1. The physical and chemical properties tests are performed to determine the physical proportion of soil (gravel, sand, silt and clay content) as well as chemical compositions of soil and fly ash material in order to evaluate the chemical reactions between the materials used during the stabilized process .

2. Single and double oedometer tests are carried out to determine the collapse potential (C_p%) at different loadings, de-saturated steps, different fly ash content as well as to plot the stress-strain curve of soils used.

3. In the recent research, the hydraulic-mechanical behavior of unsaturated collapsible soil is investigated by determining the soil-water characteristic curve under several initial conditions: the influence of moisture content, void ratio, suction state, the influence of net stress, loading path directions (drying and wetting path) and flow conditions using testing devices, which measure water content and/or water pressure and/or cumulative water outflow and inflow. In the present work, a new condition is added to others and deals with the influence of the condition of fly ash stabilization material on the hydraulic-mechanical behavior of unsaturated collapsible soils. This parameter is very important for understanding the relationship between collapse potential, the influence of fly ash stabilization and suction change on the hydraulic-mechanical properties of soils used.

4. The unconfined compressive strength of a soil is a significant factor in estimating the design criteria for use as pavement and construction material. The fly ash-stabilization of soil generally leads to an increase in the strength of the soil.

Therefore, uni-axial tests for soils used are essential for evaluating the strength development during the hardening and pozzolanic reactions of fly ash-soil mixtures.

5. The physical-chemical forces and double layer size between the clay plates can be investigated through the electromagnetic properties of the pore fluid, which is affected by several parameters such as: ion concentration, valence, pH, and permittivity. Furthermore, by using this test the change in the chemical properties of soil during the pozzolanic reactions can be evaluated and monitored.

6. The use of seismic measurements (ultrasonic test) is a simple and practical tool to evaluate shear stiffness development with curing time of stabilized soils by determining the V_s and V_p wave velocity without destroying the sample (non-destructive test).

Chapter 4

Hydro-mechanical behavior of non-stabilized and stabilized soil

4.1 Introduction

This chapter presents and discusses the hydro-mechanical properties of stabilized and non-stabilized soil as reflected in the experimental results. The experimental results of two series of soils: natural collapsible soil and natural collapsible soil mixed with different percentages of fly ash were investigated. The chapter consists of three main parts. The first part are investigated the physical properties, chemical analysis and mineralogy composition of the soils studied. The second part are represented some of the mechanical properties which include the oedometer results and unconfined compressive strength. The third part contains the hydro-mechanical properties which consist of soil water characteristic curve tests and discusses the results of oedometer-suction control test (Barcelona cell test).

4.2 Physical properties results

4.2.1 Atterberg limits results

Atterberg limits (Plastic limit PL, Liquid limit LL, and Plasticity index PI = LL-PL) play an important role in soil identification and classification. These parameters indi-

cate some of the geotechnical problems such as collapse potential, swelling potential and workability. One of the principal aims of this study was to evaluate the changes of liquid, plastic limits and plasticity index with the addition of fly ash to the studied soils. To achieve this objective, the Atterberg limits test (including PL, LL, and PI) was conducted on both natural soil and fly ash-stabilized soil. The results show that the addition of (5%, 10%, 15%, 20% and 25%) fly ash to natural soil led to a decrease in the liquid limit and an increase in the plastic limit. This resulted in a reduction of the plasticity index [PI = LL-PL] (see Table B.5 in Appendix B). This is due to the fact that the surface of clay particles of natural soil is charged with a high Na ion one valence and the presence of cationic ions in pore water causes increases in the thickness of double layers. By the addition of fly ash, the free calcium of fly ash exchanges with the adsorbed cations of the clay mineral, which results in a reduction in size of the diffused water layer surrounding the clay particles. This reduction in the diffused water layer allows the clay particles to come closer to one another, causing the flocculation and agglomeration of the clay particles.

4.2.2 Proctor test results

The geotechnical properties of soil (such as collapse potential, swelling potential and unconfined compressive strength, etc.) are dependent on the moisture and density at which the soil is compacted. Generally, a high level of soil compaction enhances the geotechnical parameters of the soil, hence the importance of achieving the desired degree of relative compaction necessary to meet specified or desired properties of soil [Nicholson et al., 1994]. The aim of the proctor test (moisture-density test) was to determine the optimum moisture content of both untreated compacted and treated fly ash stabilized soil-mixtures. Figure 4.1 illustrates the moisture-density relationship of natural untreated soil and treated soil with 5%, 10%, 15%, 20% and 25% of fly ash. The addition of fly ash to the natural soil caused an increase in optimum moisture content and a decrease in maximum dry density. The decrease in maximum dry density is due to the dominance of the low weight and specific gravity of the fly ash, hence the total dry weight of soil mixtures decreases. The increase in optimum water content is due to the fact that fly ash particles are a very fine material that causes an increase in the surface area of clay as well as an increase in amount of water content to complete

the cation exchange process and pozzolanic reaction of fly ash.

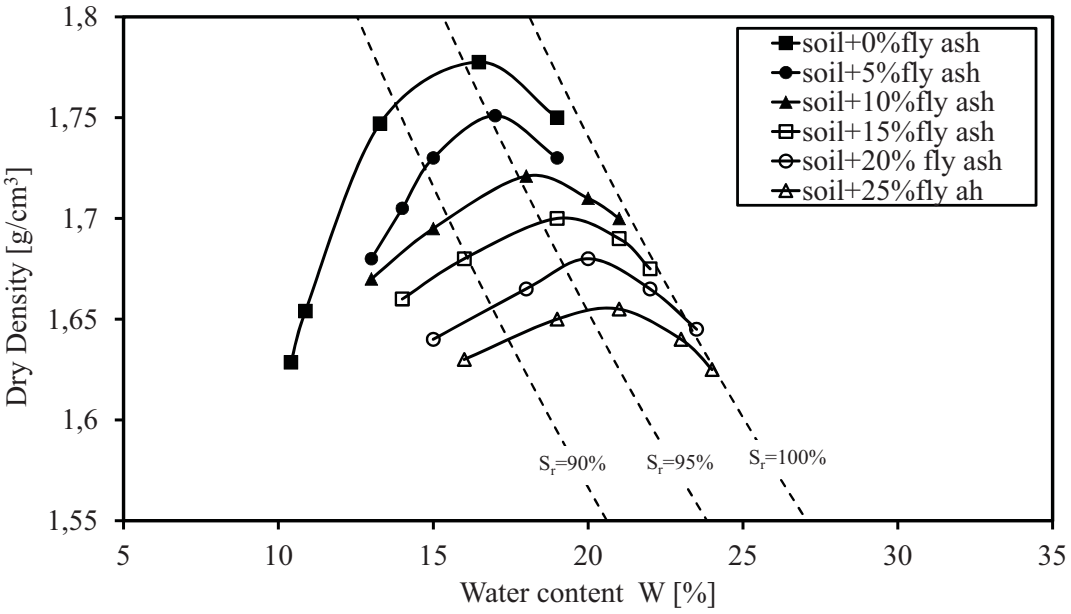

Figure 4.1: Relationship between the dry density and water content for soils studied.

4.3 Oedometer test results

4.3.1 Collapse behavior of non-stabilized soil

Single and double oedometer tests were carried out to investigate the behavior between the vertical stress-strain as well as the collapse potential. The results of the single oedometer test are studied to determine the collapse potential value (C_p [%]) for two undisturbed natural collapsible soils with different initial conditions as shown in Figures 4.2. It can be concluded that the collapse potential of a single oedometer test for natural un-compacted soil ((NUS) (e_0= 0.83) is higher than when compared with natural compacted soil (NCS) (e_0= 0.43) by 5% (see Table 4.1). This is due to the macro-physical loose structure of un-compacted soil (NUC). The resistance of clayey links between big grains is reduced by adding water to a soil subjected to a constraint. When this resistance becomes lower than the constraints of cutting, these links break and subsidence occurs. The other effect is mainly due to the cancellation of capillary

suction in soils partially saturated. The water flooding causes the migration of fine particles through their structures from one horizon to another. The suffusion phenomenon (or internal erosion) is proposed as an approach to explain the cause of collapse. In this study, collapse occurred due to the natural un-compacted soil ((NUS) (e_0= 0.83) having a loose, weak structure and large spaces between the particles. With the application of high vertical stress during the flooding process, the water helps the particles to slide and in turn causes a new rearrangement of soil particles and a great reduction in soil volume [Barden et al., 1996].

Table 4.1: Results of single Oedometer test for NUS and NCS soils

Type of soil	Void Ratio, e_0 [-]	(C_p [%])	Classification [Jennings and Knight, 1975]
Natural un-compacted soil (NUS)	0.84	9.17	Trouble
Natural compacted soil (NCS)	0.43	2.5	Moderate problem

Although natural compacted soil (NCS) has a low void ratio compared with natural un-compacted soil (NUS), it collapsed with a value of 2.5% (see Table 4.1). This is due to the effect of micro-chemical reaction behavior. The collapse phenomena in natural compacted soil (NCS) [e_o= 0.43] depends on the main parameters of ion exchange concentration and the water content. As the moisture content decreases and fine particles displace towards the menisci, the ionic concentration in the pore fluid increases, the Van der Waals attraction force increases by comparison with the repulsion force, which causes a decrease in the double layer thickness as well as strengthening soil structure. Upon wetting, most of the processes that contribute to the strengthening of soil mass are reversed: soluble salt dissociates and softens, the ionic concentration in the fluid decreases with the increase in water content and the lower the ionic concentration, the thicker the double layers that form around particles (this is aggravated by the low local confinement clay particles experience in clay bridges and buttresses). The shear stiffness and strength of the clayey formations decrease as the thickness of the hydration layers increases. Repulsion forces may become dominant and clay particles disperse. Eventually, the structure weakens and collapses even before full saturation is reached. Very low external loads are required to trigger the final collapse; in fact, self-weight alone may suffice [Victor et al., 1998].

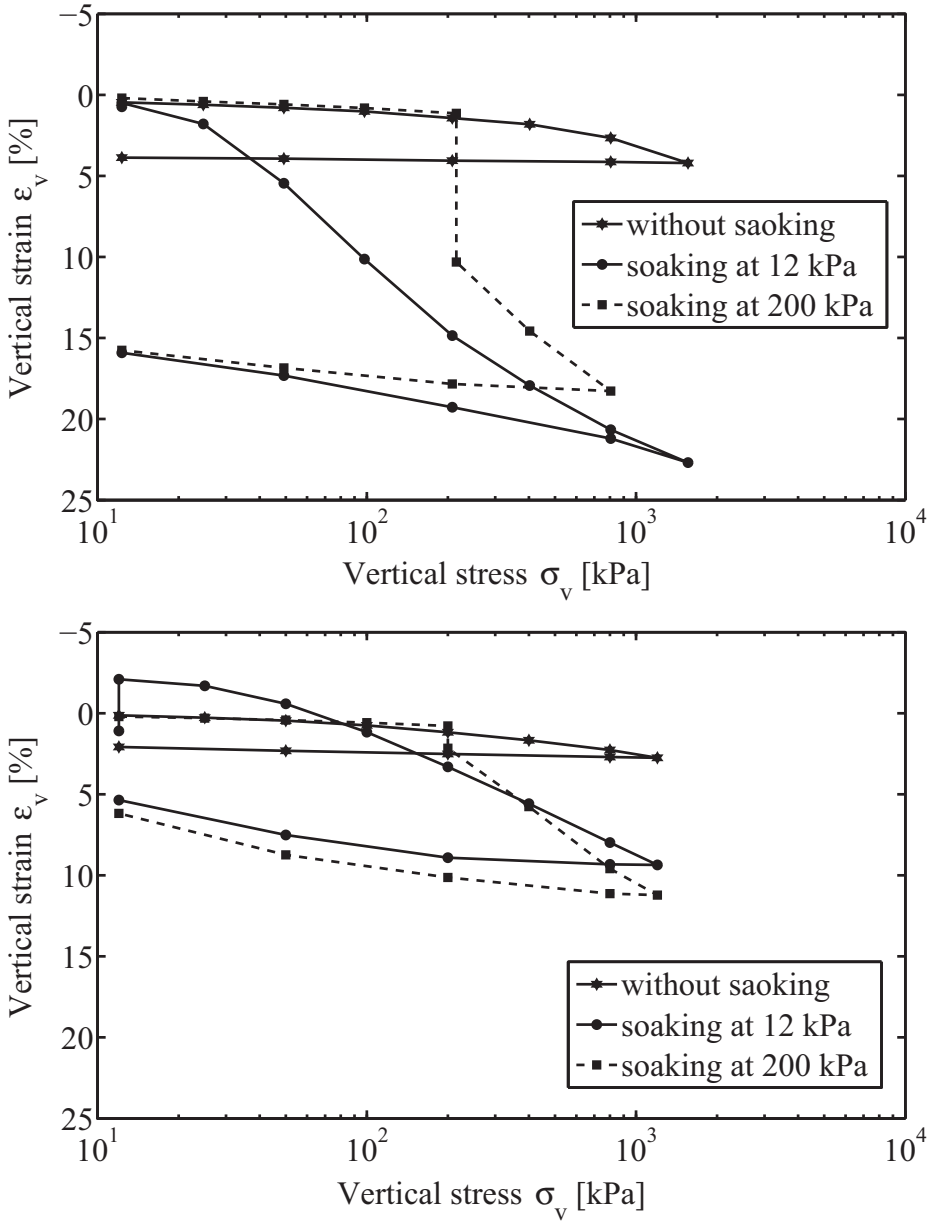

Figure 4.2: Relationship between the strain and the vertical stress for NUS soil (void ratio=0.835) (top) and NCS soil (void ratio=0.43) (bottom) of single and double oedometer test.

Figure 4.3 show the scanning electron microscopy (SEM) images which are obtained with a FEI/Philips XL30 ESEM FEG energy dispersive X-ray (EDX) scanning electron microscope. The (SEM) images show that at low water content (natural initial condition), the structure of collapsible soil has high space (i.e. high void ratio) and the bond forces between the soil particles are sufficient to provide strength. At soaking, the water causes the breaking and removing of the bonding/cementation material, causing a reduction in the strength and friction force between particles soil.

Table 4.2 shows the results of the double oedometer test for NUS and NCS soils. It

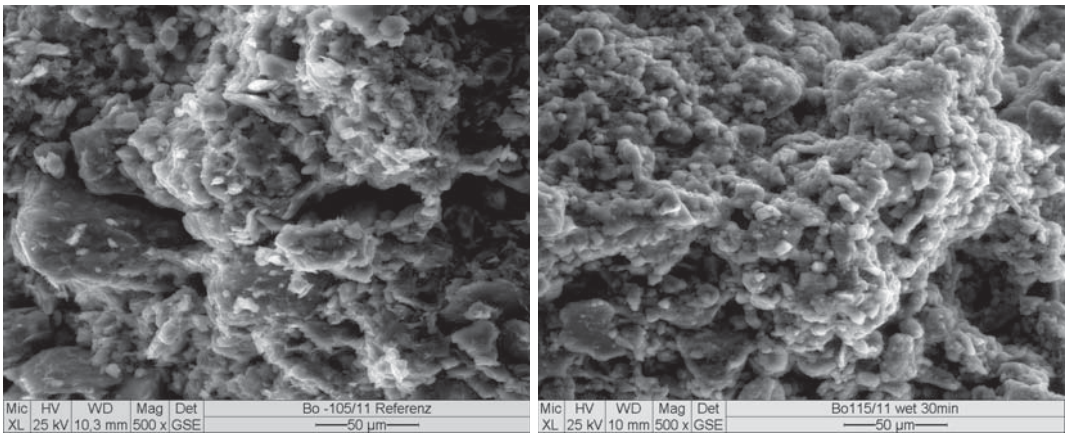

Figure 4.3: Microscope Scanning test for soil (right) before soaking and (left) after soaking.

can be seen that these soils exhibit high collapsibility strength when dry, and by comparing failure envelopes of dry specimens with those of saturated specimens, a loss of strength, basically in cohesion, is observed. Furthermore, the (C_p [%]) for NUS soil was 1.5 times higher than in the single oedometer test at load 200 kPa. A clear decrease in the collapsibility of NUS compared with NCS can be seen, as shown in Figure 4.4, due to the fact that the flooding during the double oedometer test starts at load 12 kPa so that the soaking period of the double oedometer test is longer, which causes increases in water content, the degree of saturation and collapse potential [Victor et al., 1998] and [Dibben, 1998].

Table 4.2: Results of double Oedometer test for NUS and NCS soils

Stress [kPa]	Natural compacted soil (NCS) (C_p [%])	Natural Un-compacted soil (NUS) (C_p [%])
25	-	1.2
50	-	4.7
100	1	9.1
200	3.1	13.4
400	5.2	16.4
800	7.5	18
1600	8.8	18.5

Table 4.3: Results of single Oedometer test for NUS and soils mixed with fly ash

Type of soil	Curing Time [days]	C_p [%]
N	-	9.17
N + 5% FA	1	5.2
	3	4.5
	7	4
N + 15% FA	1	3.5
	3	3.3
	7	2.8
N + 25% FA	1	3.6
	3	3.2
	7	3.1
N = Natural soil FA = Fly Ash		

4.3.2 Collapse behavior of fly ash stabilized soil

Single and double oedometer tests were carried out to determine the collapse value of natural soil mixed with different percentages of fly ash (5, 15 and 25%) at (1, 3, 7 days) of curing period. The results of single oedometer show that the collapse value (C_p= 9.17 [%]) of natural untreated soil decreases with range (5.2-4%), (3.5-2.8%) and (3.6-3.1%) when mixed with 5, 15 and 25% fly ash, respectively, after different curing days (see Table 4.3 and Figures 4.5, 4.6 and 4.7).

The effects of the fly ash chemical reaction in two level macro and micro structural behavior can be described as follows:-

In macro-physical behavior of soil, when fly ash is mixed with soil in the presence

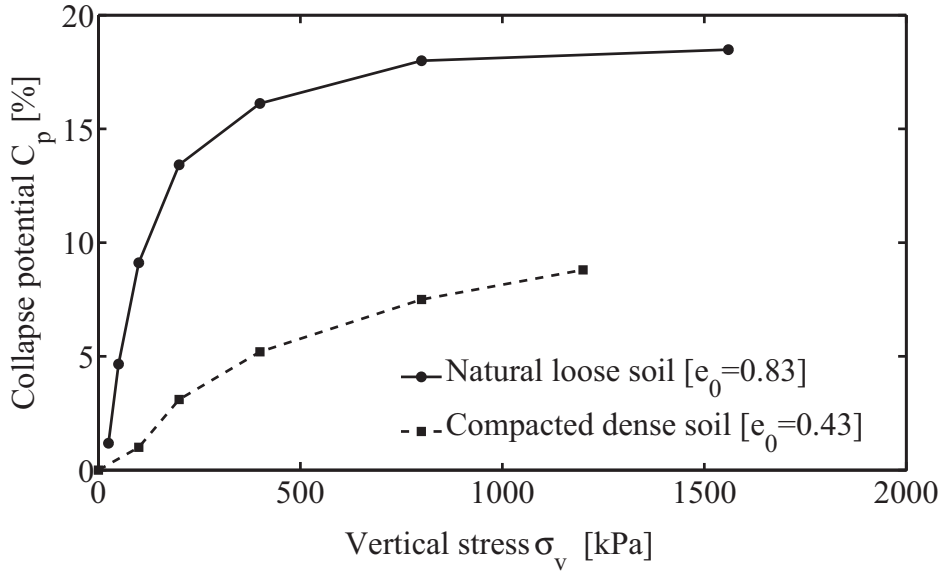

Figure 4.4: Collapse potential vs. vertical stress of double Oedometer test for NUS and NCS.

of water, a set of reactions occur that result in the dissociation of lime (CaO) in the binders and the formation of cementations and pozzolanic gels [calcium silicate hydrate gel (CSH) and calcium aluminate silicate hydrate gel (CASH)]. These reactions are referred to as cementations and/or pozzolanic reactions that result in the formation of cementations gels. The decrease in collapse value and increase in strength were found to be roughly related to the type and quantity of possible reaction products (i.e., CSH for short-term strength and pozzolanic reaction product, CASH for long-term strength gain) [Rogers and Glendinning, 2000].

In micro-chemical behavior, the effect of fly ash depends on the double layers theory which states that the interaction force between the layers in clay plates depends on the ion concentration at the mid-plane between the two adjacent parallel plates named ”attraction force” [Mitchell, 1993]. According to the chemical analysis (SAR$\geq$ 8), the untreated soil treatment is rich in bentonite by Na-type [Burden and Sims, 1999]. The surface of clay plates is charged with a high Na ion one valence and the presence of cationic ions in pore water causes increases in the thickness of double layers as well as increasing the attraction force among the clay plates. When the dry bentonite reacts with water, the hydration of Na ion one valence in surfaces of clay plates and

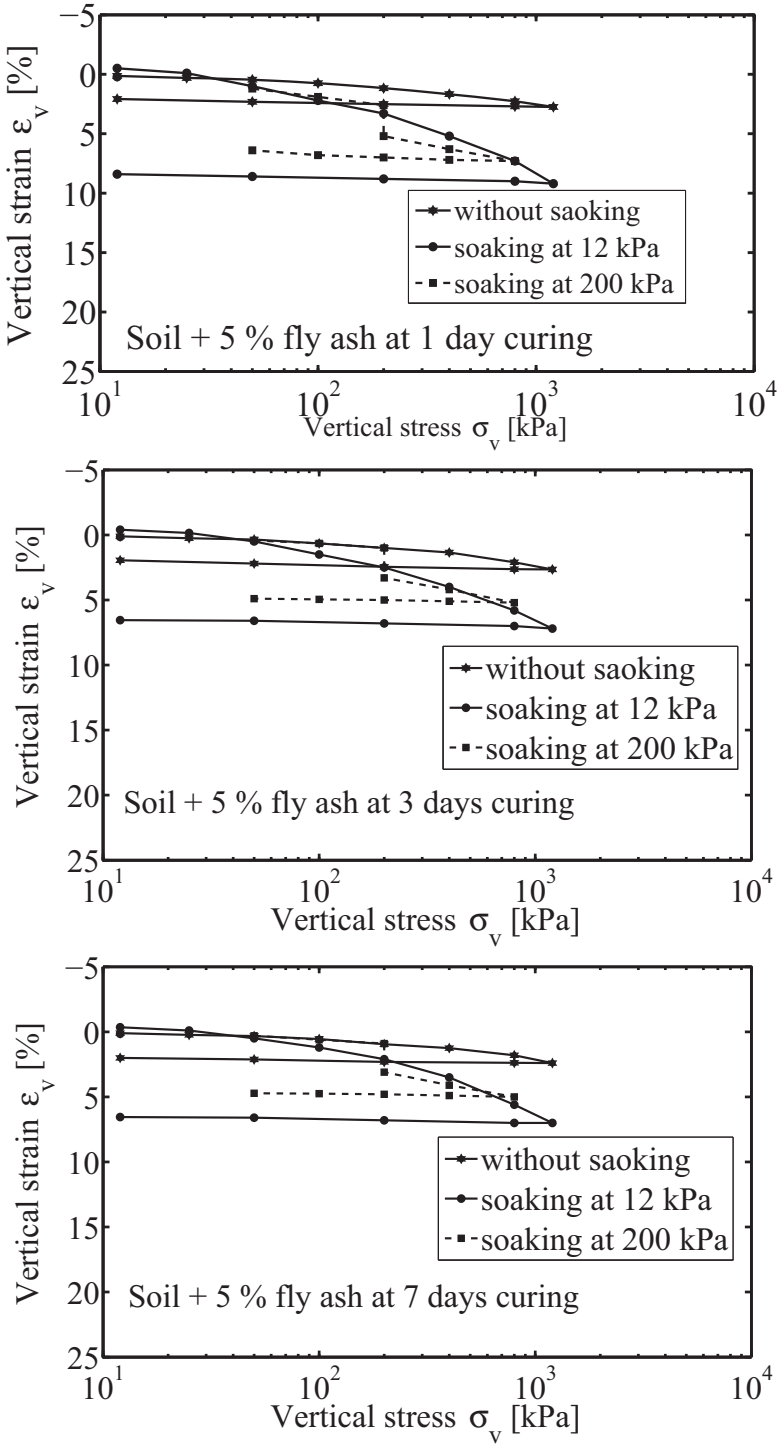

Figure 4.5: Relationship between the strain and the vertical stress of soil mixed with 5 % fly ash after 1 day (top), 3 days (middle) and 7 days (bottom) of curing period for single and double oedometer test.

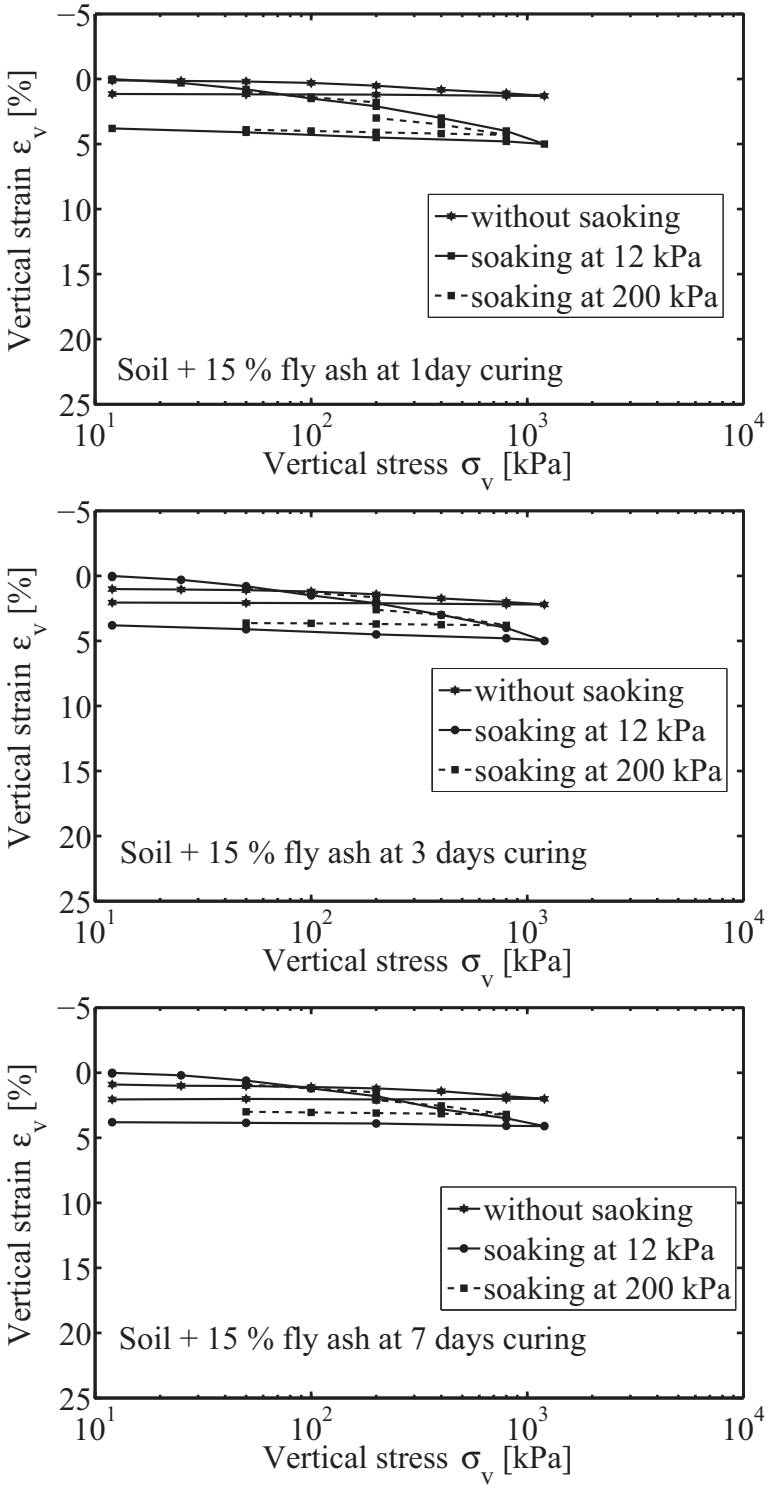

Figure 4.6: Relationship between the strain and the vertical stress of soil mixed with 15 % fly ash after 1 day (top), 3 days (middle) and 7 days (bottom) of curing period for single and double oedometer test.

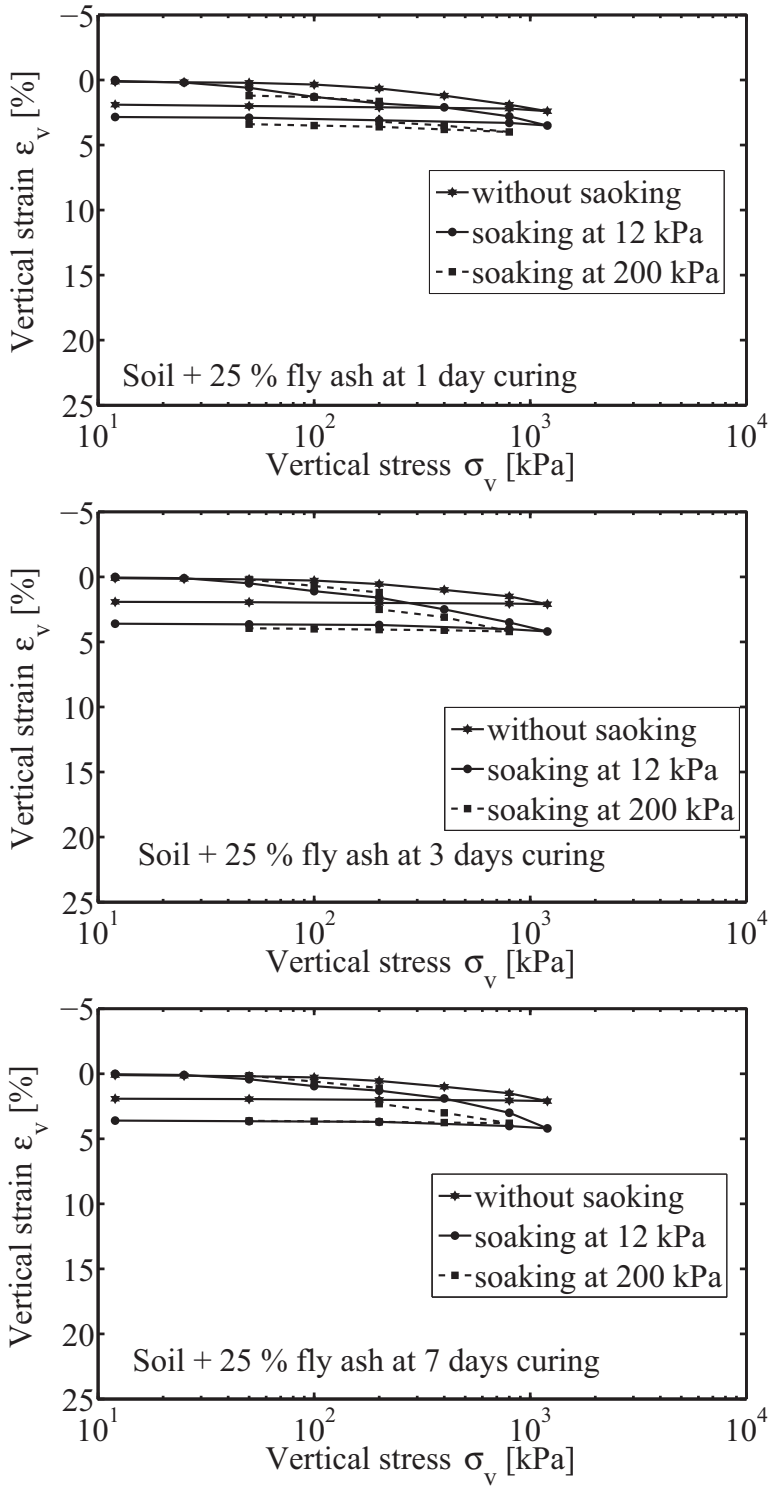

Figure 4.7: Relationship between the strain and the vertical stress of soil mixed with 25 % fly ash after 1 day (top), 3 days (middle) and 7 days (bottom) of curing period for single and double oedometer test.

exchangeable cations will occur, which causes an increase of the inter layer separation distance [Pusch, 1982]. For the soil treated with 15% fly ash, the hydration of fly ash releases calcium ions, which in turn replace original cations (most commonly sodium ions) in clay particles. This process is called the cation exchange process. The free calcium with higher valency cations (Ca^{+2}) of fly ash replace the lower ion valency (Na^{+1}), and any cation will tend to replace one to the left of it, which leads to a reduction in the amount of (Na^{+1}) ions in the bentonite surface as well as decreasing the size of the diffused double layer surrounding the clay particles. This decrease in the diffused double layer allows the clay particles to come closer to one another. The reactions occur quite rapidly when fly ash is added to soil, depending on the availability of various types of cations in the pore fluid, cation replacement can take place.
From the results, it can be observed that the C_p decreases slightly when the soil is mixed with more than 15% of fly ash. This could be because the pozzolanic reaction begins with great intensity when the (clay content/fly ash) in soil is high (with high silica and/or alumina) and then slows down when the (clay content /fly ash) ratio in soil is very low (with increasing fly ash content). Collapse during double oedometer tests was higher than in single oedometer testing because the period of soaking in double oedometer tests is longer (started at 12 kPa), which causes the removal of all the interaction forces (capillary force and cementation force).
The structure of soil mixed with 15% fly ash was scanned by scanning electron microscopy (SEM), as shown in Figure 4.8, and the images show that the fly ash particles provide the soil particles with a binder cementation material which causes an increase in strength and stiffness through chemical reactions. The binder is intended to cement the soil solids, thereby increasing strength and stiffness.

4.4 Uni-axial test results

The compressive strength of a soil is a significant factor in estimating the design criteria for its use as pavement and construction material. The fly ash-stabilization of soil, generally, leads to an increase in the strength of the soil. Therefore, fly ash has become a cost-effective and efficient material for use in road construction, embankments, and earth fills.
The strength gain of fly ash-stabilized soil is primarily caused by the formation of

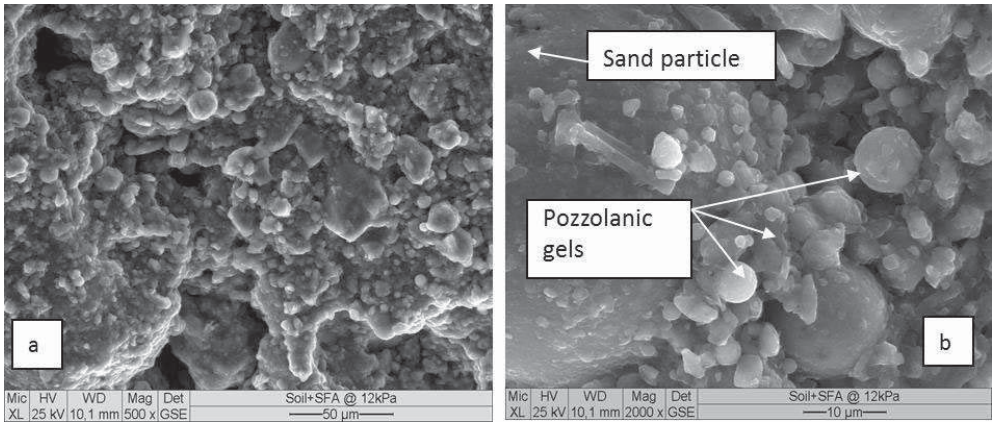

Figure 4.8: Microscope scanning test for soil with 15% fly ash [A] with 50 μm [B] with 10 μm.

various calcium silicate hydrates and calcium aluminate hydrates. The exact products formed, however, depend on the type of clay mineralogy and the reaction conditions including temperature, moisture, and curing conditions.

Unconfined compression tests were conducted to characterize the strength of natural soil and fly ash-stabilized soil. The test procedures and the preparation of the specimens were performed according to the procedures described in Chapter 3.

Fly ash-stabilized soil mixtures are prepared by mixing 5, 10, 15, 20 and 25% of fly ash. All the mixtures were compacted at optimum water content, two hours after mixing with water to simulate the construction delay that typically occurs in the field before sub-grade compaction due to construction operations. Each fly ash-stabilized soil mixture is tested at 1, 3, 7, 14 and 20 days of curing time. Figures 4.9 [A-D] show the relationship between the stress-strain curve of natural soil and all fly ash-stabilized soil mixtures with different fly ash content at different curing times. It can be observed from these Figures (as well as Table B.6 in Appendix B) that the failure occurs at a stress of 132 kPa corresponding to a strain of 2.34 % for natural soil. This behavior can be attributed to the fact that natural soil has a high amount of bentonite by Na-type (based on the chemical composition test (SAR$\geq$ 8). The surface of clay particles is charged with a high Na^{+1} and the presence of cationic ions in pore water caused increases in the thickness of double layers as well as increasing the attraction force among the clay plates. During the reaction of water with dry bentonite, a new hydration of Na ion one valence in surfaces of clay plates and exchangeable cations will

occur, which causes an increase in the inter-layer separation distance [Pusch, 1982], leading to a softer and weaker soil structure with low unconfined compressive strength. Observations from Table B.6 that the unconfined compressive strength of fly ash mixed soil increases with increasing fly ash content up to 15%, beyond which it slightly increases. This indicates that fly ash content of 15% is a fly ash fixation point, [Herrin and Mitchell, 1961], an optimum fly ash content for pozzolanic reaction with the soil. Increasing fly ash content beyond the above optimum value results in a slight increase in the strength of sample, which may be due to insufficient availability of silica and/or alumina in the soil for pozzolanic reaction. [Eades and Grim, 1960] also reported that the optimum amount of lime for maximum strength gain in stabilizing soil with lime was 46% for Kaolinite and about 8% for illite and montmorillonite.
Further, it is observed that for a given fly ash content the development of UCS occurs at a higher rate with an increase of the curing period of up to 7 days, after which the improvement is nominal and almost stabilizes. At 15% fly ash contents and after 7 days curing period, the strength gain with increasing curing period moderates to a slower rate and improvement is negligible when curing exceeds 14 days.
The mechanism to explain this fact is discussed in the following lines. The pozzolanic reaction takes place as silica and alumina present in clay react with calcium from fly ash to form cementitious products such as calcium-silicate-hydrates (CSH) and calcium-aluminate-hydrates (CAH). This pozzolanic reaction slows down when the clay content in soil is very low (with less silica and/or alumina). Above 15% fly ash content (i.e. at 20% and 25%) the increases in UCS are slight because of the insufficient amount of silica and/or alumina in clay for continuous and pozzolanic reaction resulting in some of the fly ash particles remaining without reaction. The fly ash which remains causes a reduction in the total bulk density of soil and strength (fly ash has low specific gravity and low density).

4.5 Soil water characteristic curve results (SWCCs)

4.5.1 Effect of initial void ratio on SWCCs for natural soil

Soil water characteristic curves (SWCCs) are carried out to study the hydro-mechanical behavior during changes in water content and suction value. They are plotted with ma-

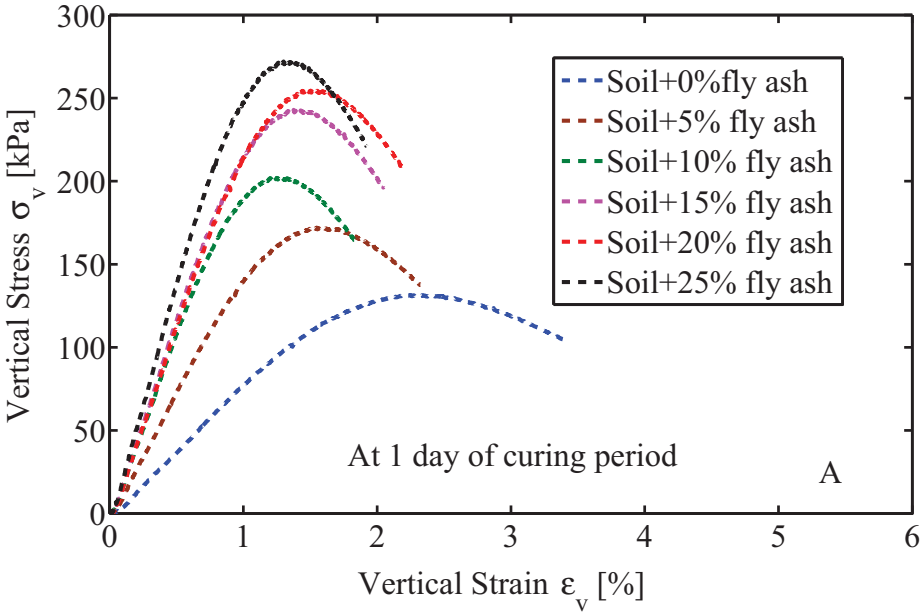
Vertical Stress σv [kPa]
Vertical Strain εv [%]
Soil+0%fly ash
Soil+5% fly ash
Soil+10% fly ash
Soil+15% fly ash
Soil+20% fly ash
Soil+25% fly ash
At 1 day of curing period
A

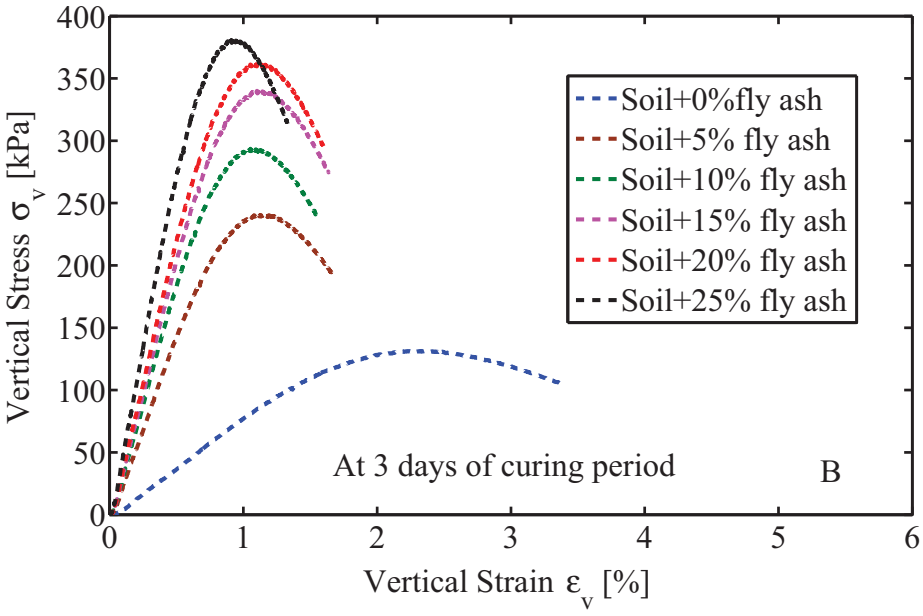
Vertical Stress σv [kPa]
Vertical Strain εv [%]
Soil+0%fly ash
Soil+5% fly ash
Soil+10% fly ash
Soil+15% fly ash
Soil+20% fly ash
Soil+25% fly ash
At 3 days of curing period
B

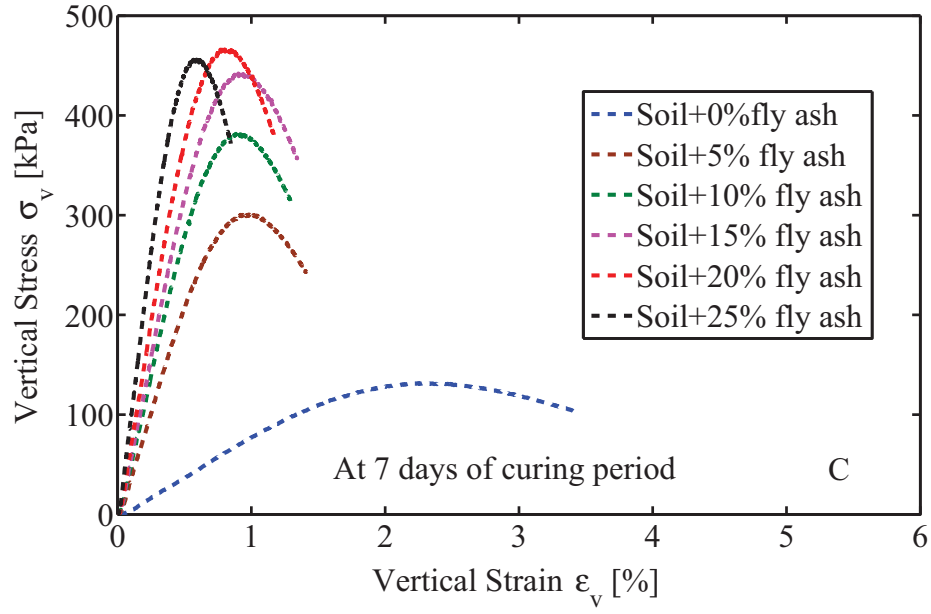
Vertical Stress σv [kPa]
Vertical Strain εv [%]
Soil+0%fly ash
Soil+5% fly ash
Soil+10% fly ash
Soil+15% fly ash
Soil+20% fly ash
Soil+25% fly ash
At 7 days of curing period
C

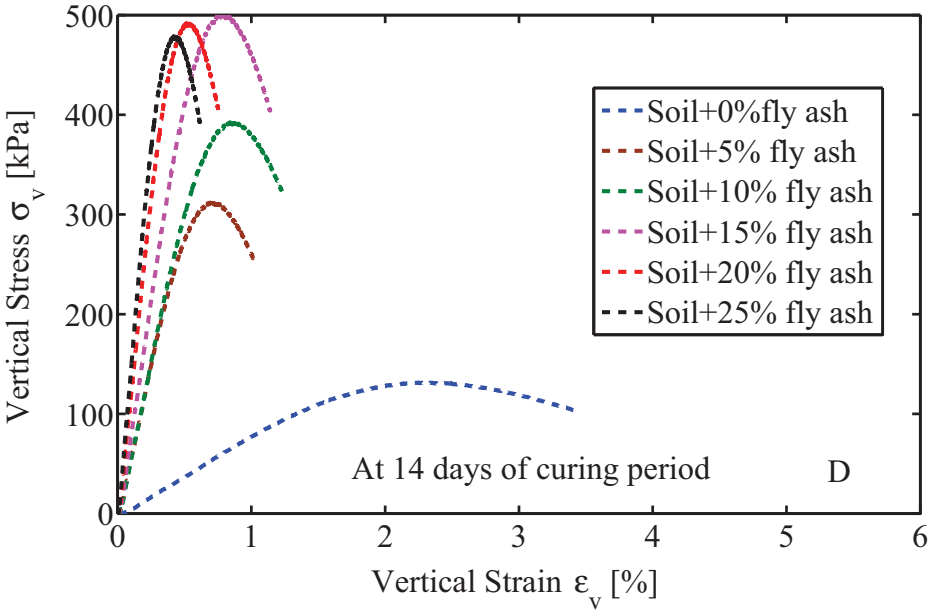
Vertical Stress σv [kPa]
Vertical Strain εv [%]
Soil+0%fly ash
Soil+5% fly ash
Soil+10% fly ash
Soil+15% fly ash
Soil+20% fly ash
Soil+25% fly ash
At 14 days of curing period
D

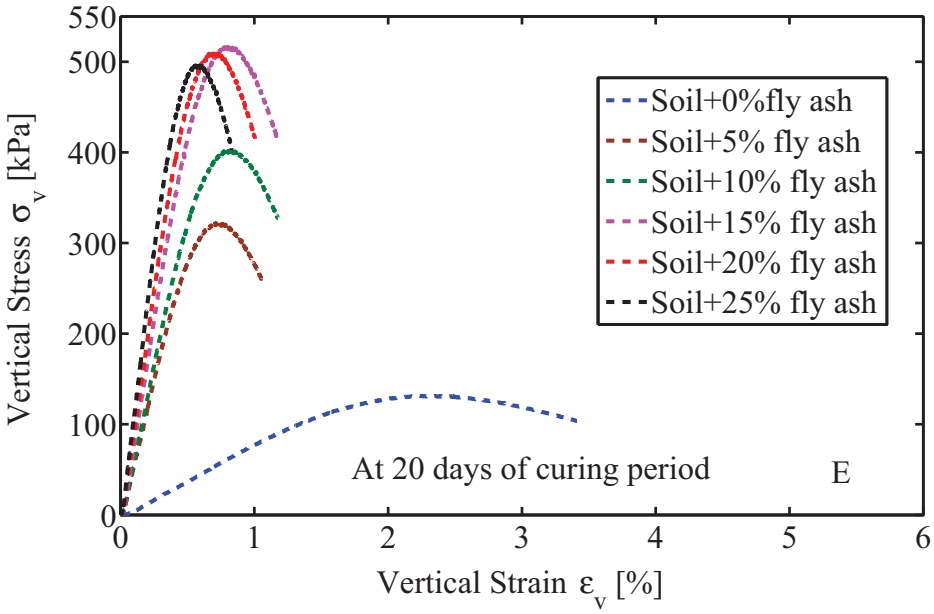

Figure 4.9: Relationship between the vertical stress [kPa] and vertical strain [%] at (A) 1 day, (B) 2 days, (C) 7 days, (D) 14 days and (E) 20 days of curing period for soils used.

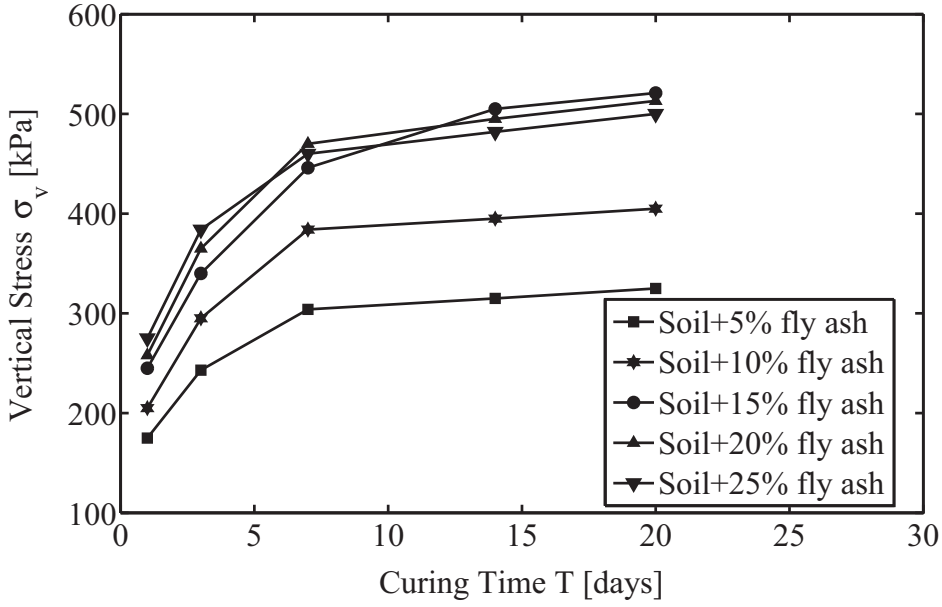

Figure 4.10: Relationship between the vertical stress [kPa] and curing period of soil used.

trix suction on the x-axis (log scale) against volumetric water content, θ [%], water content, w [%]; and the degree of saturation, S_r [%] ; on the y-axis. The soil water characteristic curves for all soils. Soil line and dish line in all Figures 4.11 [A-C] represent the fit curves, and the points represent actual experimental data. Two types of samples were prepared from undisturbed samples with different initial void ratio, soil with initial void ratio (e_o=0.83), namely (S-0.83) and soil with initial void ratio (e_o= 0.43), namely (S-0.43). From these Figures it can be analyzed that in both soils, volumetric water content, θ [%], water content, w [%] and degree of saturation, S_r [%] decrease with increases in matrix suction. Figure 4.11[A] shows the air-entry value (AEV= 280 [kPa]), which is defined as the matrix suction for which air starts to enter the largest pores in the soil, for compacted soil (S-0.43) is higher than with compression for compacted soil (S-0.83) (AEV= 100 kPa). SWCCs were affected with an increase in effort and this behavior could be attributed to the decrease in void ratio caused by the increase in compacted effort; hence, a more closed skeleton for water loss under a certain applied suction was obtained and leads to higher water holding capacity [Vanapalli et al., 1996]. The shape of the de-saturated zone for natural soil (S-0.83), which ranged between the air-entry value and the residual water content, had a steeper slope than the SWCC shape for the compacted soil (S-0.43). This is due to the open structure of compacted soil (S-0.83) and when the increase in the suction is greater than the air-entry value it causes a rapid outflow of water inside the large spaces between the particles. For compacted soil (S-0.83), the decrease in all hydro-mechanical properties can be seen to be less than when comparing with the soil (S-0.83) because the strong bond between particles requires greater suction to remove the molecules of water.

4.5.2 Effect of fly ash material on SWCCs

In the recent research, the hydraulic-mechanical behavior of unsaturated collapsible soil has been investigated by determining the soil-water characteristic curve under several initial conditions: the influence of moisture content, void ratio, suction state, the influence of net stress, loading path directions (drying and wetting path) and flow conditions using testing devices which measure water content and/or water pressure and/or cumulative water outflow and inflow. In the present work, a new condition is studied

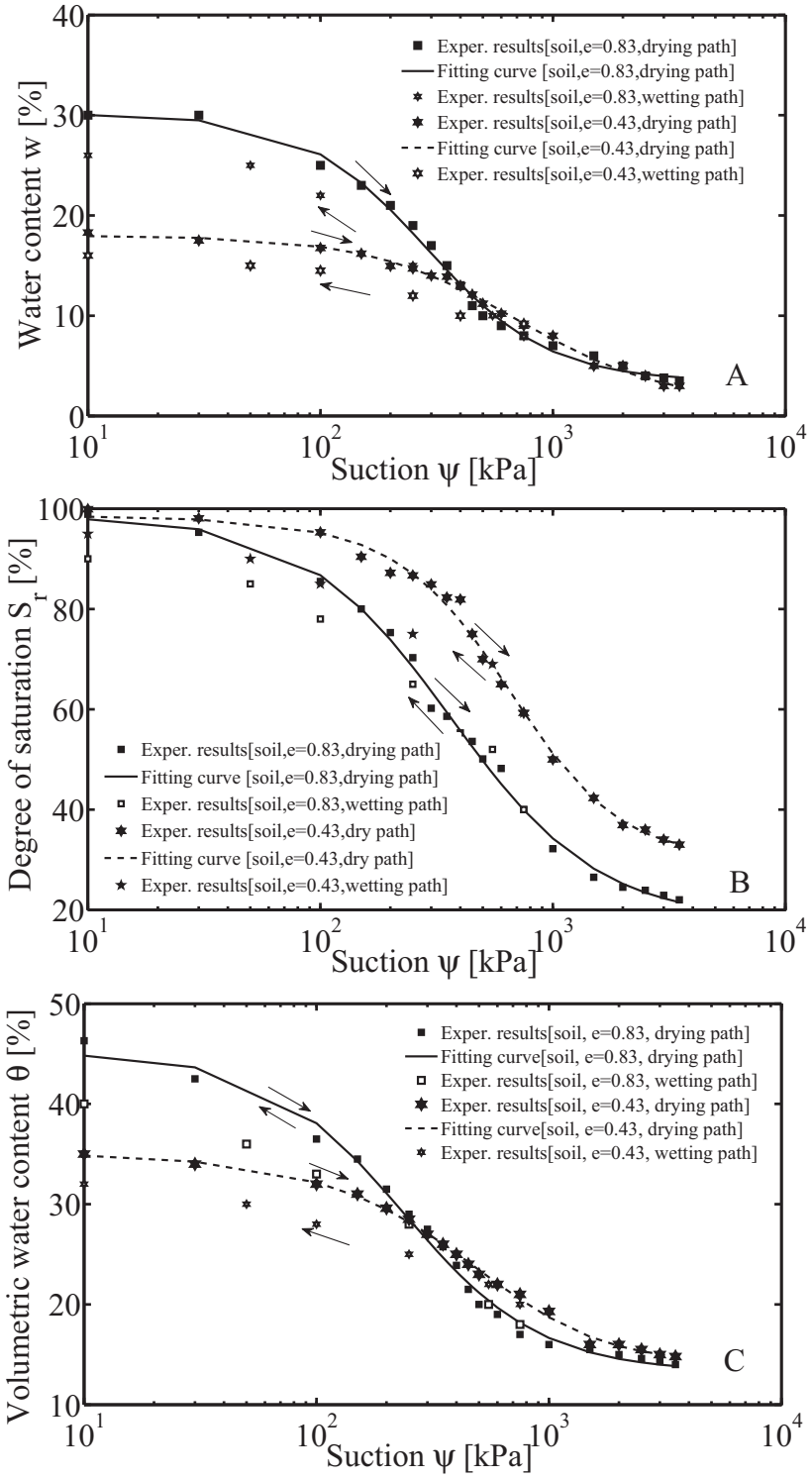

Figure 4.11: Relationship between the suction and (A) water content, w [%], (B) degree of saturation, S_r [%] and (C) volumetric water content, θ [%] for natural soil with e_o =0.83 and natural soil with e_o=0.43.

in addition to others which deals with the influence of the condition of fly ash stabilization material on the hydraulic-mechanical behavior of unsaturated collapsible soils. This parameter is very important for understanding the relationship between collapse potential and the mechanism of fly ash stabilization on the hydraulic-mechanical behavior of unsaturated collapsible soils.
Two soils, natural compacted soil (S-0.83) and soil mixed with 15% fly ash (S15FA), were prepared to study the effect of fly ash stabilization on the SWCCs. All Figures 4.12 show that the water holding capacity of the sample increased when mixed with fly ash. This could be explained by the fact that the added fly ash causes more pozzolanic products. These products are crystallized due to the pozzolanic reaction, which is expected to block the opened pores. This can be seen clearly in Figure 4.12 [C] (void ratio) which shows that the rate of decrease in the void ratio of sample (S15FA) is greater than when compared with sample (S-0.83). However, fly ash addition will usually cause a needle-like interlocking metalline structure, but the crystallization of pozzolanic products would block this opening.

4.6 Suction controlled oedometer test results

4.6.1 Suction-collapse behavior of natural soil

The suction controlled oedometer test (UPC-Barcelona cell test) was carried out to investigate the collapse potential under various water content levels and suction with applied vertical stress. The results show that the collapse value (C_p [%]) increases as suction decreases. Figures 4.13 show the change in void ratio in natural soil related to each suction value under different vertical stresses for soil (S-0.83) and (S-0.43).
It can be seen that the sample tested under vertical of 50 kPa presented an almost negligible collapse potential when suction was decreased from 400 to 100 kPa. The largest part of collapse developed when the suction was reduced from 100 to 0 kPa. At the other extreme, a rather different behavior is observed. At 200 and 400 kPa vertical stress, the collapse potential begins to increase for suction less than 250 kPa. Thus, the soil is capable of supporting the suction reduction up to a limit value, after which collapse strain begins to develop more intensively and this behavior should be related to the associated water retention characteristics of the soil. It was considered

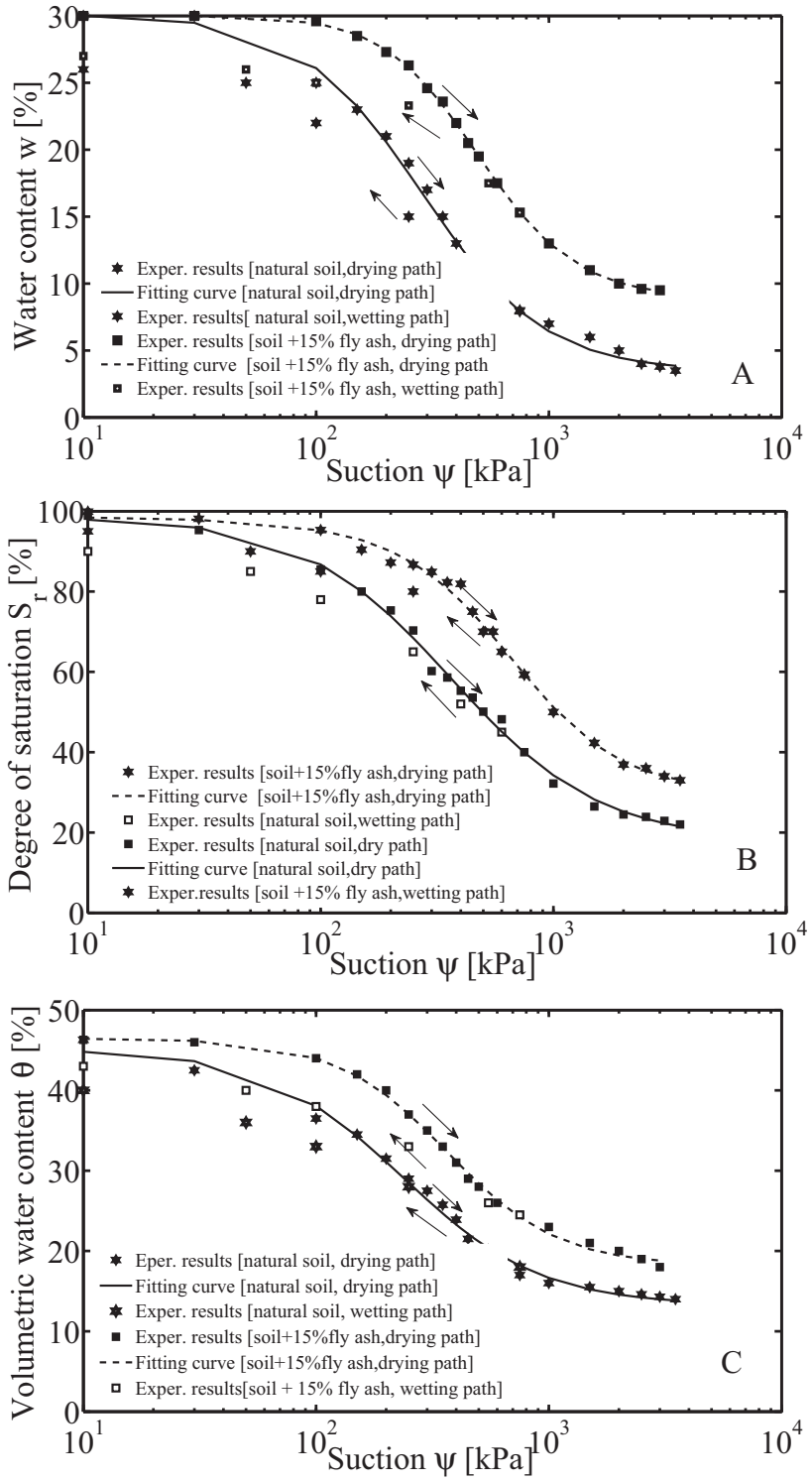

Figure 4.12: Relationship between the suction and (A) water content, w [%], (B) degree of saturation, S_r [%] and (C) volumetric water content, θ [%] for natural soil with e_0= 0.83 and soil mixed with 15% fly ash e_0= 0.83.

that the collapse potential for suction = 0 kPa corresponds to 100 % of collapse. For soil (S-0.83), at 50 kPa of vertical stress, the reduction in suction from 400 to 100 kPa caused 8.06% of collapse potential but when the suction is reduced from 100 to 0 kPa, the accumulated collapse potential rises from 40% to 100 %. At a vertical stress of 200 and 400 kPa, the reduction in suction from 400 - 250 kPa caused 2.63% and 2% of collapse potential, respectively. As suction is reduced from to 250 to 0 kPa, the accumulated collapse potential rises from 40 % to 100 % for 200 kPa and 400 kPa of vertical stress, respectively. Furthermore, the results show that collapse strains start to increase at a faster rate at suction values above air-entry level. As shown in SWCC curves, larger collapse seems to be associated with the de-saturation zone of SWCC, thus it is reasonable to suppose that this critical value is associated with the residual suction that depends on the load applied to the sample.

For soil (S-0.43) at all vertical stresses (50, 200 and 400 kPa), the reduction of the suction value from initial suction 400 to the 0 kPa caused a slight reduction in void ratio and low collapse values. This is due to the strong bond between the particles of this soil, needing more suction to remove the water molecules.

4.6.2 Suction-collapse behavior of fly ash stabilized soil

The results show that the mixing of fly ash with natural soil (S) causes an increase in the resistance and strength of soils and a reduction in void as well as collapse potential. The highest reduction in voids was recorded at 200 kPa vertical stress and they decreased from 0.83 to 0.7. Further, a decrease in collapse was observed from (9.2% to 4%) of soils (S) when mixed with 15% fly ash. This is due to the fact that, in the macro-structure of soil, when fly ash is mixed with soil in the presence of water, a set of reactions occur that result in the dissociation of lime (CaO) in the binders and the formation of cementations and pozzolanic gels [calcium silicate hydrate gel (CSH) and calcium aluminate silicate hydrate gel (CASH)]. These reactions are referred to as cementations and/or pozzolanic reactions that result in the formation of cementation gels. The decrease in collapse value and increase in strength in natural soil were found to be roughly related to the type and quantity of possible reaction products (i.e. CSH for short-term strength and pozzolanic reaction product, CASH for long-term strength gain). These new pozzolanic products fill the voids, leading the soil structure to be-

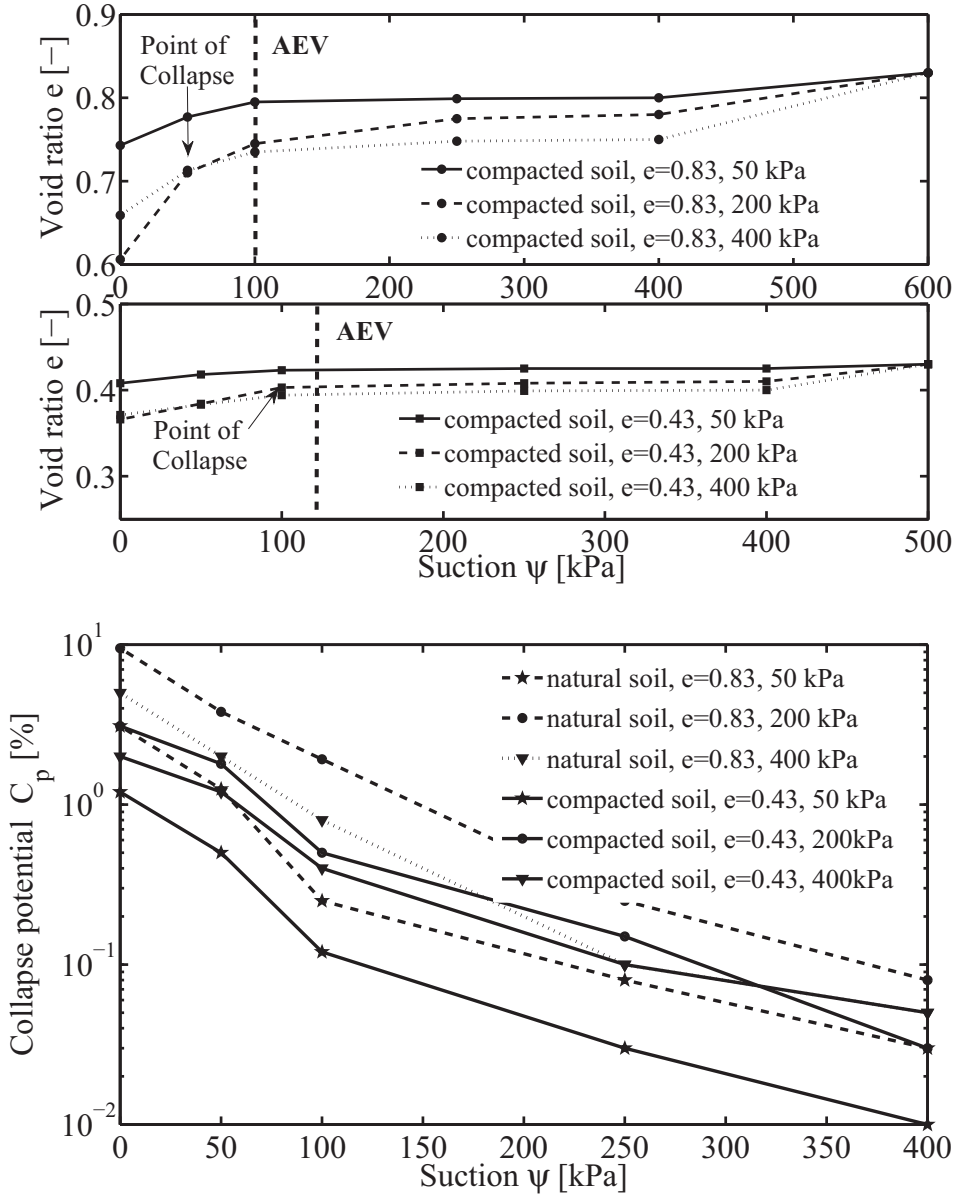

Figure 4.13: Void ratio vs. suction (top) and collapse potential vs. suction (bottom) for natural soil (S-0.83) and (S-0.43).

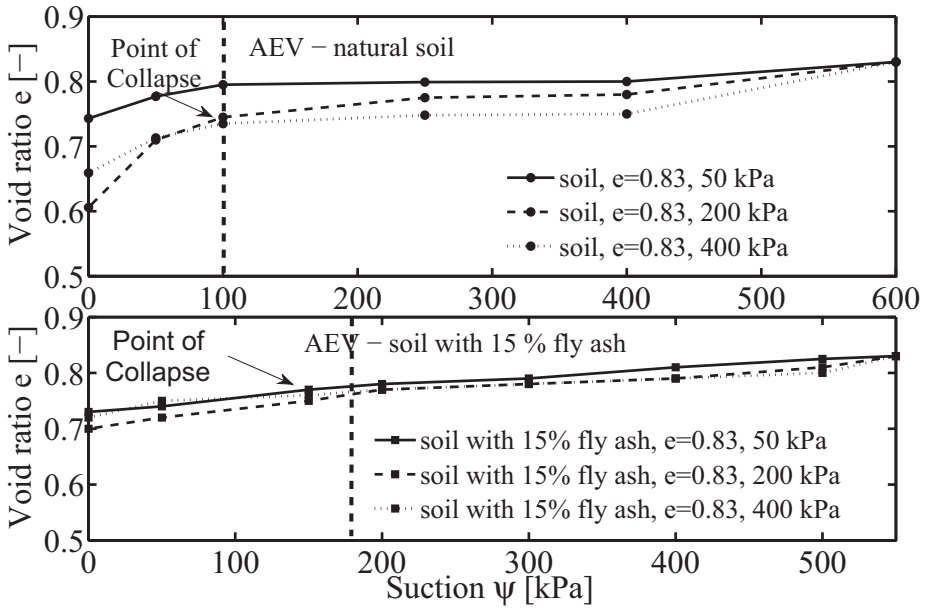

Figure 4.14: Void ratio vs. suction for natural soil and soil mixed with fly ash.

come denser [Rogers and Glendinning, 2000].

4.7 Summary

The addition of fly ash to natural soil led to a reduction of the plasticity index and contributed to an increase in the optimum moisture content and a decrease in the maximum dry density. By the addition of fly ash, the free calcium of fly ash exchanges with the adsorbed cations of the clay mineral, which results in reduction in size of the diffused water layer surrounding the clay particles. This reduction in the diffused water layer allows the clay particles to come closer to one another, causing flocculation and agglomeration of the clay particles.

The collapse potential of undisturbed natural soils with loose material (e_0= 0.83) and undisturbed field compacted soil (e_0= 0.43) depends on the hydro-mechanical properties of the soil skeleton, on the physical-chemical properties, double layer size and attractive / repulsive forces of pore fluid. The collapse potential is decreased when increasing fly ash content is mixed with the addition of chemical stabilizing agents (fly ash). The cementitious / pozolanic products formed as a result of the chemical reac-

tions between the silica and the alumina and the additives joins the soil particles, and ion exchange decreases the size of the double layer.
The magnitude of collapse potential depends on the gradient of the SWCC slope inside the de-saturated zone, the air-entry value and the fabric water holding capacity. The stepwise reduction of suction causes collapse, while the magnitude of collapse depends on vertical stress and initial void ratio. The addition of fly ash to natural soil causes higher air-entry value (AEV), increased water holding capacity and changes in the hydro-mechanical properties due to the increase in density as a result of new pozolanic products as well as of ion exchange.
In the case of the studied stabilized soils, unconfined compressive strength (qu) and elasticity modulus (E_{secant}) increased and failure axial strain (ε_f) decreased dramatically with the addition of fly ash. The mechanical behavior of fly ash stabilized soils was changed from ductile to brittle through long-term curing.

Chapter 5

Wave based analysis of non-stabilized and stabilized soil

5.1 Introduction

In this chapter are presented and discussed the experimental results of wave based analysis of soil behavior in this study. It consist of two main parts: the first part are presented and discussed the electromagnetic properties results of non-stabilized soil (natural collapsible soil). Moreover, the results of the electromagnetic properties of fly ash-stabilized soil are provided for two cases: (i) at natural water content without loading and (ii) with different loadings in order to study the collapse phenomenon in relation to electromagnetic properties. The second part contain the results of seismic waves propagation in the soil in non-stabilized state and for fly ash stabilized state which include shear stiffness - collapse test results during the loading and de-saturation processes and the ultrasonic test results (P and S wave) of fly ash-stabilized soil.

5.2 Electromagnetic soil properties results

5.2.1 Electromagnetic properties results of non-stabilized soil

In Figure 5.1, determined dielectric relaxation behavior is represented in the frequency range from 1 MHz to 5 GHz for a sample of undisturbed natural loose material soil

at a water content of 5.6% and a void ratio of 0.83 as well as a disturbed lab sample compacted and nearly saturated with w = 22.6% and e_0= 0.64.

The high frequency range is dominated by free water relaxation (called primary process). The relaxation strength of the process is quantitatively related to the volume fraction of free pore water [Wagner and Lauer, 2012]. Typically, the frequency range below 1 GHz down to about 1 MHz is dominated by two secondary relaxation processes. These two relaxation processes are related to interactions between the aqueous pore solution and mineral surfaces such as interface water relaxation, counter ion relaxation and Maxwell Wagner-Polarisation [Ishida et al., 2000] and [Wagner et al., 2011]. In addition, in the lower frequency range, the imaginary part of the complex effective relative permittivity is dominated by the apparent direct current conductivity contribution. The results of the electromagnetic properties test on the unsaturated and nearly saturated samples conclude that saturated soil has a high apparent direct current conductivity contribution (σ'_{Dc} = 1.47 [S/m]) when compared to unsaturated soil (σ'_{Dc} = 0.058 [S/m]), (see Figure 5.1). Hence, it can be considered that this type of soil undergoes great changes in physical and chemical properties during wetting and compaction, which makes collapse easier to understand. The results at low water content indicate a high apparent direct current conductivity contribution which dominates the imaginary part of the spectrum in the low frequency range. In comparison to a silty clay loam with a certain amount of swelling, clay minerals are in the range of 1 [mS/m] at the same water content [Wagner et al., 2011]. The high direct current conductivity contribution induces a strong low frequency relaxation process. The contribution of free pore water to the relaxation dynamics in the high frequency range is also strongly overlapped, leading to dispersion in the real part of the permittivity in the frequency range above 1 GHz coupled with strong absorption in the imaginary part. Hence, there is a small amount of free pore water and thus the magnitude of the apparent direct current conductivity is expected to be related to the surface conductivity rather than conductivity in the pore solution at these low water contents. The comparison of the electromagnetic properties of the unsaturated with the nearly saturated sample clearly indicates the water content effect. As expected, permittivity as well as conductivity increases with increasing water content. However, the real part of the permittivity in the low frequency range around 1 MHz of the unsaturated soil is higher than the permittivity of the nearly saturated soil. The dispersion decreases with water content

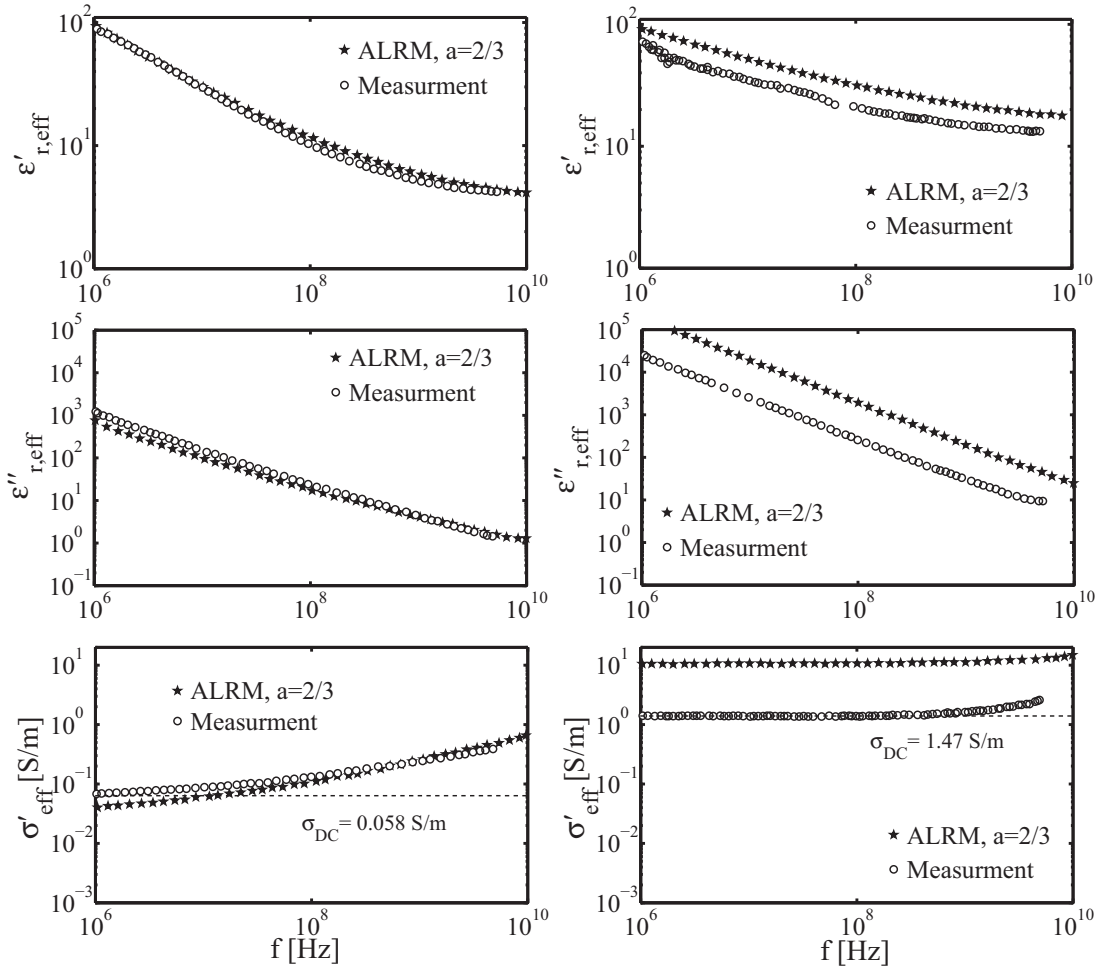

Figure 5.1: (from top to bottom) Real $\varepsilon'_{r,eff}$ and imaginary part $\varepsilon''_{r,eff}$ of the complex effective relative permittivity $\varepsilon^*_{r,eff}$ and real part σ'_{eff} of the complex effective electrical conductivity (σ^*_{eff}) as a function of frequency (left) undisturbed natural loose material sample at gravimetric water content w = 5.6 % and void ratio e_0= 0.82 and (right) a nearly saturated disturbed compacted sample at with w = 22.6 % and e_0= 0.64.

and a reduction of the relaxation strength of the process from 50 to 17 coupled with a decrease of the relaxation time from 61 ns to 1.1 ns was observed. Furthermore, the apparent direct current conductivity of the soil at near saturation is high. This is a clear indication of chemical processes in the soil with changes in water content strongly affecting pore water chemistry and thus interface processes. Moreover, the high apparent electrical conductivity reflects a concentrated pore solution which further reduces the formation of an electrical double layer. From the electromagnetic test, the observed dielectric relaxation dynamics of the nearly saturated soil sample support this microscopic level due to the high apparent direct current conductivity, the strong increasing of the free water process, as well as the strong reduction coupled with the shift to higher frequencies of the process with increasing water content.

5.2.1.1 Influence of hydro-mechanical properties on electromagnetic properties

The results of electromagnetic properties tests on collapsible soils in relation to the hydro-mechanical and collapse mechanism are presented and discussed in this section. The broadband electromagnetic measurements were performed at a frequency range from 10 MHz to 10 GHz at room temperature and atmospheric pressure by means of TDR technique with an open ended coaxial line [Wagner et al., 2011]. Remolded samples of collapsible soil with varying porosity and gravimetric water content were used for the electromagnetic tests. The first set of tests were performed on samples with initial void ratio of e_0= 0.83 (natural loose condition) and varying water content. The second set comprised of samples with initial void ratio of e_0= 0.43 (lab compacted condition) and with varying water contents. To identify the effects of changes in both porosity and water content on the electromagnetic properties at the same time, a third set of samples with varying void ratios and water content was used. The results of electromagnetic measurements on collapsible soil samples at natural loose condition (e_0= 0.83), lab compacted condition (e_0= 0.43) and with varying void ratios are shown in Figures 5.2, 5.3 and 5.4, respectively. In these Figures, it can be seen that the complex effective relative permittivity of the soil is highly influenced by changes in water content of the soil as compared to changes in porosity.

The dielectric properties of soil were affected by the porosity (n) and volumetric

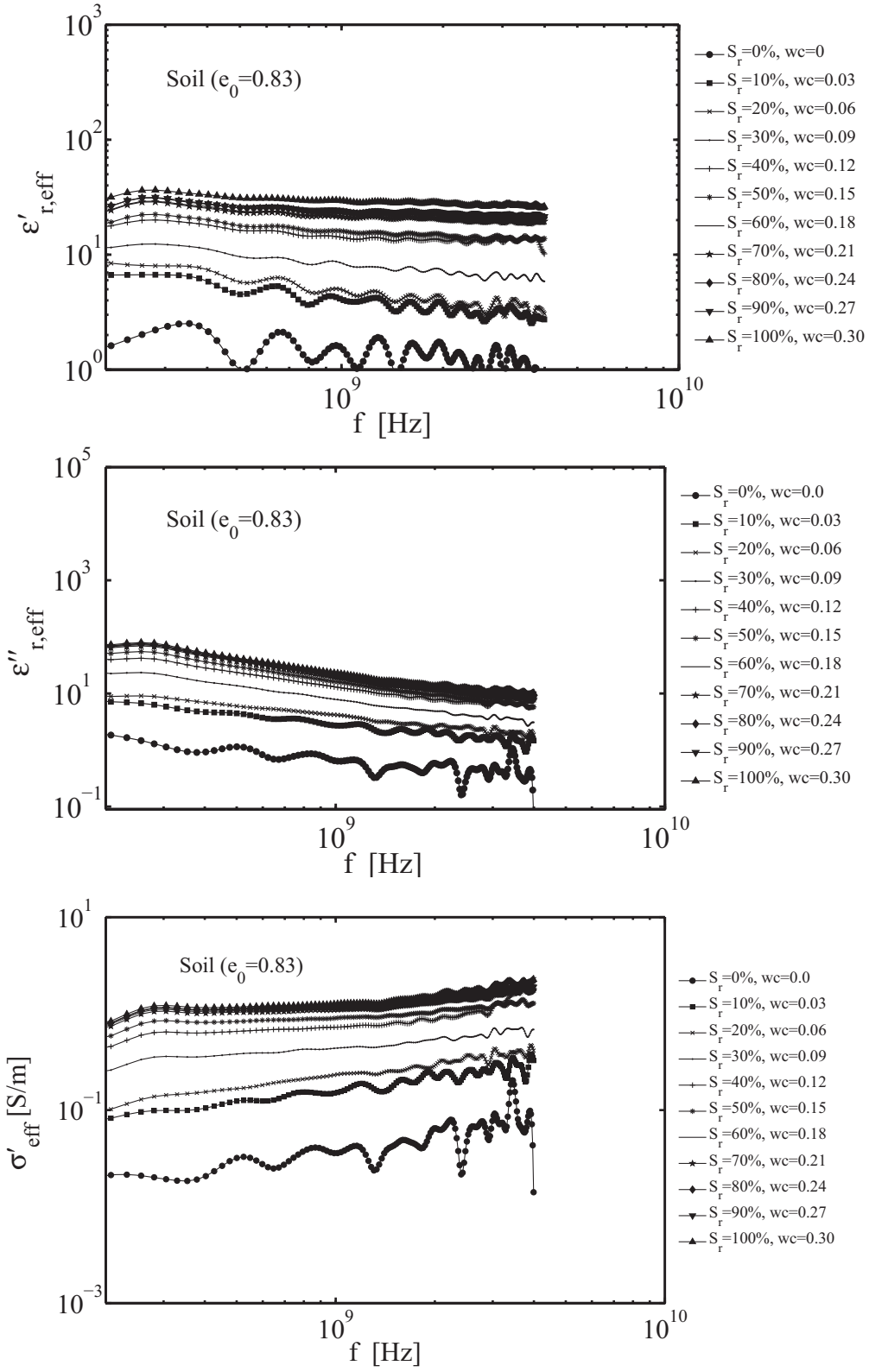

Figure 5.2: (From top to bottom) relationship between frequency, $\varepsilon'_{r,eff}$, $\varepsilon''_{r,eff}$ and σ'_{eff} of the natural soil (e_0= 0.83) with different water content.

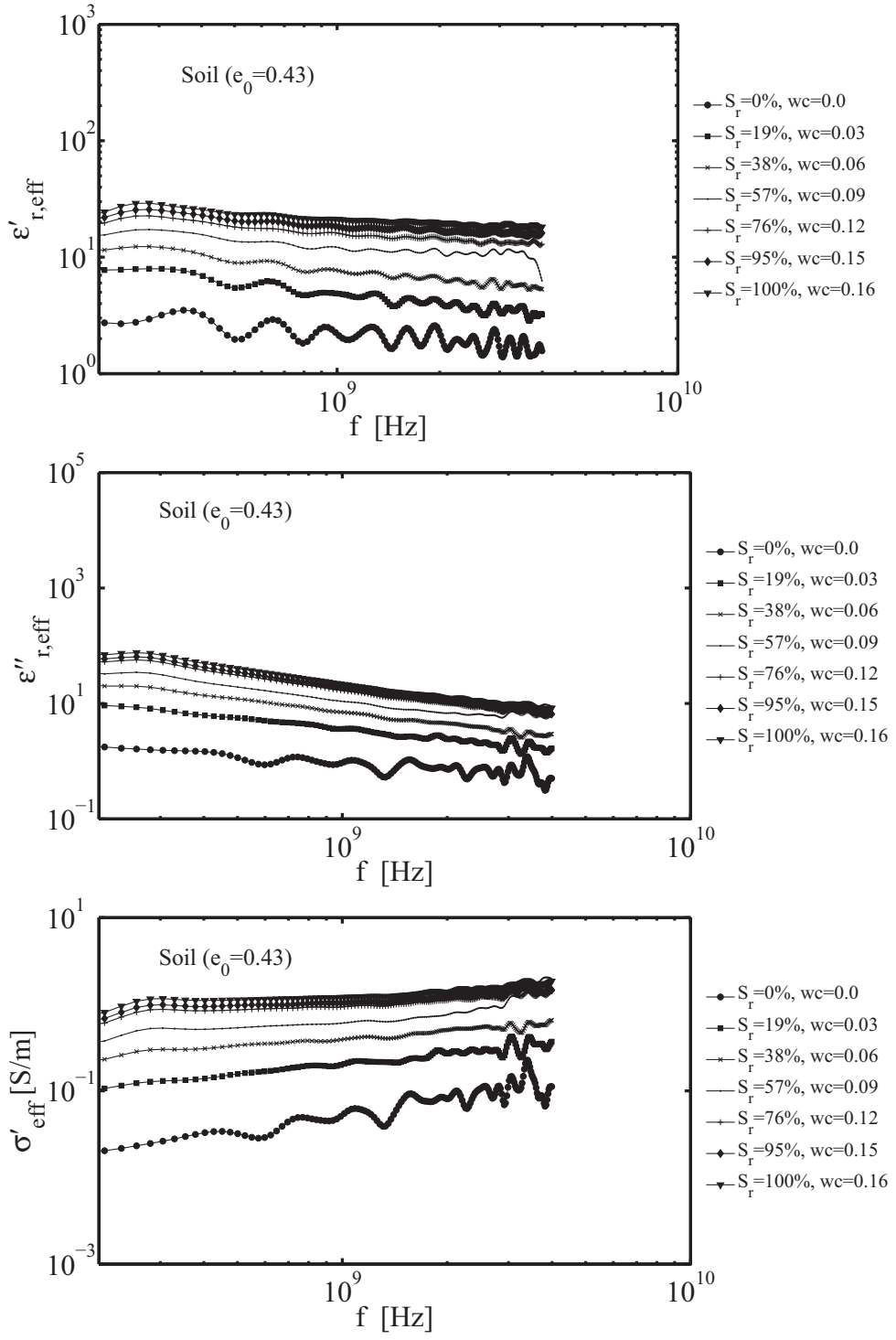

Figure 5.3: (From top to bottom) relationship between frequency, $\varepsilon'_{r,eff}$, $\varepsilon''_{r,eff}$ and σ'_{eff} of the natural soil (e_0=0.43) with different water content.

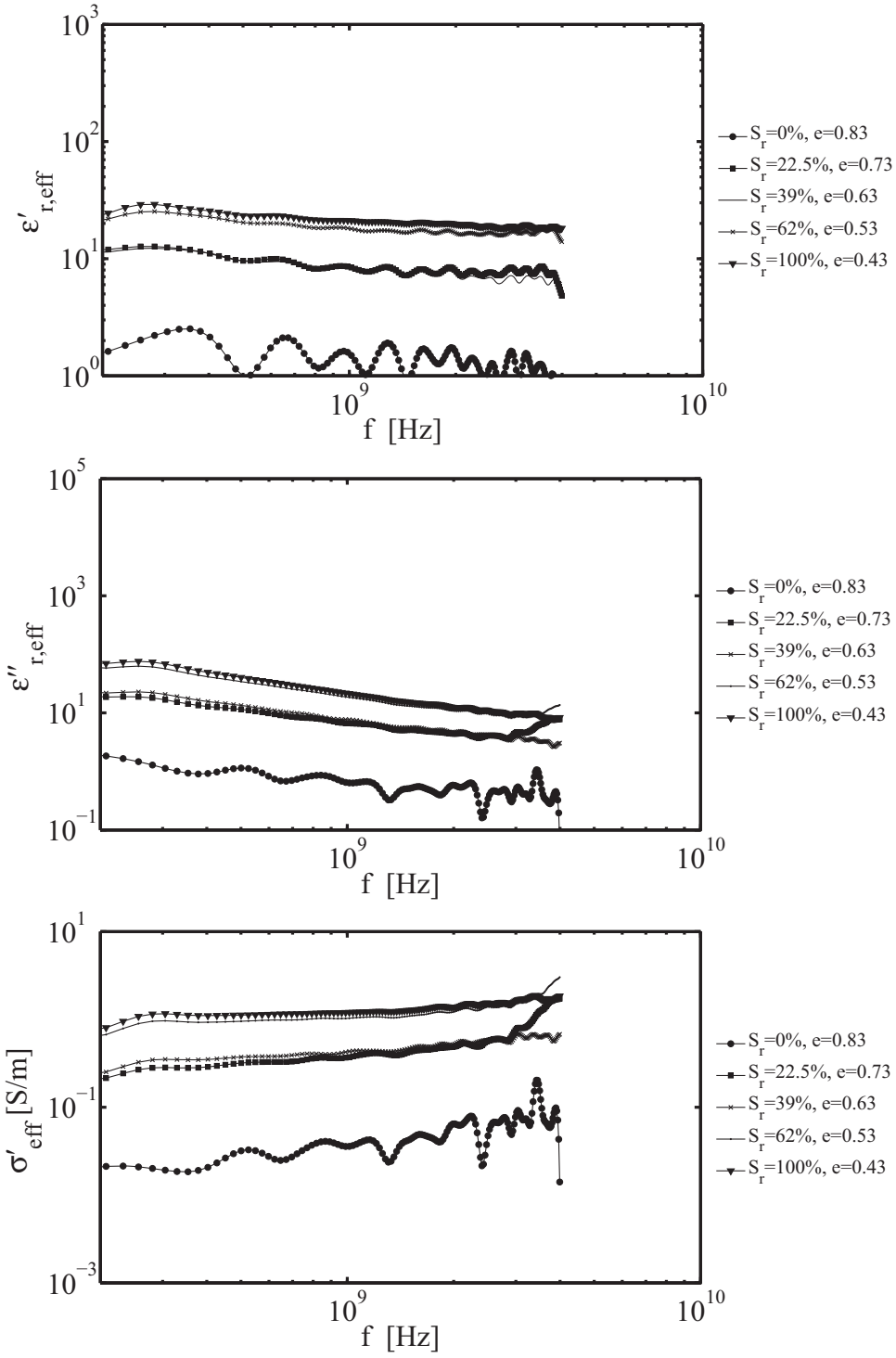

Figure 5.4: (From top to bottom) relationship between frequency, $\varepsilon'_{r,eff}$, $\varepsilon''_{r,eff}$ and σ'_{eff} of the natural soil (varying e_0) with different water content.

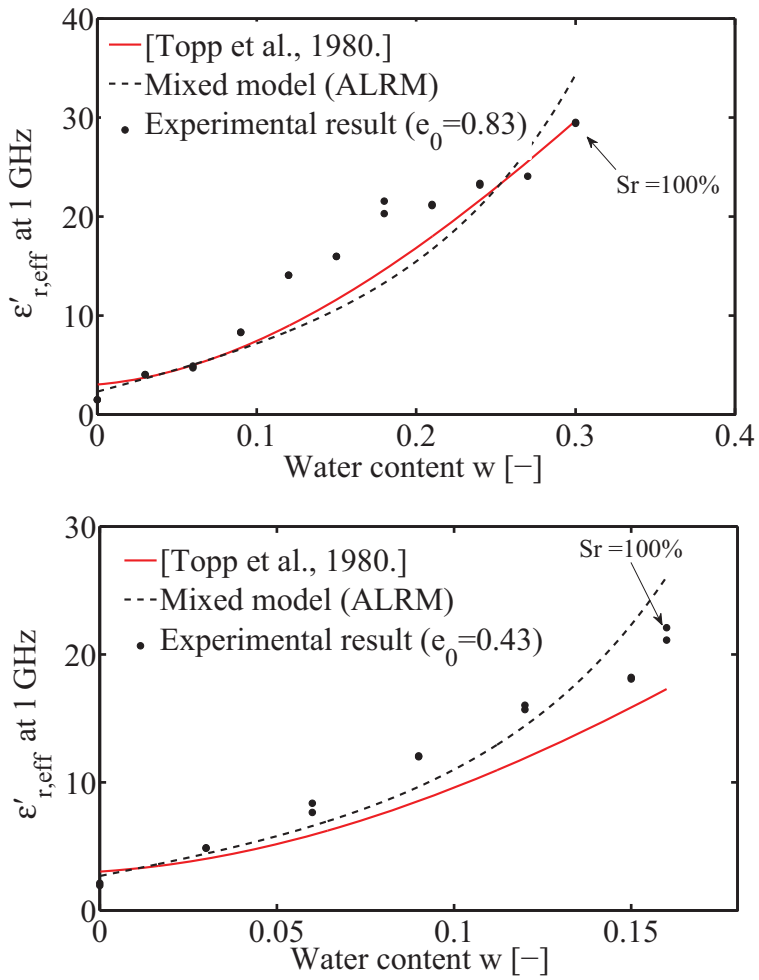

Figure 5.5: Experimental results and Simulation model based on [Top et al.,1980] and Mixed model (ALRM) between the ($\varepsilon'_{r,eff}$ at 1GHz) with water content *w* for the natural collapsible soil with initial void ratios of 0.83 and 0.43.

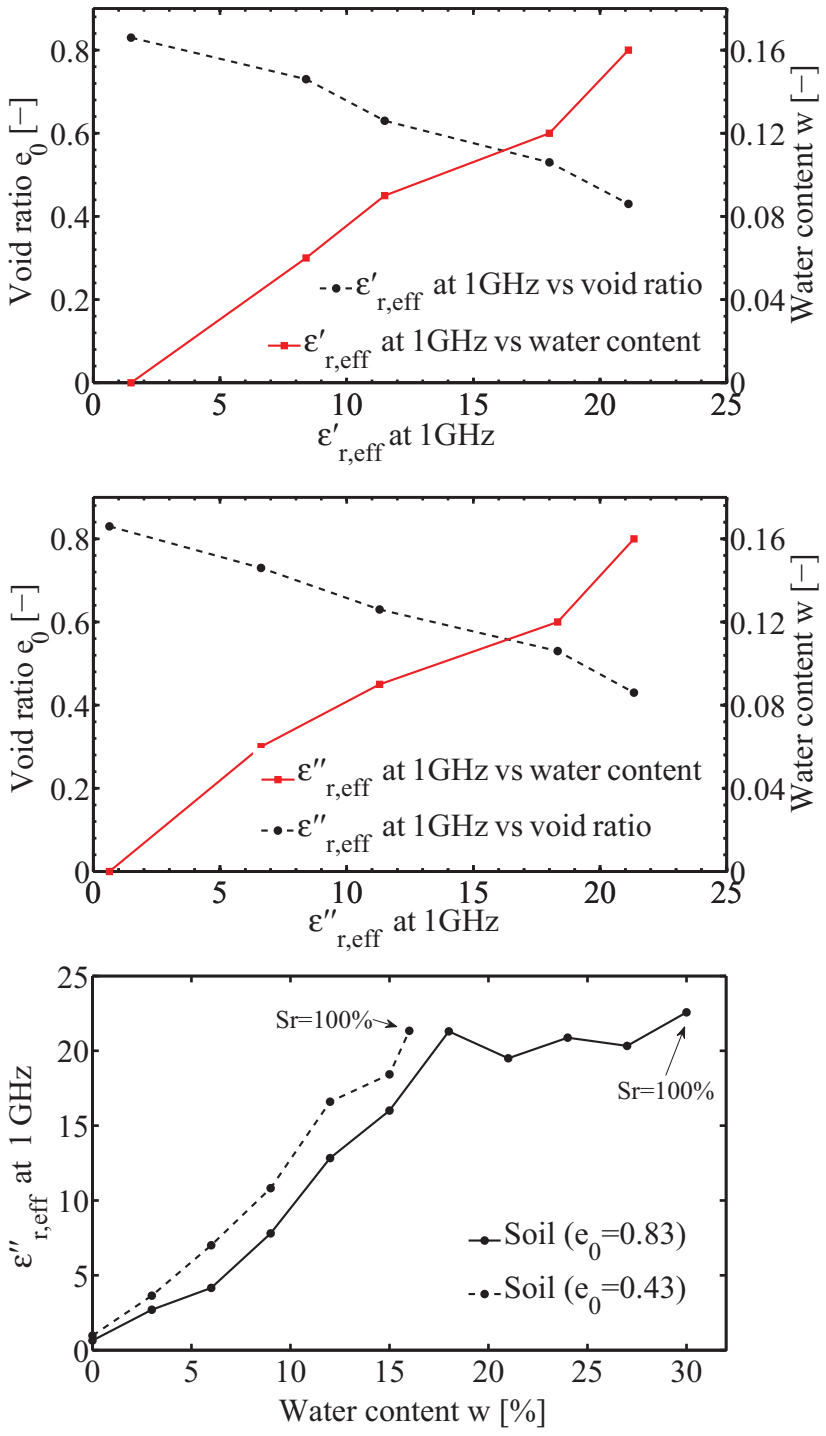

Figure 5.6: (Top and middle) relationship between $\varepsilon'_{r,eff}$ and $\varepsilon''_{r,eff}$ at 1GHz with different water content w and void ratio e_0, (bottom) variation $\varepsilon''_{r,eff}$ at 1GHz with different water content of the natural collapsible soil with initial void ratios of 0.83 and 0.43.

water content (θ). From this fact, it can be seen that the $\varepsilon'_{r,eff}$, $\varepsilon''_{r,eff}$ and $\sigma_{eff}{}'$ of both soils (soil with e_0= 0.83 and soil with e_0= 0.43) increase with rising water content at constant void ratio. This is due to the fact that during the de-saturation process, the water helps to dissolve a great amount of salts in this soil which leads to the release of high Na in the pore water. The greater mobility of Na causes the increase of the repulsive force, the double layer size and finally the dielectric properties of soil. The results further show that the rate of increase in the $\varepsilon'_{r,eff}$, $\varepsilon''_{r,eff}$ and σ'_{eff} of soil (e_0= 0.83) was higher in comparison with soil (e_0= 0.43) because the higher void ratio causes greater ion mobility in the pore water. The results of the dielectric properties of soil when both void ratio and water content changes show that the effect of porosity change is less than when compared with the water content change, which makes it clear that this type of soil (collapsible soil) is a highly sensitive to the water.

5.2.1.2 Influence of vertical stress on electromagnetic properties

In Figures 5.7 and 5.8 the results are shown of electromagnetic measurements taken during a one dimensional loading test on a collapsible soil at optimum moisture condition (w = 18%). The sample was loaded with predefined loading steps up to a maximum of 400 kPa, followed by un-loading back to initial condition. The electromagnetic measurements were made before and after each load step with the help of the open ended coaxial line. The complex effective relative permittivity of the soil increased significantly with each load increment on the soil until the maximum applied load of 400 kPa was reached. This is indicated in Figure 5.7, where with each application of a vertical stress increment there is an equivalent jump in the complex effective relative permittivity of the soil. The increase in the complex effective relative permittivity of the collapsible soil is attributed to the reduction in the porosity of the sample with an increase in vertical stress. As expected, during the unloading stage, insignificant changes in the complex effective relative permittivity of the soil were recorded. This is primarily due to the low deformation recovery (elasticity) of collapsible soils upon unloading, which in turn induces negligible changes in soil porosity.

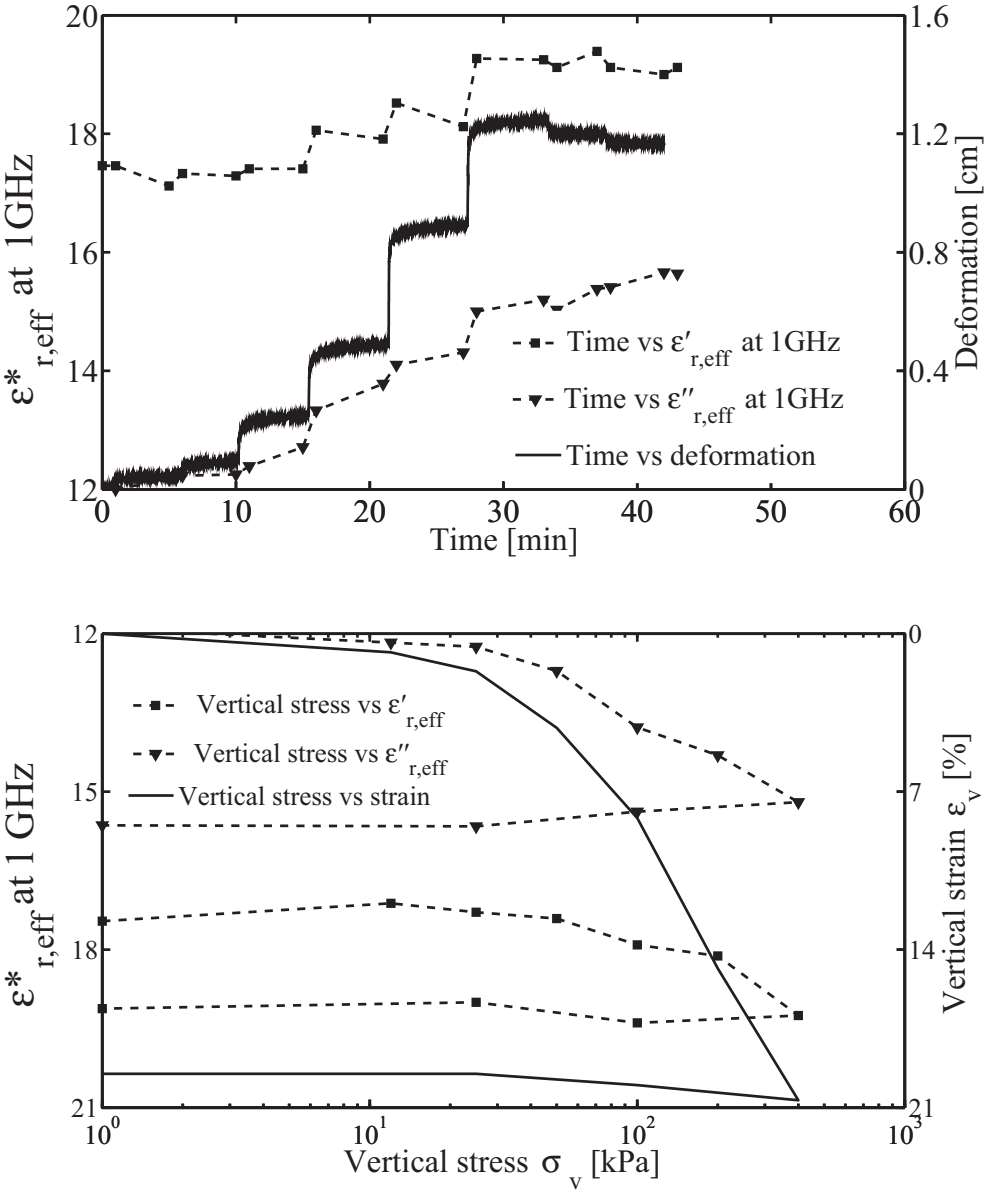

Figure 5.7: Relationship between $\varepsilon'_{r,eff}$ and $\varepsilon''_{r,eff}$ at 1GHz at different vertical deformation with time (top) and with different vertical stresses (bottom) of the natural collapsible soil (e_0=0.83).

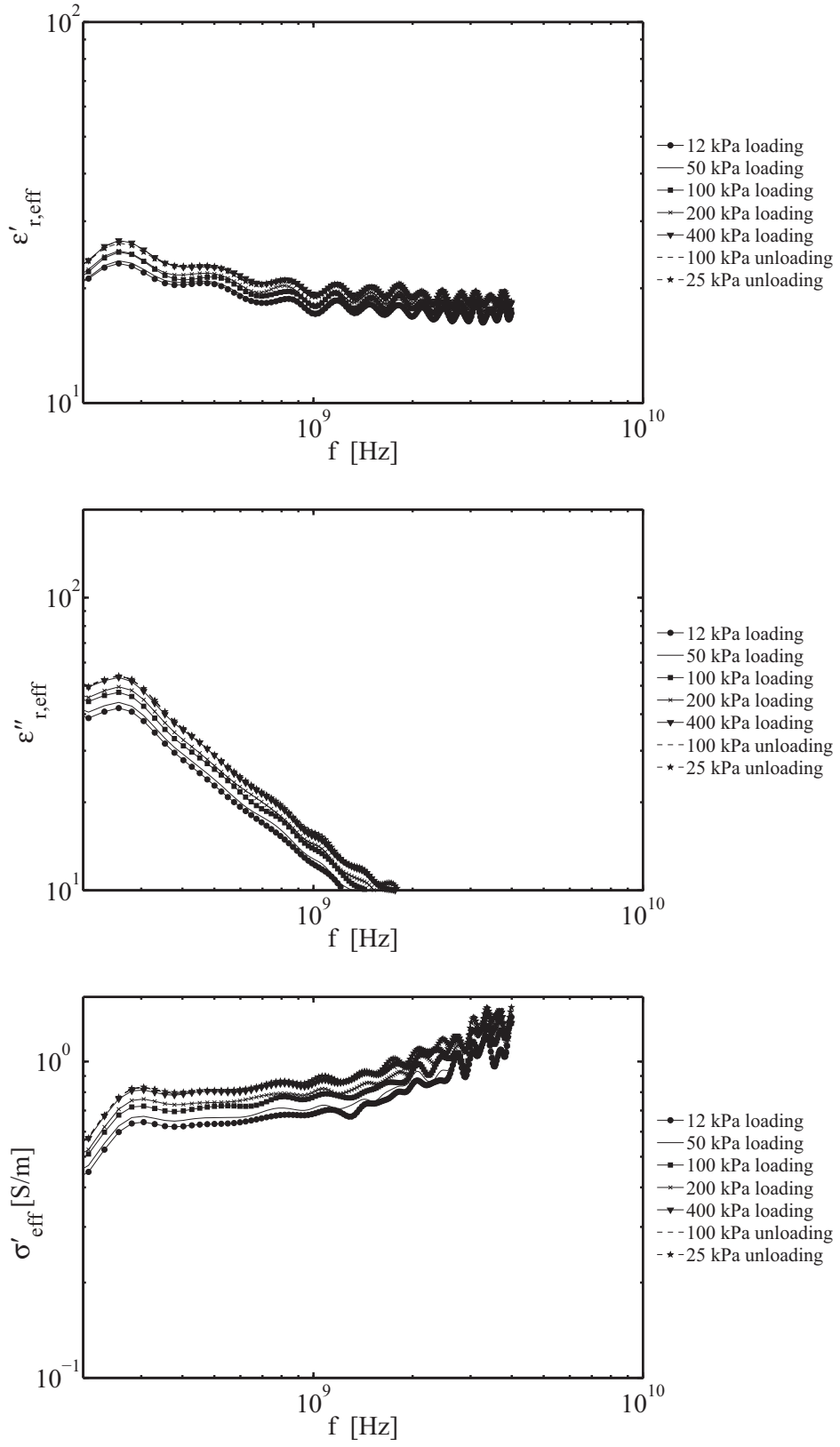

Figure 5.8: (From top to bottom) relationship between frequency, $\varepsilon'_{r,eff}$, $\varepsilon''_{r,eff}$ and σ'_{eff} of the natural collapsible soil (e_0=0.83) with with different vertical stress.

5.2.2 Electromagnetic properties results of fly ash-stabilized soil

5.2.2.1 Influence of fly ash content and curing time on electromagnetic properties

Figures 5.9, 5.10, 5.11 and 5.12 show the experimentally determined electromagnetic material properties of fly ash-mixed soils at a bulk soil case and at a pore water case of mixed soil which is extracted from the soils investigated, respectively, in terms of real part $\varepsilon_{r,eff}^{'}$ and imaginary part $\varepsilon_{r,eff}^{''}$ of complex effective relative permittivity and real part $\sigma_{eff}^{'}$ of complex effective electrical conductivity. All fly ash-stabilized soils show a clear dispersion and strong absorption in the investigated frequency range. However, the high frequency part of ($\geq$ 1 GHz) as well as the low frequency part of ($\leq$ 10 MHz) has low dispersion. The results of the electromagnetic properties tests on the soils investigated at a bulk state indicate an appropriate contribution of water relaxation at high frequencies. Hence, the comparison between $\varepsilon_{r,eff}^{'}$ of the different fly ash-soils mixed at the high frequency of ($\varepsilon_{r,eff}^{'} \geq$1 GHz) of different fly ash percentages imply that the change in chemical properties of solid soil particles influence dielectric soil properties. It is observed that the higher the fly ash content, the higher the dielectric properties $\varepsilon_{r,eff}^{'}$, $\varepsilon_{r,eff}^{''}$ and $\sigma_{eff}^{'}$. This is due to the fact that the hydration of fly ash with water causes an increase in Ca^{+2} and pH values of the pore water [Suzuki et al., 1981.]. Calcium silicate hydrate C-S-H begins to form and the clay is transformed into a calcium-clay through ion exchange with calcium ions produced by fly ash hydration. The increased concentration of Ca^{+2} in the pore water of the double layer causes a strengthening of the attraction force which leads to flocculation of particles. The new pozzolanic products block the voids, which results in decreasing porosity and increasing permittivity [Broderick and Daniel, 1990]. As shown in Figure 5.13, the dielectric properties show a high value after 5 hours of curing time which then decreases up to 3 days. This could be due to the first reaction of the fly ash causing ion exchange between the Na^{+1} in clay and Ca^{+2} in the fly ash, thus increasing ionic mobility and increasing the surface area. After 3 days of curing time, the dielectric properties show a gain, increasing up to 14 days and then decreasing. This behavior can be attributed to the second reaction of fly ash (pozzolanic reaction). At this stage, the free water will change to the bound water in the structure of the new pozzolanic products which cause blocking, reducing the porosity and finally reducing the amounts of Ca^{+2} in pore water

[Santamarina and Fam, 1995].

Figure 5.9: Relationship between frequency, $\varepsilon'_{r,eff}$ (top), $\varepsilon''_{r,eff}$ (middle) and σ'_{eff} (bottom) for the fly-stabilized soils with 0%, 5% and 10% of fly ash content and at different curing time as a bulk soil state.

Figure 5.10: Relationship between frequency, $\varepsilon'_{r,eff}$ (top), $\varepsilon''_{r,eff}$ (middle) and σ'_{eff} (bottom) for the fly-stabilized soils with 15%, 20% and 25% of fly ash content and at different curing time as a bulk soil state.

Figure 5.11: Relationship between frequency, $\varepsilon'_{r,eff}$ (top), $\varepsilon''_{r,eff}$ (middle) and σ'_{eff} (bottom) for the fly-stabilized soils with 0%, 5% and 10% of fly ash content and at different curing time as a pore water state.

Figure 5.12: Relationship between frequency, $\varepsilon'_{r,eff}$ (top), $\varepsilon''_{r,eff}$ (middle) and σ'_{eff} (bottom) for the fly-stabilized soils with 15%, 20% and 25% different fly ash content and at different curing time as a pore water state.

5.3 Seismic wave results

5.3.1 Seismic wave results of non-stabilized soil

5.3.1.1 Influence of vertical stress and de-saturated processing on seismic wave properties

Stiffness-collapse tests are essential tests which can describe the relation between the vertical stress - strain and the stiffness change under collapse potential. Shear wave velocity V_s and longitudinal wave velocity V_p were determined based on the first arrival method. From these velocities, G_{max} and E_0 are calculated with equation 3.1 (see chapter 3). The velocity readings were taken at four stages: at initial condition without loading, at loading before saturation, at loading during de-saturation and at fully saturated. The results of V_s, V_p), G_{max} and E_0 are shown in Figures 5.14 and 5.15. The results indicate that the V_s, V_p, G_{max} and E_0, at the loading stage before wetting (during the consolidation process), increase to (210 m/sec, 310 m/sec, 63 MPa and 145 MPa), (340 m/sec, 405 m/sec, 160 MPa and 230 MPa) and (325 m/sec, 375 m/sec, 155 MPa and 200 MPa) at 50, 200 and 400 kPa vertical stress, respectively. The increase of stiffness is due to that the soil starts to compact during this stage until maximum density is reached, after which there is no deformation change because it is fully compacted. Additionally, the soil in this stage has high suction stress (low water content) which in turn provides the soil structure with a high strength. Furthermore, in a dry state, the clay of this type of soil charge with a amount of Na^{+1} (based on the chemical analysis test), which causes strong attraction forces between the clay plates. This increasing leads the particles to be close together and thereby the soil exhibit a high stiffness. After starting with water (at the de-saturation process), the V_s, V_p, G_{max} and E_0 values decrease suddenly to (50 m/sec, 110 m/sec, 5 MPa and 18 MPa), (120 m/sec, 155 m/sec, 24 MPa and 40 MPa) and (90 m/sec, 90 m/sec, 12.5 MPa and 12.5 MPa) at 50, 200 and 400 kPa vertical stress, respectively. During saturation at a high loading, the breaking in cementation and/or changes in physical-chemical forces between soil particles occur because this type of soil (collapsible soil) is strongly dependent on the water. It is suggested that the reduction in the stiffness is due to two main reasons: (i) In macro-physical structure of collapsible soil with a high void ratio (loose structure), the resistance of clayey links between large grains is reduced by adding water

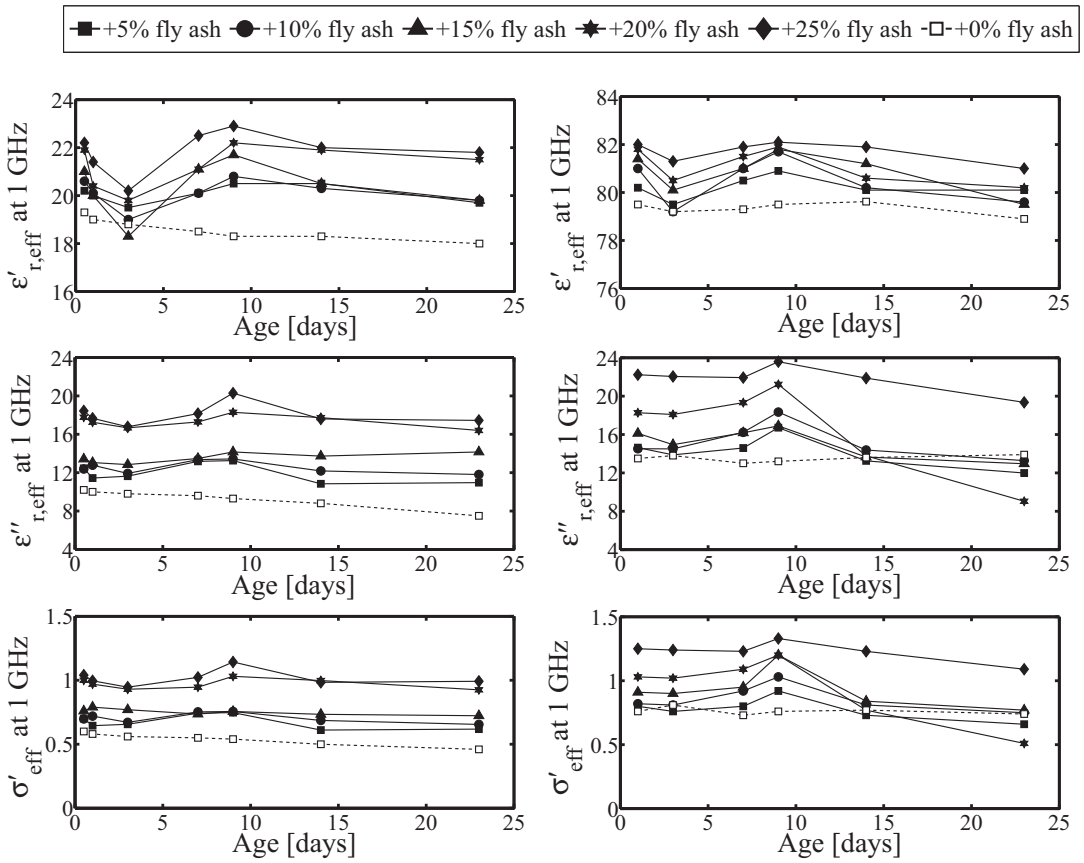

Figure 5.13: Relationship of $\varepsilon_{r,eff}^{'}$ (top), $\varepsilon_{r,eff}^{''}$ (middle) and $\sigma_{eff}^{'}$ (bottom) at different curing time for the fly-stabilized soil as a bulk soil state (left) and as a pore water state (right) with different fly ash content.

to a soil subjected to a constraint that causes a new radical rearrangement of particles and great loss of volume strain and stiffness. When this resistance becomes lower than the constraints of cutting, these links break and subsidence occurs. The other effect is mainly due to the cancellation of capillary suction in partially saturated soils. The water flooding causes the migration of fine particles through their structures from one horizon to another. (ii) In micro-elector-chemical process based on the structure of the double layer, the increase in the water content of soil causes decreasing of the ion concentration at the particles- water contact which causes an strengthening of repulsive forces and a weakening of attraction forces, along with a decrease in double layer size, which in turn reduce the bonding forces between particles as well as shear stiffness. The results also show that there is a strong link between soil water characteristics and shear stiffness results. The considerable reduction in stiffness occurred as the soil suction value was decreasing (during increases in water content) and is located in the de-saturated zone of SWCC after the air-entry value AVE. At the nearly saturated stage, the rates of decrease in the V_s, V_p, G_{max} and E_0 were slight and lasted until full saturation was reached. After this stage, there were obviously no changes in stiffness and there were no waves traveling through the soil, indicating very low shear stiffness.

5.3.2 Ultrasonic results of fly ash stabilized soil

5.3.3 Influence of fly ash content and curing time on (V_s) and (V_p) wave results

Ultrasonic velocity tests were conducted to evaluate the mixtures with fly ash to determine the variation and the correlation of the velocity with the percentage of fly ash stabilizing agent and curing time. As shown in Figures 5.16 5.17, the results of (V_s), (V_p), (G_{max}) and (E_0) rose when natural collapsible soil was mixed with fly ash (see Tables B.7 and B.8 in Appendix B). This is due to the fact that when fly ash is mixed with soil in the presence of water, two types of reaction occur: the hydration of fly ash releases calcium ions, which in turn replaces original cations (most commonly sodium ions) in clay particles. This process is known as the cation exchange process. The free calcium with higher valency cations (Ca^{+2}) of fly ash replaces the lower ion valency (Na^{+1}), and any cation will tend to replace one to the left of it, which leads to a reduc-

tion in the amount of (Na^{+1}) in the bentonite surface as well as the reduction in size of the diffused double layer surrounding the clay particles. This decrease in the diffused double layer allows the clay particles to come closer to one another. The reactions occur quite rapidly when fly ash is added to soil, and depending on the availability of various types of cations in the pore fluid, cation replacement can take place. The second reaction, which occurs in soil macro-structure, is cementation and/or pozzolanic reaction that results in the dissociation of lime (CaO) in the binders and the formation of cementations and pozzolanic gels [calcium silicate hydrate gel (CSH) and calcium aluminate silicate hydrate gel (CASH)]. These cementation gels act as binder cementation material around the soil particles that cause an increase in the contact area of soil particles. The increase of velocity values and stiffness were found to be roughly related to the type and quantity of possible reaction products (i.e., CSH for short-term strength and pozzolanic reaction product, CASH for long-term strength gain). The results indicate that the (V_s), (V_p), (E_0) and (G_{max}) values rise significantly with increases in the amount of fly ash for mix proportions of up to 15% fly ash. After this percentage, the values show only slight increases when compared to that of 15% fly ash. The reason could be that fly ash cementation/pozzolanic reaction starts with great intensity at the lower fly ash percentages (5, 10 and 15%) and high amounts of SiO_2 and Al_2O_3 in clay soil. As a result of this, the hydration reaction of the fly ash particles with the soil generates large amounts of cementation and pozzolanic production. For fly ash mixes with percentages higher than 15% (i.e. at 20 and 25%), there are not sufficient amounts of SiO_2 and Al_2O_3 in clay, and hence less hydration reaction and cementation. In these particular cases, the extra amount of fly ash particles lowers the bulk density and stiffness of the soil.

5.4 Summary

The electromagnetic properties test is used as a new tool to investigate the change in the hydro-mechanical properties (including change in water content, void ratio, vertical stress, collapse potential and fly ash-stabilized content). The electromagnetic results noted that the electrical permittivity and conductivity of the soil is highly influenced by changes in the water content, soil porosity and the chemistry of soil pore water. Therefore, the experiments provide the basis for understanding the functional relation-

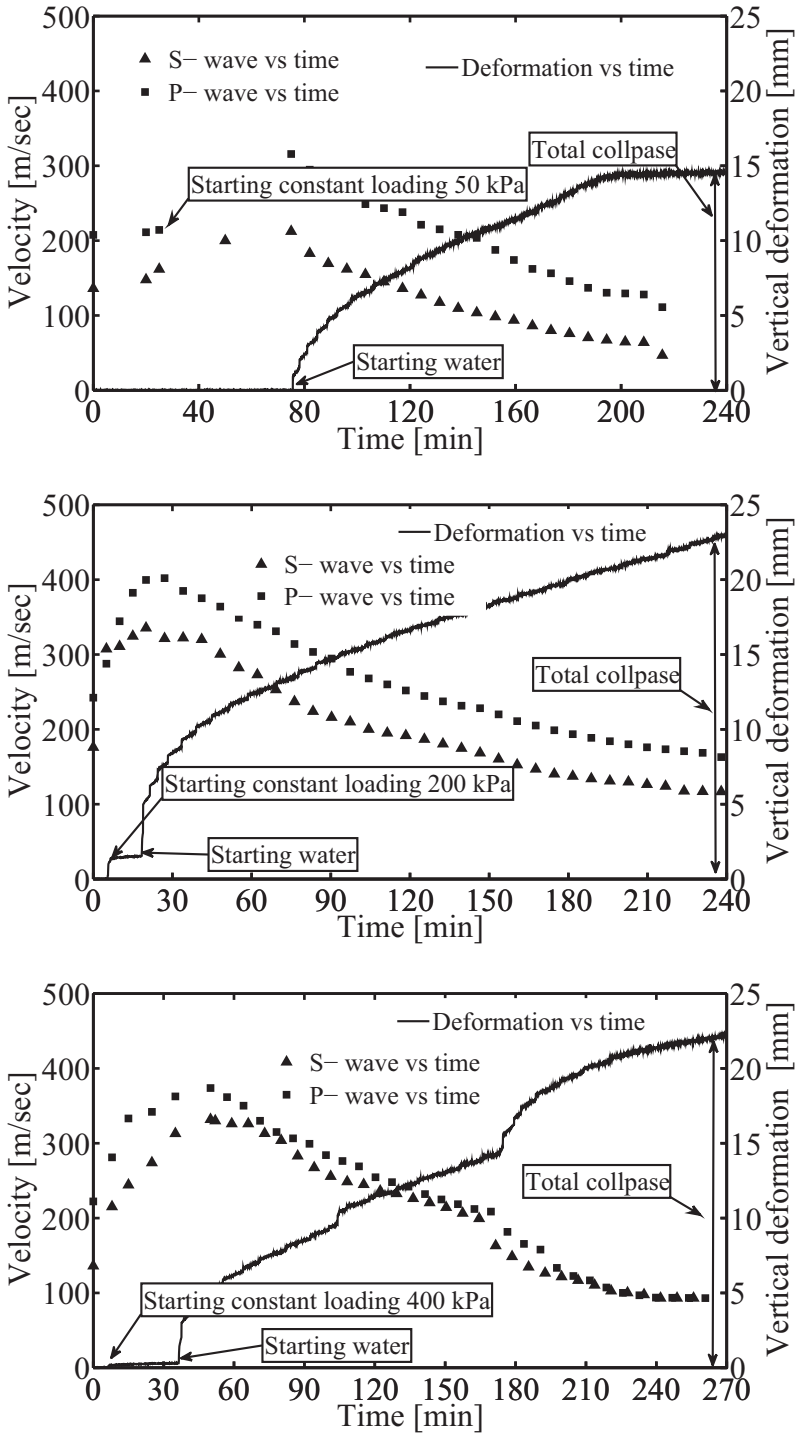

Figure 5.14: Relationship between Shear waves velocity (V_s), Longitudinal wave velocity (V_p) and vertical strain with time from (top) to (bottom) at vertical stress 50, 200 and 400 kPa.

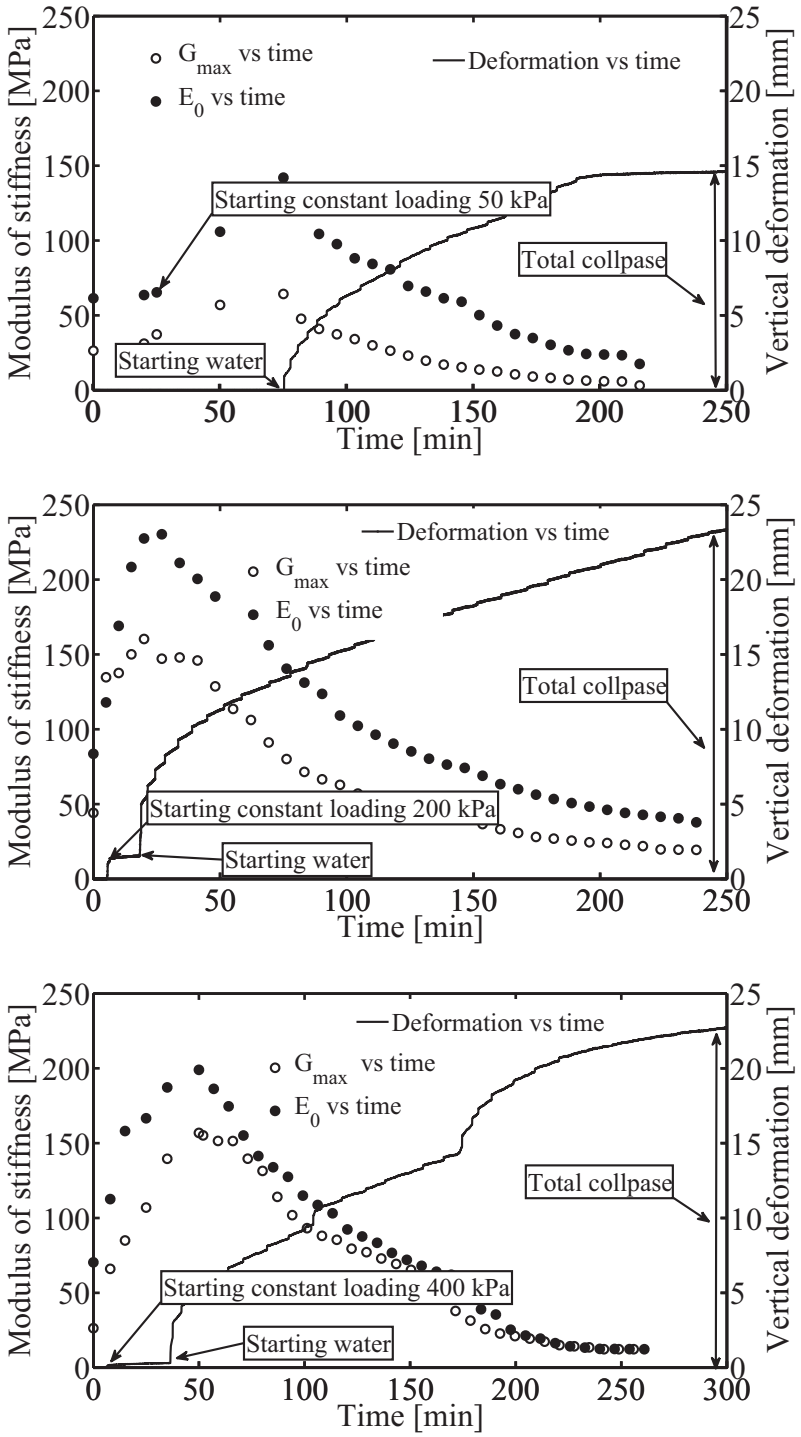

Figure 5.15: Relationship between Shear stiffness G_{max} based on waves velocity (V_s), Longitudinal wave velocity (V_p) and vertical strain with time from (top) to (bottom) at vertical stress 50, 200 and 400 kPa.

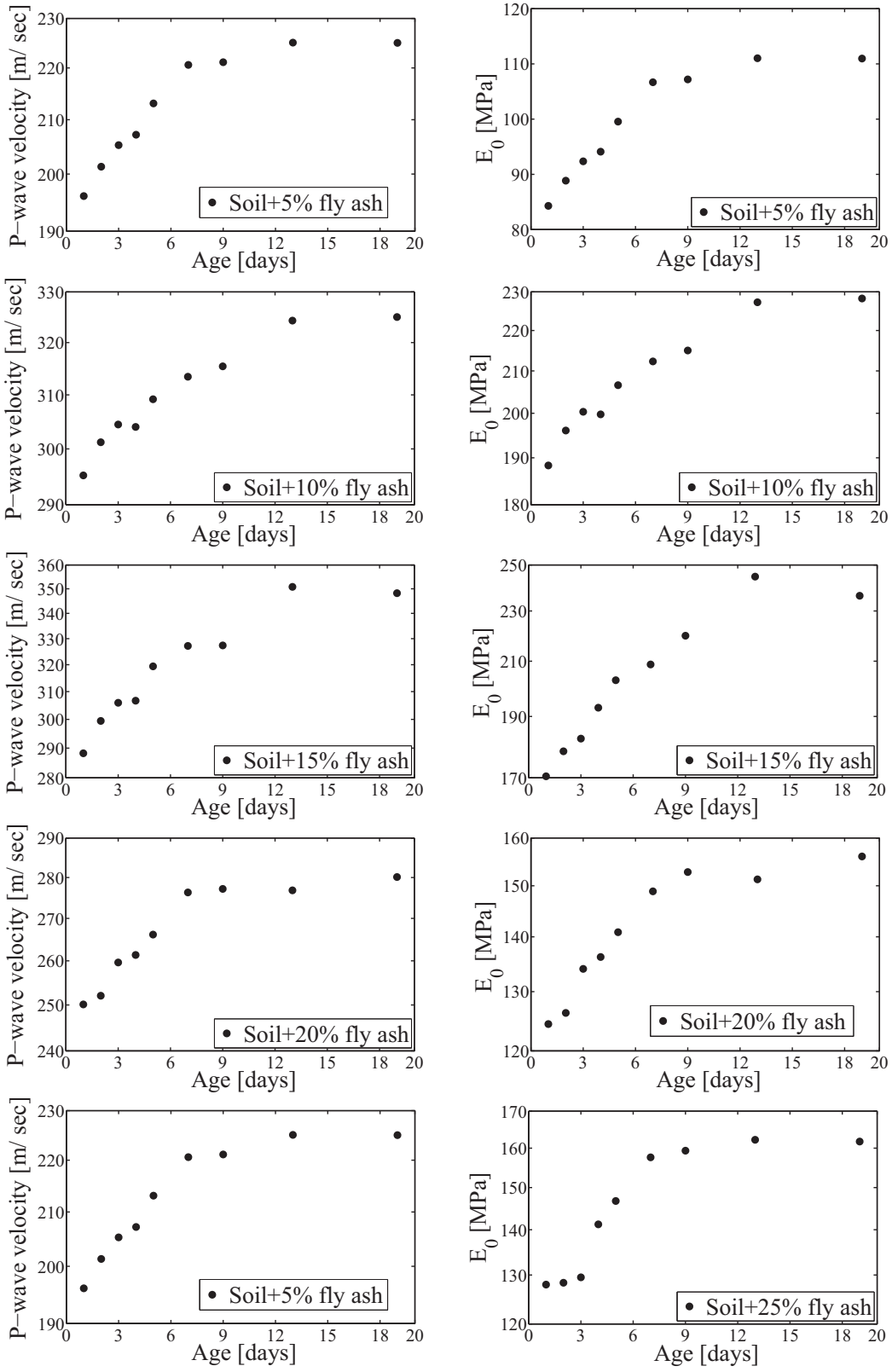

Figure 5.16: Relationship between the V_p velocity (left) and (E_0) (right) at different curing time for fly ash stabilization soils studied.

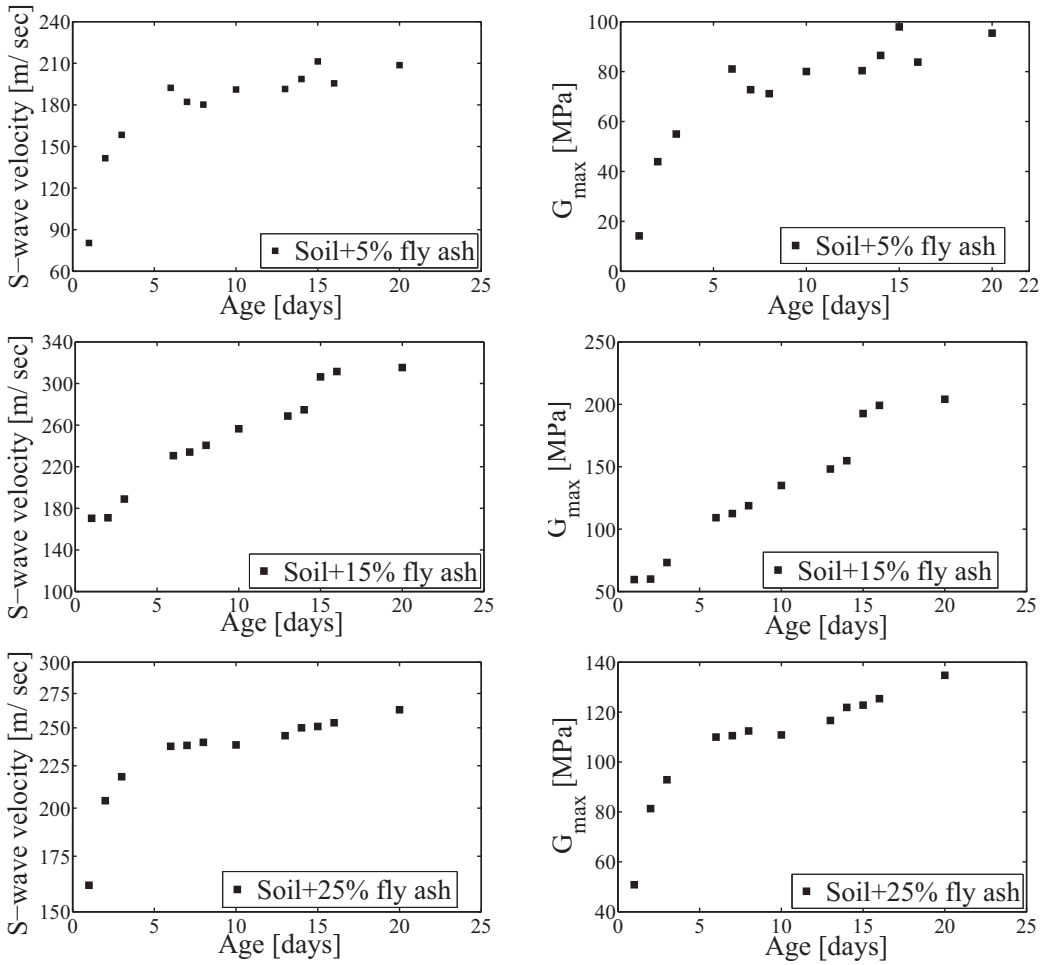

Figure 5.17: Relationship between the V_s (left) and (G_{max}) (right) at different curing time for fly ash stabilization soils studied.

ships between macro and micro hydro-mechanical behavior as well as electromagnetic properties and collapse phenomena.

The seismic P and S - wave velocity test is used in this study to investigate shear stiffness of natural collapsible soil and of soil with fly ash stabilized material during setting and hardening, by using the collapse-shear test and the non-destructive ultrasonic test. Stiffness-collapse tests are very important tests which can describe the relationship between the vertical stresses - strain and the stiffness change during collapse potential. The seismic results show that natural collapsible soil has low shear stiffness during the wetting process with high vertical stress loadings due to the breaking and removal of cementation material as the collapse progresses. The Ultrasonic show that (V_p), (V_s), (E_0) and (G_{max}) values increase significantly with the increase in the amount of fly ash for mix proportions of up to 15% fly ash. Above this percentage, the values show a slight increase when compared to that of 15% fly ash. The reason could be that the fly ash cementation pozzolanic reaction starts with great intensity at lower fly ash percentages (5, 10 and 15%) and high amounts of SiO_2 and Al_2O_3 in clay soil. As a result of this, the hydration reaction of the fly ash particles with the soil produces great amounts of cementation and pozzolanic production. For fly ash mixes with percentages above 15% (i.e. at 20 and 25%), there are insufficient amounts of SiO_2 and Al_2O_3 in clay, and hence less hydration reaction and cementation. In these particular cases, the extra amount of fly ash particles lowers the bulk density and stiffness of the soil. Finally, it can be used successfully as a tool to monitor the fabric change of collapsible soil during the hydration in cementation materials.

Chapter 6

Collapse assessment method and practical procedures methods of stabilized soil

6.1 Monitor the collapse development based on Electromagnetic properties

Figures 6.1 show the relationship between the experimental results of vertical deformation and real, imaginary part of complex effective relative permittivity with different vertical loading at different saturation stages. The electromagnetic properties $\varepsilon'_{r,eff}$ and $\varepsilon''_{r,eff}$ measured were taken every 10 minutes at four stages: at initial condition, at loading with constant vertical stress (50, 200 and 400 kPa) before starting water, at saturation process and at fully saturated.

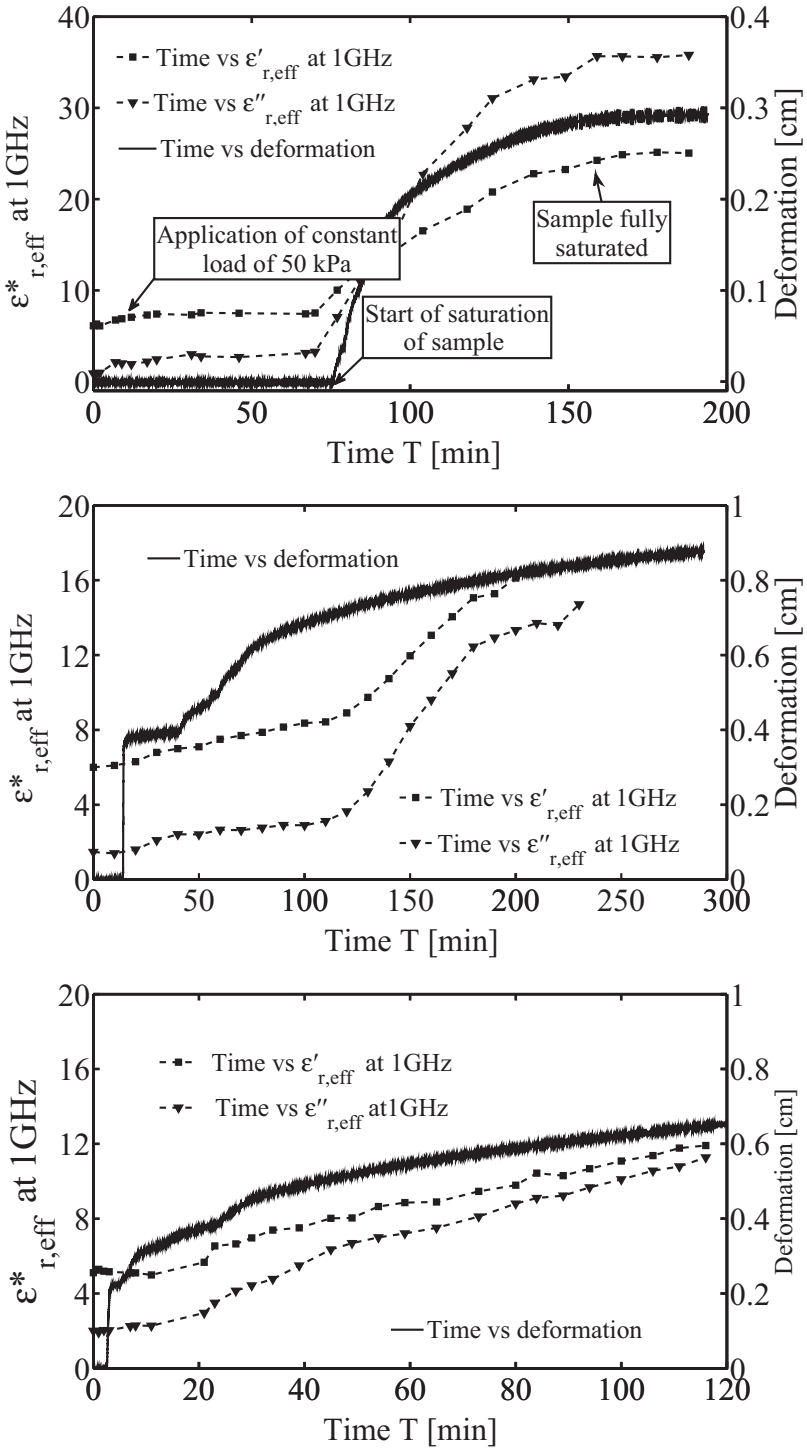

Figure 6.1: Relationship between real part $\varepsilon'_{r,eff}$, imaginary part $\varepsilon''_{r,eff}$ and deformation with time at 50 kPa (top), at 200 kPa (middle) and at 400 kPa (bottom) of vertical stress.

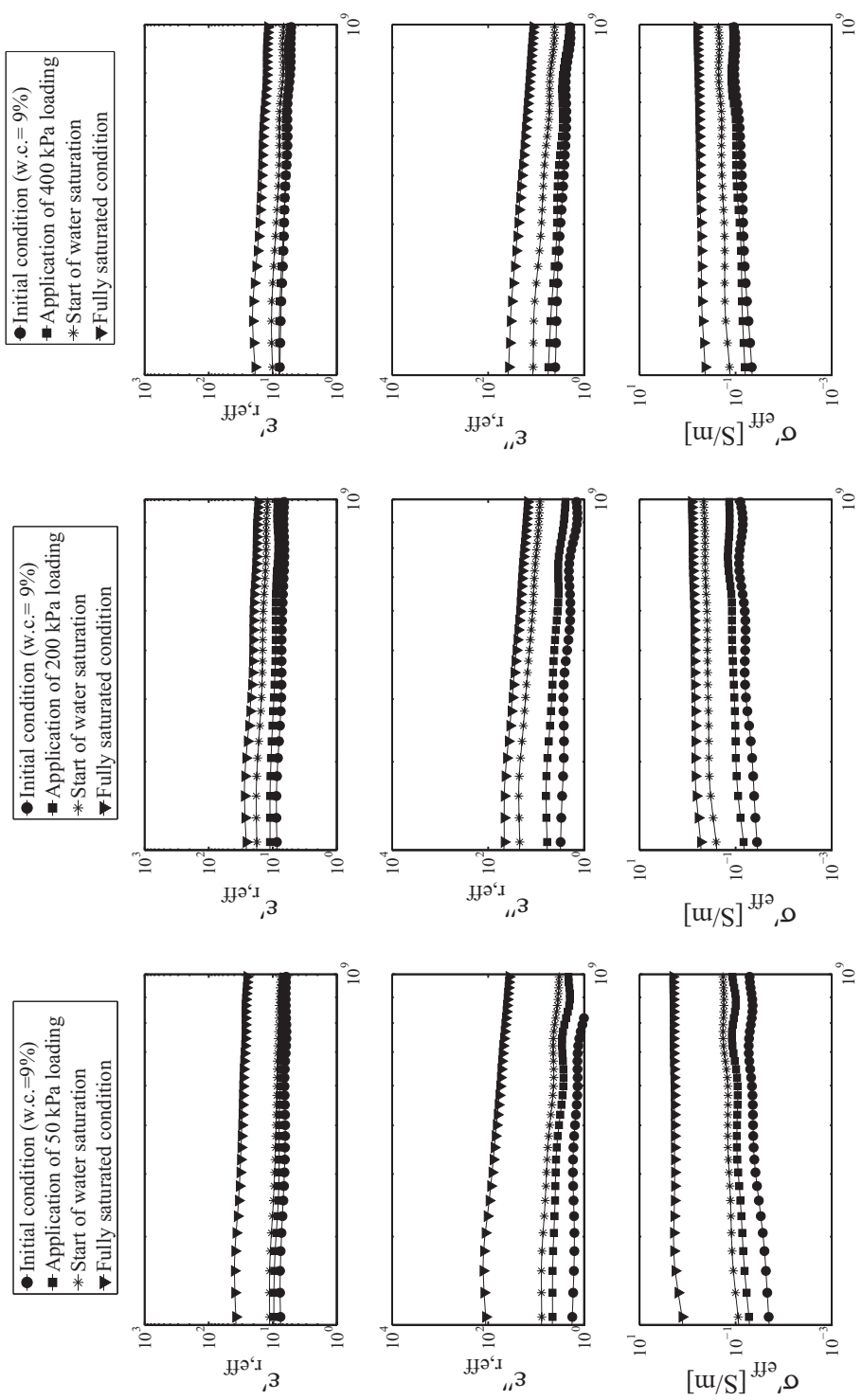

Figure 6.2: Relationship between frequency, $\varepsilon'_{r,eff}$ (top), $\varepsilon''_{r,eff}$ (middle) and σ'_{eff} (bottom) for the non-stabilized soil at 50 kPa, 200 kPa and 400 kPa (from left to right).

A clear difference in behavior can be seen between real and imaginary parts of the complex effective relative permittivity as well as the real part of the conductivity of soil used (see Figures 6.2). At initial condition, $\varepsilon'_{r,eff}$ and σ'_{eff} are ranged (5-6.5) and (1.8-2.8), respectively. The lower values of $\varepsilon'_{r,eff}$ and σ'_{eff} are due to the fact that the permittivity of soil, a corroding of the modified equation 6.4, is affected by the main two parameters porosity (n) and volumetric water content (θ), where the soil at this stage has high porosity and lower initial water content. Furthermore, at the loading stage before starting water, the electromagnetic properties measurements increase slightly because of the reduction in the initial void ratio during the consolidation process.

As shown in Figure 6.1, the results indicate that at lower vertical stress (50 kPa) the real part experiences no change at both initial condition and during the loading stage because the loading is very low and there is no change in void ratio, porosity or volumetric water content, which are the main parameters affecting permittivity. However, when the vertical stress is increased to 200 and 400 kPa, $\varepsilon'_{r,eff}$ decreases slightly from (5.4) to (4) and from (5.3) to (5) respectively. This is due to the fact that at these higher vertical stresses, the void ratio (e_0) and the porosity (n) decrease continuously until they reach maximum density (full compaction), although the water content of the soil is kept constant.

After starting to inject the water into the soil (at saturation stage), the results indicate that at 50, 200 and 400 kPa vertical stresses, the $\varepsilon'_{r,eff}$ of soil increases to (25), (17) and (12), respectively. This is because of during this stage the soil starts to collapse due to the breaking of bonds between the soil particles as well as suction stress reduction. During the collapse process, the void ratio and porosity of soil structure decrease rapidly. As expected, collapsible loose soil has a high void ratio (e_0= 0.83), so that the soil structure is saturated with a large amount of water that caused a greatly increasing of permittivity. This is a clear indication of chemical processes in the soil, with changes in water content strongly affecting pore water chemistry and thus interfaces processes. [Barden et al., 1973] has demonstrated that a portion of the fine-grained fraction of the soil exists as bonding material for the larger grained particles and that these bonds undergo local compression in the small gaps between adjacent grains resulting in the development of strength. When the loaded soil is exposed to moisture, and certain critical moisture content is exceeded, the fine silt or clay bridges that pro-

vide the cementation will soften and weaken and/or dissolve to some extent. Eventually, the binders reach a stage where they can no longer resist the deformation forces and the structure collapses. This principle explains the rapid increase in the complex effective relative permittivity of the soil, as with progressive collapse in the soil, the porosity decreases rapidly and hence the complex effective relative permittivity of the soil is increased. More importantly, the increase in the water content of the soil during collapse gives rise to the value of the complex effective relative permittivity of the soil as stated in the earlier sections of this paper. The rate of increase of the complex effective relative permittivity of the soil is faster at the beginning of the start of saturation, but then gradually slows down to a constant value during the latter stages of the test. This is directly related to the fact that the rate at which the water reacts with the fine cementing particles is very high at the initial stage of saturation and then gradually slows down to zero within a time frame of 2 to 3 hours.

Furthermore, at nearly full saturation (S_r =100%), it was observed that the permittivity of soils at all vertical stress levels (50, 200 and 400 kPa) is constant, with no change in void ratio or porosity.

It can also be seen that, at 50 kPa vertical stress, the real permittivity at full saturation $\varepsilon'_{r,eff}$ = 25 was highest when compared with 200 kPa $\varepsilon'_{r,eff}$ = 17 and 400 kPa $\varepsilon'_{r,eff}$ = 12. This is due to the fact that the reduction in void ratio of the soil at 50 kPa was less and the soil structure still had a high void and porosity which was not compacted. Hence, soil voids fill with large amounts of water at full saturation.

From these facts, it can be concluded that the real permittivity of soil at full saturation S_r=100% gives a strong indication as to the change in void ratio as well as collapse potential. Furthermore, the high values of $\varepsilon'_{r,eff}$, high initial void ratio (loose soil) and high collapse potential. At the low $\varepsilon'_{r,eff}$, low initial void ratio (dense soil) and low collapse potential.

The experimental data for the variation of collapse potential with electrical permittivity has been verified against the electrical permittivity measurement from the experimental results. A suitable equation which can be used to give an accurate estimation of collapse potential based on electrical permittivity measurements and the collapse load is suggested by equation 6.1.

The constants $x_1(\sigma)$ and $x_2(\sigma)$ are a fitting parameters form the fitting curve of the experimental results for the analysis soil (collapsible soil) which can present the verti-

cal stress value (σ). For the others types of soils, It can determine $x_1(\sigma)$, $x_2(\sigma)$ from the equation of the fitting curve of the experimental results between the real part of permittivity (at 1 GHz) and collapse potential values at different vertical stress.

$$C_p(\sigma,\theta,n) = x_1(\sigma) + \frac{x_2(\sigma)}{(\varepsilon'_{r,eff})^2} \tag{6.1}$$

$$x_1(\sigma) = -0.0003 * \sigma^2 + 0.1585 * \sigma - 2.6703 \tag{6.2}$$

$$x_2(\sigma) = 0.0083 * \sigma^2 - 3.859 * \sigma - 44.937 \tag{6.3}$$

Where,
$C_p(\sigma,\theta,n)$: Collapse potential value [%].
$\varepsilon'_{r,eff}$: Real part of complex permittivity.
σ : Vertical stress [kPa].
$x_1(\sigma)$, $x_2(\sigma)$: coefficients dependent on (σ).
To validate the equation 6.1 which show the experimental results of real part $\varepsilon'_{r,eff}$ and collapse behavior, a model was developed based on equation 6.4 in the following simplified form:

$$\varepsilon_{r,eff}^{a(\theta,n)} = \theta * \varepsilon_w^{a(\theta,n)} + (1-n) * \varepsilon_G^{a(\theta,n)} + (n-\theta) \tag{6.4}$$

$$\varepsilon'_{r,eff} = (\theta * \varepsilon_w^{a(\theta,n)} + (1-n) * \varepsilon_G^{a(\theta,n)} + (n-\theta))^{1/a(\theta,n)} \tag{6.5}$$

$$C_p(\sigma,\theta,n) = x_1(\sigma) + \frac{x_2(\sigma)}{(\varepsilon'_{r,eff})^2} \tag{6.6}$$

$$C_p(\sigma,\theta,n) = x_1(\sigma) + \frac{x_2(\sigma)}{((\theta * \varepsilon_w^{a(\theta,n)} + (1-n) * \varepsilon_G^{a(\theta,n)} + (n-\theta))^{1/a(\theta,n)})^2} \tag{6.7}$$

Where,

$C_p(\sigma, \theta, n)$: Collapse potential value [%].

$\varepsilon'_{r,eff}$: Real part of complex permittivity.

σ : Vertical stress [kPa].

ε_G (ε_G= 5.59) : Relative real permittivity of the solid grain particles based on the empirical equations by [Campbell, 2002], [Dobson, 1985] and [Olhoeft, 1974].

ε_G : relative real permittivity of the solid grain.

θ $(m^3 m^{-3})$: volumetric water content of the soil.

n : soil porosity.

ε_w : relative real permittivity of water.

$a(\theta, n)$: coefficient dependent on (θ, n).

According to suggestions by [Wagner and Lauer, 2012], in the low water content range the advanced Lichtenecker-Rother model (ALRM) was used with a=1/3, and in the nearly saturated case was used with a=2/3.

The porosity (n) and volumetric water content (θ) of the soils which are measured in the oedometer-electromagnetic control test and the real part ε'_w= 80 of the complex effective relative water permittivity $\varepsilon^*_{r,eff}$ taken at 1 GHz frequency from the electromagnetic test were implemented in equation 6.4 to calculated the real part $\varepsilon'_{r,eff}$ based on the (ALRM) model.

In this study, the real part value of the complex effective relative permittivity at 1 GHz is used in the equation 6.4 in relation to the collapse value because all the techniques which use the electromagnetic test to determine the physical properties of soils in practical applications like (TDR, GDR, etc.) have used the real part value as well as the frequency chosen at 1 GHz because the real part above this value gives a strong indication of the changing in porosity (n) [Wagner et al., 2011].

By using the equation 6.1, collapse potential were calculated based on the real part $\varepsilon'_{r,eff}$ calculated by the (ALRM) model. As shown Figures 6.4, the trends of the simulation and experimental results are more identical. The advantages of the new model (equation 6.1) as following :

- For this type soil (collapsible soil), the new model can predict directly the collapse potential (C_p) by measurement the real part of permittivity $\varepsilon^*_{r,eff}$.

- It is a new model which can present the effect of the vertical stress value (as parameters $x_1(\sigma)$ and $x_2(\sigma)$) on the collapse potential (C_p) based on the real part of permittivity $\varepsilon^*_{r,eff}$ measured.

6.2 Methods and optimization of soil stabilization

Collapsible soils are widely distributed in the many regions of the world recognized as having one of the problematic soils. Therefore, during recent years there have been many attempts to improve these soil characteristics. Fly ash is one of the many types of solid waste product created in large amounts in Germany (around than 65 million metric tons per year) as a waste product of coal burning electric power plants. The benefit of using fly ash as stabilizing material in soil has increased significantly in many countries due to increased availability and the introduction of new environmental regulations that encourage the use of fly ash in geotechnical applications since it is environmentally safe. From the results of this study, some guidelines and standard specifications for the fly ash-stabilization process are summarized and recommended as follows:

1. The oedometer and uni-axial results show that the geotechnical properties of soil are improved (decrease in collapse potential (C_p [%]) and increase in unconfined compressive strength (qu)) by increasing the amounts of added fly ash up to 15%. At more than this percentage (20% and 25% of fly ash), soil strength increased slightly. This study therefore recommends that a mixture with 15% fly ash is optimal for providing the soil with the required strength.

2. The pozzolanic reactions of fly ash depend on the chemical properties of clay soil (the amount of silica /alumina). Therefore, before using the stabilizing process, various investigations into chemical properties for both fly ash and soil used should be carried out in order to evaluate the identification and classification of the pozzolanic reactions.

3. Electromagnetic properties tests give a strong indication as to the change of chemical properties during the fly ash stabilizing process (ion exchanges and pozzolanic reactions). Therefore, in addition to basic chemical analyses, this

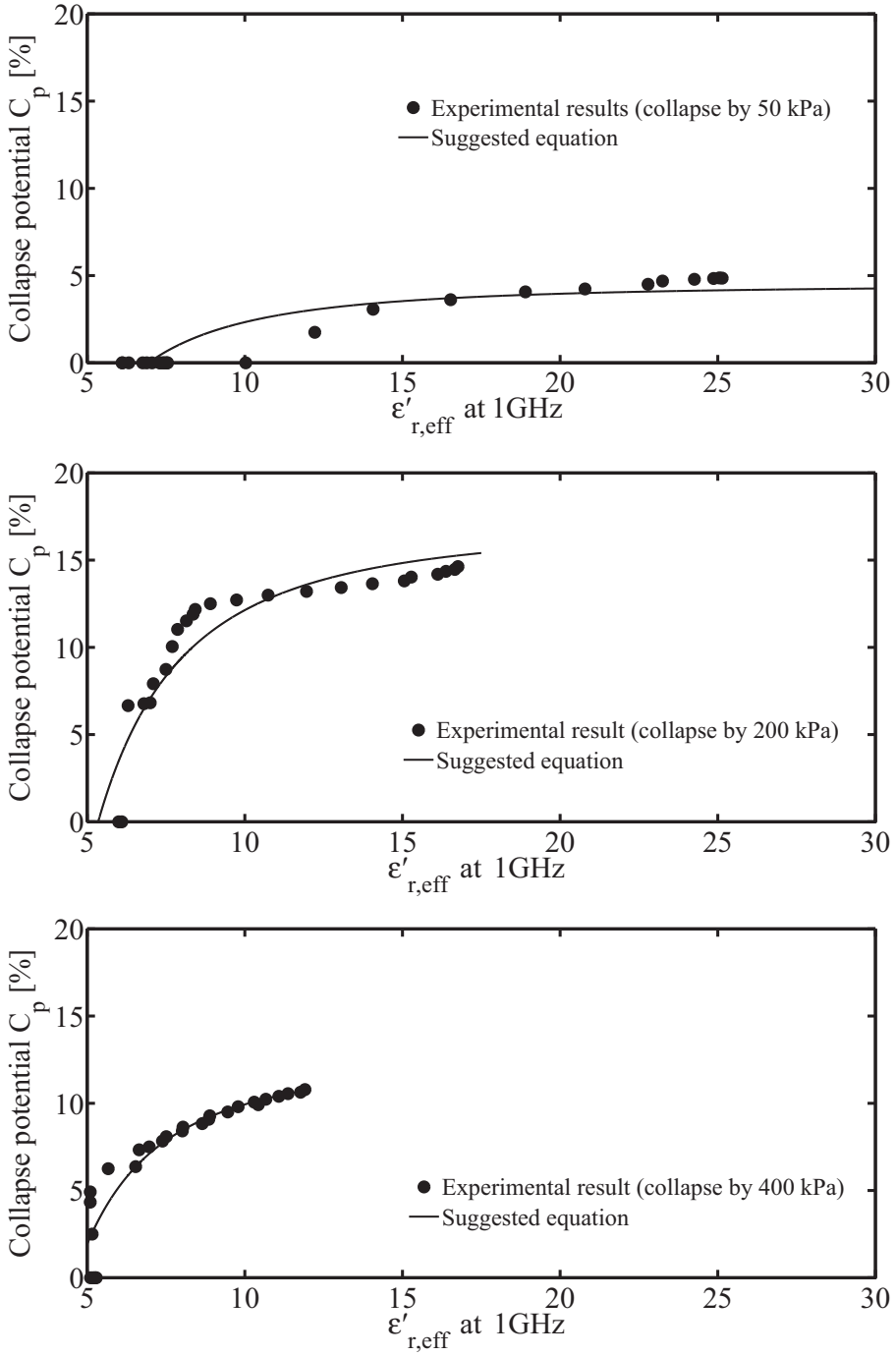

Figure 6.3: Experimental results and the suggested equation of real part $\varepsilon'_{r,eff}$ and collapse potential (C_p) at 50 kPa (top), at 200 kPa (middle) and at 400 kPa (bottom) of vertical stress.

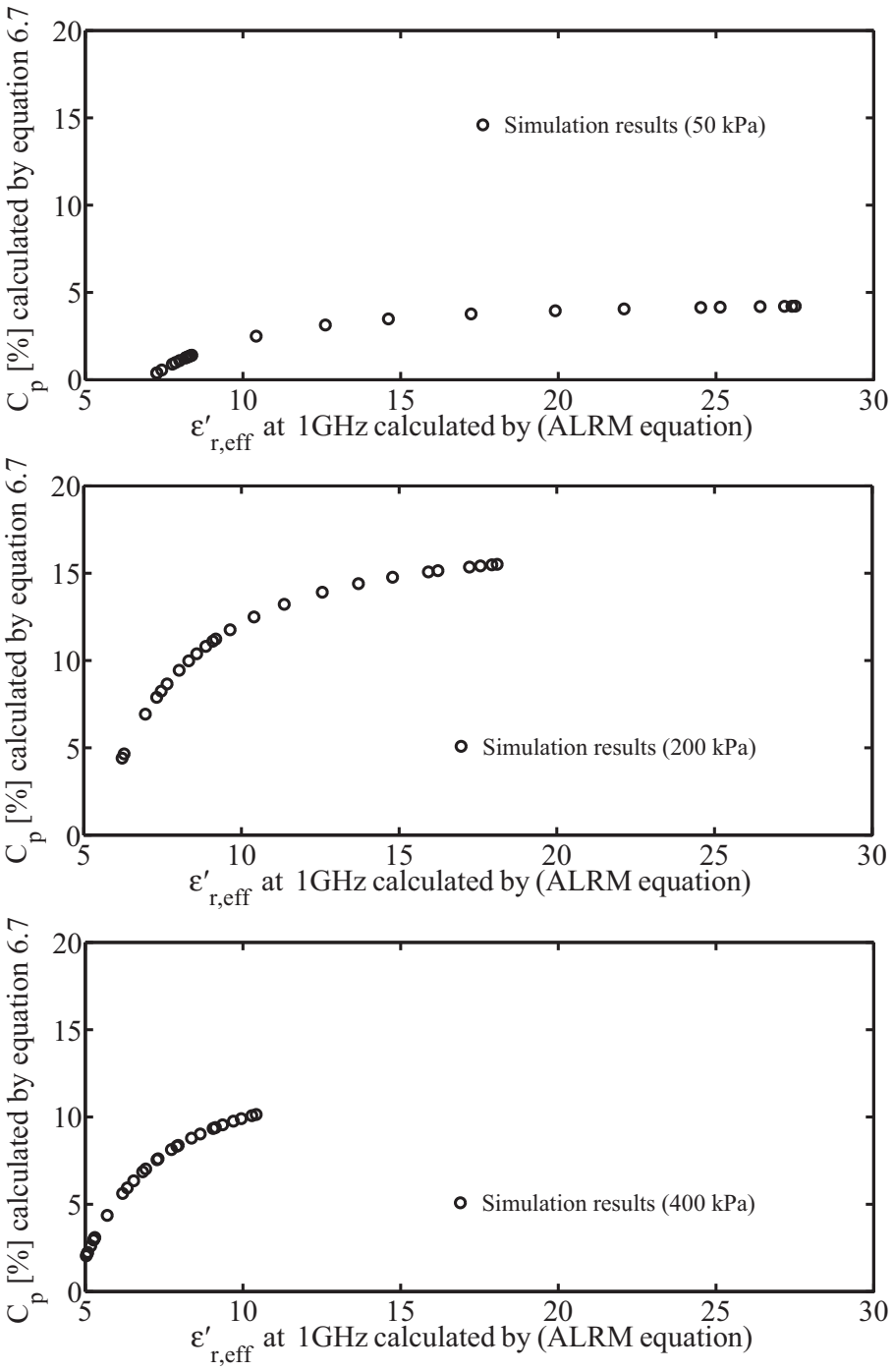

Figure 6.4: Simulation results of real part $\varepsilon'_{r,eff}$ [calculated by ALRM equation] and collapse potential (C_p) [calculated by equation 6.1] at 50 kPa (top), at 200 kPa (middle) and at 400 kPa (bottom) of vertical stress.

new tool can be used in a trial with a small stabilized soil sample to evaluate the intensity of pozzolanic reaction before starting to stabilize the soil.

4. The use of ultrasonic V_s and V_p velocity methods is a simple and practical (non-destructive) tool to evaluate the hardening, strength and shear stiffness development over time for fly ash-stabilized soils. It would need many studies to establish guidelines and standard specifications. However, to fully understand the observed electromagnetic properties and ultrasonic behavior in view of the collapse mechanisms, it is suggested that further systematic coupled mechanical, hydraulic and broadband electromagnetic investigations are carried out.

6.3 Summary

The results show that it is possible to use electromagnetic measurement to monitor the fabric change of soil during the changes in cementation materials which are directly related to the collapse potential. The outcome of this investigation gives the engineers a useful new tool for determining the collapse potential depending on void ratio, water content, vertical stress and electromagnetic behavior for the given soil.

Chapter 7

General summary and Outlook

7.1 General Summary

Plasticity and compaction

The addition of fly ash to the tested soil led to a reduction in the plasticity index. This reduction occurs because of the decreasing thickness of the double layer of the clay particles as a result of cation exchange reactions, which cause an increase in the attraction force leading to flocculation of the particles. Unlike the pozzolanic reaction, flocculation tends to modify the soil without producing new secondary minerals .

The addition of fly ash increased the percentage of the sand particles fraction and decreased the percent of fines. This increase of coarse grain size also resulted in a reduction of the plasticity index. The addition of fly ash to the studied soil contributed to an increase in the optimum moisture content and a decrease in the maximum dry density. The maximum dry density decreases with increasing fly ash content. The decrease in maximum dry density is due to the domination of the low weight and specific gravity of fly ash, hence the total dry weight of soil mixtures decreases. The increase in optimum water content is due to fly ash particles being a very fine material and causing an increase of the surface area of clay as well as the amount of water content to complete the cation exchange process and pozzolanic reaction of fly ash.

Oedometer test

The collapse potential of undisturbed natural soils in loose material (e_0 = 0.83) depends on the hydro-mechanical behavior of the soil skeleton. This type of collapse is due to the breaking of clay bonds during wetting, causing a re-arrangement of the particles as well as a total collapse. The open structure that encourages strong root development makes the soil susceptible to collapse upon the application of load and/or water. In fact, the collapse of such open structures can cause a reduction in volume of up to 30%. The large voids in these soils are maintained as a result of various bridging and bonding systems between the main structural silt particles or due to the breaking or reduction of capillary suction in soils. The collapse is caused by the internal erosion of fine particles through the soil structures. In this study, the collapse probably happened due to a mix of new arrangement distribution of void ratio clay bridge dissolution and changes in chemical bonding.

Although natural compacted soil (NCS) has a low void ratio compared with natural uncompacted soil (NUS), it collapsed with a value of 2.5%. This is due to the effect of micro-chemical reactions. The collapse phenomena in natural compacted soil (NCS) [e_o = 0.43] depends on the main parameters: ion exchange concentration and water content. As moisture content decreases, fine particles displace towards the menisci, the ion concentration in the pore fluid increases, Van der Waals attraction force increases in comparison to the repulsion force which decreases the double layer thickness. Soil structure is thus strengthened. Upon wetting, most of the processes contributing to a strengthening of the soil mass are reversed: soluble salt dissociates and softens, and the ion concentration in the fluid decreases with the increase in water content. The lower the ion concentration , the thicker the double layers that form around particles (this is aggravated by the low local confinement of clay particles experienced in clay bridges and buttresses). The shear stiffness and strength of the clayey formations decreases as the thickness of the hydration layers increases. Repulsion forces may become dominant and clay particles disperse. Eventually, the structure weakens and collapses even before full saturation is reached

Results of oedometer tests show that the collapse value (C_p = 9.17%) of natural untreated soil decreases with range (5.2-4%), (3.5-2.8%) and (3.6-3.1%) when mixed with 5, 15 and 25% fly ash, respectively. This fact can be described by the effects of

fly ash chemical reactions in two level macro and micro structural behaviors as follows: In the macro-physical behavior of soil, when fly ash is mixed with soil in the presence of water, a set of reactions occur that result in the dissociation of lime (CaO) in the binders and the formation of cementations and pozzolanic gels [calcium silicate hydrate gel (CSH) and calcium aluminate silicate hydrate gel (CASH)]. These reactions are referred to as cementations and/or pozzolanic reactions that result in the formation of cementation gels. The decrease in collapse value and increase in strength were found to be roughly related to the type and quantity of possible reaction products. At the micro-chemical level, the hydration of fly ash releases calcium ions, which in turn replaces original cations (most commonly sodium ions) in clay particles. This process is known as the cation exchange process. The free calcium with higher valency cations (Ca^{+2}) of fly ash replace the lower ion valency (Na^{+1}), and any cation will tend to replace one to the left of it, leading to a reduction in the amount of (Na^{+1}) ions in the bentonite surface as well as a decrease in the size of the diffused double layer surrounding the clay particles. This decreasing in the diffused double layer allows the clay particles to come closer to one another.

Unconfined compressive strength

The results indicate that the unconfined compressive strength of fly ash mixed soil increases with higher fly ash content up to 15%, beyond which it increases only slightly. This suggests that a fly ash content of 15% is a fly ash fixation point, an optimum fly ash content for pozzolanic reaction with the soil. Increases in fly ash content beyond the above optimum value results in a slight increase in the strength of the sample, which may be due to insufficient availability of silica and/or alumina in the soil for pozzolanic reaction.

Further, it is observed that for a given fly ash content the development of UCS occurs at a higher rate with an increase of the curing period of up to 7 days, after which the improvement is nominal and almost stabilizes. At 15% fly ash content and after 7 days curing, the strength gain with longer curing periods slows down and improvement is negligible when curing exceeds 14 days.

The mechanism behind this fact can be explained along the following lines. The pozzolanic reaction takes place as the silica and alumina present in clay react with calcium

from fly ash to form cementitious products such as calcium-silicate-hydrates (CSH) and calcium-aluminate-hydrates (CAH). This reaction slows when the clay content in soil is very low (with less silica and/or alumina). Above 15% fly ash content (i.e. at 20% and 25%) the increase in UCS is slight because there is insufficient amount of silica and/or alumina in clay for continuous pozzolanic reaction which means some of the fly ash particles remain without reaction. The remaining fly ash causes a reduction in the total bulk density of soil and strength (fly ash has low specific gravity and low density).

Soil water characteristic curves (SWCC)

Soil water characteristic curves (SWCCs) are carried out to study the hydro-mechanical behavior during changes in suction value. The results show that in both soils, volumetric water content, θ [%], water content, w [%] and degrees of saturation, S_r [%] decrease with increases in matrix suction. The air-entry value (AEV = 280 kPa) for compacted soil (S-0.43) is higher than with comparison for compacted soil (S-0.83) (AEV= 100 kPa). SWCCs were affected with increases in effort and this behavior could be attributed to the decrease in void ratio caused by the increase in compacted effort; as a result, a more closed skeleton for water loss was obtained under a certain level of applied suction, leading to a higher water holding capacity. The shape of the de-saturated zone for natural soil (S-0.83), which ranged between the air-entry value and the residual water content, had a steeper slope than the SWCC shape for compacted soil (S-0.43). This is due to the open structure of compacted soil (S-0.83) and when the increase in suction is greater than the air-entry value this causes a rapid outflow of the water inside the large spaces between the particles. For compacted soil (S-0.83), the decrease in all hydro-mechanical properties can be seen to be less than when comparing with soil (S-0.83) because the strong bond between particles requires greater suction to remove the molecules of water. The air-entry value and water holding capacity of the natural soil increases when mixed with fly ash. This is due to added fly ash causing more pozzolanic products. These products will be crystallized due to the pozzolanic reaction and this is expected to block the opened pores. The fly ash addition usually produces a needle like interlocking metalline structure, but the crystallization of pozzolanic products would block this opening.

Electromagnetic properties

Electromagnetic properties tests are used as a new tool to investigate the change in the hydro-mechanical properties (including changes in water content, void ratio, vertical stress, collapse potential and fly ash-stabilized content). The results of the electromagnetic tests show that a saturated soil has a much higher apparent direct current conductivity (1.47 S/m) compared with unsaturated soil (0.058 S/m) because of the higher change in physical-chemical behavior of the clay particles during wetting. Moreover, the high apparent electrical conductivity reflects a concentrated pore solution which further reduces the ion formation at the electrical double layers. The results of one-dimension load with natural water content show that the electrical permittivity and conductivity of the soil increases significantly with each load increment on the soil until the maximum applied load of 400 kPa is reached, and with every increment of vertical stress there is an equivalent jump in the measured values of electrical soil permittivity and conductivity. The increase in the electrical permittivity and conductivity of the collapsible soil is attributed to the decrease in porosity of the sample together with an increase in vertical stress. During the unloading stage however, as expected, the changes recorded in electrical soil permittivity and conductivity were insignificant. This is primarily due to the low deformation recovery (elasticity) of collapsible soils upon unloading, which in turn produces negligible changes in soil porosity. The results of one-dimension load with de-saturation processing show that the stages of initial condition and loading with constant vertical stress (at 50, 200 and 400 kPa), the electrical permittivity and conductivity of the soil increased slightly due to the reduction in porosity. After starting to inject water into the soil (at the de-saturated stage), the results indicate that at vertical stresses of 50, 200 and 400 kPa, the permittivity of soil increases to (25), (17) and (12), respectively. This is may be because the soil during this stage starts to collapse due to the breaking of bonds between the soil particles as well as the reduction of suction stress. During the collapse process, the void ratio and porosity of soil structure decease rapidly. Furthermore, at near full saturation (S_r =100%), it is observed that the permittivity of soils at all different vertical stresses (50, 200 and 400 kPa) is constant, not changing in either void ratio or porosity.

Furthermore, it can be seen that, at 50 kPa vertical stress, real permittivity at full saturation ($\varepsilon'_{r,eff}$ = 25) was highest when compared with 200 kPa ($\varepsilon'_{r,eff}$ = 17) and 400 kPa

($\varepsilon'_{r,eff}$ = 12). This is due to the fact that the reduction in the void ratio of soil at 50 kPa was less and soil structure still had a high void and porosity which was not compacted. Hence, soil voids fill with large amounts of water at full saturation.

From these facts, it can be concluded that the real permittivity of soil at full saturation (S_r = 100%) gives a strong indication as to the change in void ratio as well as collapse potential. Furthermore, the high values of ($\varepsilon'_{r,eff}$), high initial void ratio (loose soil) and high collapse potential. At the low ($\varepsilon'_{r,eff}$) , low initial void ratio (dense soil) and low collapse potential. The results of the electromagnetic properties of soils investigated in bulk state indicate an appropriate contribution of water relaxation at high frequencies. Hence, the comparison between ($\varepsilon'_{r,eff}$) of the different fly ash-soils mixed at the high frequency of ($\geq 1GHz$) at different fly ash percentages imply that the change in chemical properties of solid soil particles influence the dielectric properties.

The results show that the higher the fly ash content mixed, the higher the dielectric properties ($\varepsilon'_{r,eff}$, $\varepsilon''_{r,eff}$ and σ'_{eff}). This is due to the hydration of fly ash with water causing an increase in Ca^{+2} and the pH value of pore water and the calcium silicate hydrate C-S-H beginning to form and the clay being transformed into a calcium-clay through ion exchange, with calcium ions produced by fly ash hydration. The increased concentration of Ca^{+2} in the pore water of the double layer cause an increase in the attraction force leading to the flocculation of particles. The new pozzolanic products block the voids and finally cause a reduction in porosity. The dielectric properties are highest after 5 hours of curing time and then decrease up to 3 days curing. This is could be due to the first reaction of fly ash, causing ion exchanges between the Na^{+1} in clay and Ca^{+2} in the fly ash, thus increasing ion mobility and increasing the surface area. After 3 days of curing time, the dielectric properties show a gain, increasing up to 14 days and then decreasing. This behavior can be attributed to the second reaction of fly ash (pozzolanic reaction). At this stage free water changes to bound water in the structure of the new pozzolanic products which cause blocking and a reduction in porosity and finally a reduction in the amounts of Ca^{+2} in pore water.

The seismic V_s and V_p wave velocity

The seismic V_s and V_p wave velocity results show that natural collapsible soil has low shear stiffness during the wetting process at high vertical stress loading due to

the breaking and removing of cementation material during the collapse process. The ultrasonic P and S - wave velocity results show that (V_s), (V_p), (G_{max}) and (E_0) values significantly increase with increasing amounts of fly ash for mix proportions of up to 15% fly ash. Above this percentage, the results show only slight increases when compared to that of 15% fly ash. The reason could be that the fly ash cementation pozzolanic reaction starts with great intensity at the lower fly ash percentages (5, 10 and 15%) and with high amounts of SiO_2 and Al_2O_3 in clay soil. As a result of this, the hydration reaction of fly ash particles with soil produces high cementation and pozzolanic production. For fly ash mixes with percentages higher than 15% (i.e. at 20 and 25%), there are not sufficiently high amounts of SiO_2 and Al_2O_3 in clay, and hence less intense hydration reaction and cementation takes place. In these particular cases, the extra amount of fly ash particles lowers the bulk density and stiffness of the soil. Finally, it can be used as a successful tool to monitor the fabric change of collapsible soil during hydration in cementation materials.

7.2 Outlook

The collapse potential of a silty collapsible soil depends on the hydro-mechanical behavior of the soil skeleton, the physic-chemical behavior and the electromagnetic forces between the clays plates forming the soil skeleton. The analysis of the electromagnetic soil properties provides a useful tool for characterization and quantification of the collapse potential of collapsible soils as well as it gives a strong indication to the change of chemical properties during the fly ash stabilizing process (ion exchanges and pozzolanic reactions) of fly ash-stabilized soil.

In the presented studies, experimental results correlating the collapse potential of silty collapsible soils with electromagnetic measurements for different collapse loads are presented. An empirical equation which can be used to predict the collapse potential depending on the (e_0), ($w\%$), (σ_v) and ($\varepsilon'_{r,eff}$) for both in-situ and lab conditions is presented.

However, to fully understand the observed dielectric relaxation behaviour in view of the collapse mechanisms it is suggested to study the relationship between the electromagnetic properties and collapse potential for different type of soil (expansive soil, organic soil or gypsum soil) to compare and validate with electromagnetic properties

results for collapsible soil as well as collection wide data base for this relation to model the electromagnetic properties-collapse potential results.

The present study recommends to carry out a further systematic coupled mechanical, hydraulic and broadband electromagnetic investigations by development a large equipment to apply both of the electromagnetic measurements and seismic wave tools in suit which can help the engineering applications to predict the collapse potential value of the soil in the field.

Also, the study recommends to investigate the hardening and setting of stabilization soil mixed with other stabilized material (for example lime, lime + fly ash or cement) by using the electromagnetic properties tool.

References

H. A. Acosta. *Stabilization of soft subgrade soils using fly ash*. PhD thesis, University of Wisconsin-Madison, 2002. 45

S.S. Agus. *An experimental study on hydro-mechanical characteristics of compacted bentonitesand mixtures*. PhD thesis, Bauhaus-Universität Wiemar, Germany, 2005. 172, 176, 177, 178

G. D. Aitchison. Relationships of moisture stress and effective stress functions in unsaturated soils. pages 47–52, Butterworths. London, 1960. 27

G. D. Aitchison and I. B. Donald. Effective stresses in unsaturated soils. pages 192–199, 1956. 26

M.D. Al-Janabi. Compressibility of gypseous soils stabilized with lime. 1997. 36

M. Al-Khashab and M. Al-Hayalee. Stabilization of expansive clayey soil modified by lime with an emulsified asphalt addition. *Eng. Technology*, 26(10), 2008. 39

A. A. Al-Mufty. *Effect of Gypsum Dissolution on the Mechanical Behavior of Gypseous Soils*. phd, Baghdad University, 1997. 3, 15

Q. J. AL-Obaydi. Studies in geotechnical and collapsible characteristics of gypseous soil. 2003. 36

A. A. Al-Rawasa, A.W. Hagoa, and H. Al-Sarmib. Effect of lime, cement and sarooj (artificial pozzolan) on the swelling potential of an expansive soil from oman. *Building and Environment*, 40:681687, 2005. 32

M. Al-Zoubi. Undrained shear strength and swelling characteristics of cement treated soil. *Jordan Journal of Civil Engineering*, 2(1), 2008. 34

A. Alonso, A. Gens, and D. W. Hight. Special problems soils. In *9th Eur. Conf. Soil Mech*, pages 1087–1146, Dublin, 1987. 18

E. E. Alonso, A. Gens, and A. Josa. A constitutive model for partially saturated soils. *Géotechnique*, 40(3):405–430, 1990. 29

S. Alper, I. H. Gozde, Recep Y., and Kambiz.R. *Utilization of a very high lime fly ash for improvement of Izmir clay*. Izmir, Turkey, 2004. 43

J. G. Alphen and F. D. Romero. Gypsiferous soils. *Bulletin-21, Int., Inst. for land Reclamation and Improvement Wageningen, Holland*, 1971. 15

K. Arulanandan. Soil structure: In situ properties and behavior. Depart. of Civil and Environ. 2003. 59

M. Asslan and F. Wuttke. An experimental study on the initial shear stiffness in granular dry and saturated material using bender elements test. In *14th European Conference of Earthquake Engineering*, 2010. 53

ASTMC593. Standard specification for fly ash and other pozzolans for use with lime for soil stabilization. pages 10.1520/C0593–06R11. 2001. 47

ASTMC618. Standard specification for coal fly ash and raw or calcined natural pozzolan for use in concre. page ICS Number Cod 91.100.30. 2003. 5, 40

ASTMD6913. Standard test method for particle-size analysis of soil. 1978. 165

J. Atkinson. Non-linaer soil stiffness in routine design. *Géotechniqueotechnique*, 50 (5):487–508, 2000. 50

J.H. Atkinson and G. Sallfors. Experimental determination of soil properties. In *10th Conference of European Soil Mechanics*, volume 3, pages 915–956, Florence, 1991. 48

R. Bahar, M. Benazzoug, and S. Kenai. Performance of compacted cement-stabilised soil. *Cement Concrete Composites*, 26, 2004. 33

L. Barden, A. McGown, and K. Collins. The collapse mechanism in partly saturated soil. *Engineering Geology*, 7:49–60, 1973. 2, 11, 12, 13, 134

L. Barden, A. O. Madedor, and G. R. Sides. Volume change characteristics of unsaturated clay. *Proc. Am . Soc.Civ. Engineers*, 95:33–53, 1996. 82

J. Behari. Microwave dielectric behaviour of wet soils. 2005. 60

F. G. Bell. Lime stabilization of clay minerals and soils. *Engineering Geology*, 42: 223–237, 1996. 37

J. Biarez and P. Y. Hicher. Elementary mechanics of soil behaviour. *Balkema journal*, 1994. 49

A. W. Bishop and G. E. Blight. Some aspects of effective stress in saturated and unsaturated soils. *Geotechnique*, 13(3):177–197, 1963. 25, 26

A.W. Bishop. The principle of effective stress. *Teknisk Ukeblad*, 106(39):859–863, 1959. 25, 26

G. Bolzon, A. Schrefler, and O. Zienkiewicz. Elasto plastic constitutive laws generalised to partially saturated states. *Géotechnique*, 46(2):279–289, 1996. 27

J. E. Bowles. *Foundation Analysis and Design*. New York, 3 edition, 1984. 4, 30

G. P. Broderick and D. E. Daniel. Stabilizing compacted clays against chemical attack. *J. Geotch. , ASCE*, 116(10):1549–1567, 1990. 116

B. Broms and P. Boman. Lime stabilized columns. *Fifth Asian Regional Conference on SM and FE, Bangalore, India,*, pages 227–234, 1987. 36

D.S. Burden and J.L Sims. Fundamentals of soil science as applicable to management of hazardous waste - epa ground water issue. *Environmental Protection Agency*, 1999. 86

J. B. Burland. *Some aspects of the mechanical behavior of partly saturated soils*. Sydney, Australia, 1965. 12, 13

D. Camapum, J. R. Guimaraes, and J. H. Pereira. Courbes de retention deau dun profil dalteration. pages 289–294, Brazil, 2002. 20

B. Campbell. Radar remote sensing of planetary surfaces. *Cambridge University Press*, page 342, 2002. 137

I. H. Chang, G. C. Cho, J. G. Lee, and L. H. Kim. Characterization of clay sedimentation using piezoelectric bender elements. *Key Engineering Materials*, 321-323(2): 1415–1420, 2006. 53

G.C. Cho and J.C Santamarina. Unsaturated particulate materials particle-level studies. *Journal of Geotechnical and Geoenvironmental Engineering, ASCE*, 127(1):84–96, 2001. 53

S. C. Chu and H. S. Kao. *A study of engineering properties of a clay modified by fly ash and slag*. New York, 1993. 40

C. R. Clayton. Stiffness at small strain: research and practice. *Géotechnique*, 61(1): 5–37, 2011. 50

S. P. Clemence and A. O. Finbarr. Design consideration for collapsible soils. *Journal of Geotechnical Engineering*, 107(GT3):305–317, 1981. 11

J. D. Coleman. Stress / strain relations for partly saturated soils. *Geotechnique*, 12(4): 348–350, 1962. 25, 26

D. Croney and J. D. Coleman. *Pore pressure and suction in soil*. London, Butterworths, 1961. 26

B. M. Das. *Principles of Foundation Engineering*. 1984. 4, 30, 55

B. M. Das. *Principles of Geotechnical Engineering*. 1990. 11

M. Datcheva and T. Schanz. Anisotropic bounding surface plasticity with rotational hardening for unsaturated frictional materials. *Journal de Physique*, IV(105):305–312, 2003. 25

S.C. Dibben. *The modeling of collapse in silty soils*. PhD thesis, Nottingham Trent University, UK., 1998. 84

R. Dobry and M. Vucetic. Dynamic properties and seismic response of soft clay deposits. In *International Symposium on Geotechnical Engineering of Soft Soils*, volume 2, pages 51–87, Mexico City, 1987. 50

F.and Hallikainen M.and El-rayes M. Dobson, M.and Ulaby. Microwave Dielectric Behavior of Wet Soil-Part II. *Dielectric Mixing Models. IEEE Transactions on Geoscience and Remote Sensing GE-23*, page 3546, 1985. 61, 137

J. H. Dudley. Review of collapsing soils. *Journal of Soil Mechanics and Foundation Division, ASCE*, 96(SM3, May):925–947, 1970. 11, 12

P. Durand, M. Vázquez, and J. Justo. The effect of treatment with fly ash and cement upon the characteristic curve of a collapsing soil. *Springer*, pages 377–383, 2012. 44

R. Dyvik and C. Madshus. Laboratory measurements of g_{max} using bender element. *ASCE Annual Convention: Advances in the art of testing soils under cyclic conditions*, pages 186–196, 1985. 52

J. L. Eades and R. E. Grim. The reaction of hydrated lime with pure clay minerals in soil stabilization. *U.S. Highway Research Board Bulletin*, 262:5163, 1960. 92

T. Edil, C. Benson, S. Shafique, W. Tanyu B.and Kim, and A. Senol. Field evaluation of construction alternatives for roadway over soft subgrade. *Geotechnical Engineering Report*, pages 02–04, 2002. 44

S.R. Evett, J. A. Schwartz, R. C.and Tolk, and T. A. Howell. Soil prole water content determination: spatiotemporal variability of electromagnetic and neutron probe sensors in access tubes. *Vadose Zone Journal*, 8:926941, 2009. 59

H. Y. Fang, S. Pamukcu, and R. C. Chaney. Soil-pollution effects on geotextile composite walls. *ASTM*, 1992. 3

FAO. Managements of gypsiferous soils. Number Bulletin-62. Rome, 1990. 2

G. Ferguson. Use of self-cementing fly ash as a soil stabilizing agent. *J. Geotech. Eng. ASCE*, 1993. 40, 42

V. Fioravante. Anisotropy of small-strain stiffness of ticino and kenya sands from seismic wave propagation measured in triaxial testing. *Soils and Foundations*, 40 (4):129–142, 2000. 49

D. G. Fredlund. How negative can pore-water pressure get. *Geotechnical News*, 9(3): 44–46, 1991. 1, 16, 17

D. G. Fredlund and N. R. Morgenstern. Stress state variables for unsaturated soils. *Journal of the Geotechnical Engineering Division*, 5(103):447–466, 1977. 25, 26, 29

D. G. Fredlund and H. Q. Pham. Independent roles of the stress state variables on volumemass constitutive relations. pages 37–44, Weimar, Germany, 2007. 26

D. G. Fredlund and A. Xing. Equations for the soil-water characteristic curve. *Canadian Geotechnical Journal*, 31(3):521–532, 1994. 18, 19, 38, 44, 68

D.G. Fredlund and H. Rahardjo. *Soil Mechanics for Unsaturated Soils*. John Wiley and Sons, 1993. 16, 26

R. H. Freeze and J. A. Cherry. New Jersey, 1979. 15

D. Gallipoli, S. J. Wheeler, and M. Karstunen. Modelling the variation of degree of saturation in a deformable unsaturated soil. *Géotechnique*, 53(2):105–112, 2003. 28

A. Gerald and A. Shahriar. Influence of soil type on stabilization with cement kiln dust. *Construction and Building Materials*, 14, 2000. 33

S. Goto, F. Tatsuoka, S. Shibuya, Y. Kim, and T. Sato. A simple gauge for local small strain measurements in the laboratory. *Soils and Foundations*, 31(1):169–180, 1991. 51

B.O. Hardin and F.E. Richart. Elastic wave velocities in granular soils. *Journal of Soil Mechanics and Foundations Division*, 89(1):33–65, 1963. 49

J.B. Hasted. Aqueous dielectrics. 1973. 59

M. Hayashi. Temperature-electrical conductivity relation of water for environmental monitoring and geophysical data inversion. pages 119128, Kluwer Academic Publishers, Netherlands. 2004. 61

M. Herrin and H. Mitchell. Lime soil mixture. Wasington, DC, 1961. 92

J. W. Hilf. An investigation of pore-water pressure in compacted cohesive soils. In *Technical Memorandum 654. Denver: US Bureau of Reclamation*, 1956. 22

D. Hillel. *Environmental soil physics*. 1998. 20

D. Y. Ho. *The relationship between the volumetric deformation moduli of unsaturated soils*. Phd thesis, Saskatoon, Canada., 1988. 26

W. G. Holtz and J. W. Hilf. Settlement of soil foundations due to saturation. In *Proceedings of the 15th International Conference on Soil Mechanics and Foundation Engineering*, volume 1, pages 673–679, Paris, 1961. 12, 13

E. Hoque and F. Tatsuoka. Effects of stress ratio on small-strain stiffness during triaxial shearing. *Géotechnique*, 54(7):429–439, 2004. 49

C. Hsu and M. Vucetic. Volumetric threshold shear strain for cyclic settlement. *Journal of Geotechnical and Geoenvironmental Engineering, ASCE*, 130(1):58–70, 2004. 48

G. Inan and A. Sezer. *A review on soil stabilization techniques and materials used*. Turkish, 2003. 41

O. G. Ingles and J. B. Metcalf. Soil stabilization: Principles and practice. 1973. 32, 35, 36

T. Ishida, T. Makino, and C. Wang. Dielectric-relaxation spectroscopy of kaolinite, montmorillonite, allophane, and imogolite under moist conditions. *Clays Miner*, 48:7584, 2000. 105

K. Ishihara. Clarendon Press - Oxford, New York, 1996. 48

P. S. Jagadish and K. P. Pradip. Effect of lime stabilized soil cushion on strength behaviour of expansive soil. *Geotech Geol Eng*, 2010. 36

J. B. Jennings, J. E.and Burland. Limitations to the use of effective stresses in partly saturated soils. *Géotechnique*, 12(2), 1962. 26, 27

J. E. Jennings and K. Knight. The addition settlement of foundations sandy subsoil on wetting. pages 316–319, 1957. 12, 26, 169

J. E. Jennings and K. Knight. A guide to construction on or with materials exhibiting additional settlement due to collapse of grain structure. In *VI Regional Conference for Africa on Soil Mechanics and Foundation Engineering*, pages 99–105, Durban, South Africa, 1975. 12, 82, 171

H.M. Jol. *Ground penetrating radar: Theory and applications*. Elsevier, Amsterdam, 2009. 59

V. Jovicic, M. Coop, and M. Simic. Objective criteria determining g_{max} from bender elements tests. *Géotechnique*, 46(2):357–362, 1996. 53

U. Kaatze. Non-conducting and conducting reference liquids for the calibration of dielectric measurement systems. *in: Proc. of the 7th International Conference on Electromagnetic Wave Interaction with Water and Moist Substances. Presented at the ISEMA, Okamura*, 2007a. 57

U. Kaatze. Reference liquids for the calibration of dielectric sensors and measurement instruments. *Measurement Science and Technology*, 18:967976, 2007b. 3, 57

S. Kanazawa, K. K., Kawai, A. Iizuka, Tachibana S. and Thirapong-P. Ohno, S. and, and T. Takeyama. A finite element simulator for mechanical behavior of unsaturated earth structures exposed to evaporation and moisturization. In *4th Asia-Pacific Conference on Unsaturated Soils*, pages 711–717, Newcastle, Australia, 2009. 26

S. Kaniraj and V. G. Havanagi. Compressive strength of cement stabilized fly ash-soil mixtures. *Cement and Concrete Research*, 5(5):673–7, 1999. 43

H. Karim. Improvement of compressibility of gypseous soil. *Iraqi Journal of civil Engineering*, 12:1–5, 2008. 33, 34

D. Karube and K. Kawai. The role of pore water in the mechanical behavior of unsaturated soils. *Geotech. Geol. Eng.*, 19:211–241, 2001. 27

S. Khaled and M. Mehedy. Mechanical stabilization of cemented soilfly ash mixtures with recycled plastic strips. *ASCE*, 10(943), 2003. 32

Geiser F. Khalili, N. and G.E. Blight. Effective stress in unsaturated soils: review with new evidence. *International Journal of Geomechanics*, 4(2):115–126, 2004. 26, 27

N. Khalili and M. Khabbaz. A unique relationship for the determination of the shear strength of unsaturated soils. *Geotechnique*, 48(5):681–688, 1998. 27, 28, 29

S. Khattab and L. AL-Taie. Soil-water characteistic curve (swcc) for lime treated expansive soil from mosul city. *ASCE library*, 40802(189), 2006. 38

C. Klein and C. S. Hurlbut. *Manual of Mineralogy after J.D DANA*. New York, 20 th edit edition, 1985. 15

Y. Kohgo, M. Nakano, and T. Miyazaki. Theoretical aspects of constitutive modeling for unsaturated soils. *Soil Mech. Found. Eng. (Engl. Transl.)*, 33(4):49–63, 1993. 28

S. Kolias, V. Kasselouri-Rigopoulou, and A. Karahalios. Stabilisation of clayey soils with high calcium fly ash and cement. In *National Technical University of Athens*, Athens, Greece., 2004. 43

S.L. Kramer. Geotechnical earthquake engineering. Prentice-Hall, 1996. 51

R. Kuwano and R. J Jardine. On measuring creep behaviour in granular materials through triaxial testing. *Public Works*, 1074:1061–1074, 2002. 49, 53

E. C. Lawton, R. J. Fragaszy, and J. H. Hardcastle. Stress ratio effects on collapse of compacted clayey sand. *J. Geotech. Eng. ASCE*, 117(5):714–730, 1991. 26

C.J. Lee and H.Y. Huang. Wave velocities and their relation to fabric evolution during the shearing of sands. *Soil Dynamics and Earthquake Engineering*, 27(1):1–13, 2007. 53

E. C. Leong and H. Rahardjo. Review of soil-water characteristic curve equations. *J. Geotech. Geoenviron. Eng.*, 123(12):1106–1117, 1997. 20

B. Lin and A.B. Cerato. Electromagnetic properties of natural expansive soils under one-dimensional deformation. *Springer*, pages Berlin, Heidelberg, 2013. 59

D. N. Litte. Handbook for stablilization of pavament subgrades & base courses with lime. Iowe, USA, 1995. 38

D. L. Little. Fundamentals of the stabilization of soil with lime. 1987. 42

D. LoPresti and M. Jamiolkowski. Discussion: Estimate of elastic shear modulus in holocene soil deposits. *Soils and Foundations*, 38(1):263–265, 1998. 49

N. Lu and W. Likos. *Unsaturated soil mechanics*. John Wiley and Sons, Inc., Hoboken,New Jersey., 2004. 17

R. Mair. Developments in geotechnical engineering research: application to tunnels and deep excavations. volume 97, pages 27–41, 1993. 48

E. L. Matyas and H. S. Radhakrishna. Volume change characteristics of partially saturated soils. *Geotechnique*, 18:432–448, 1968. 26

J. F. Meyers, R. Pichumani, and B. S. Kapples. Fly ash as a construction material for highways. *FHWA-IP-76-16, Washigton, DC*, FHWA-IP-76, 1976. 65

J. K. Mitchell. *Fundamentals of Soil Behavior*. New York, N.Y., 2nd edition, 1993. 12, 86

C. W. Ng and Y. W. Pang. Experimental investigation of soil-water characteristics of a volcanic soi. *Can. Geotechnic*, 37(6):1252–1264, 2000. 20

P. Nicholson, V. Kashyap, and C. Fuji. Lime and fly ash admixture improvement of tropical hawaiian soils. *Transportation Research Record*, (1440):71–78, 1994. 80

G.R. Olhoeft. Electrical properties of rocks. *The Physics and Chemistry of Minerals and Rocks*, page 261278, 1974. 137

K. Osinubi, M. Moyelakin, and A. Eberemu. Improvement of black cotton soil with ordinary portland cement - locust bean waste ash blend. *EJGE*, 16, Bund. F, 2011. 32

J. H. Pereira and D. G. Fredlund. Volume change behavior of collapsible compacted. *Journal of Geotechnical and Geoenvironmental Engineering*, 116(2):71–86, 2000. 11

J. M. Pestana and L. A. Salvati. Small-strain behavior of granular soils. i: Model for cemented and uncemented sands and gravels. *Journal of Geotechnical and Geoenvironmental Engineering*, 132(8):1071–1081, 2006. 53

D. L. Presti, O. Pallara, R. Lancellotta, and M. Armandi. Monotonic and cyclic loading behaviour of two sands at small strains. *Geotechnical Testing Journal, ASTM*, 16 (4):409–424, 1993. 49

R. Pusch. Mineral- water interactions and their influence on the physical behavior of highly compacted na bentonites. *Ca .Geotech. Journal*, pages 381–387, 1982. 90, 92

G. Rajasekaran and S. Narasimha. Permeability characteristics of lime treated marine clay. *Ocean Engineering*, 29, 2002. 39

S.S. Razouki and M. Al-Azawi. Long-term soaking effect on deformation characteristics of gypsiferous subgrade soil. *Engineering Journal of the University of Qatar*, 16:49–160, 2003. 54, 56

M. J. Reeve, P. D. Smith, and A. J. Thomasson. The effect of density on water retention properties of field soils. *Journal of Soil Science*, 24(355-367), 1973. 20, 21

L. A. Richards and L. R. Weaver. Moisture retention by some irrigated soils related to soil moisture tension. *Journal of Agricultural Research*, 69:215–235, 1944. 20

A. M. Ridley. *The measurement of soil moisture suction*. PhD thesis, University of London, 1993. 22, 23

A. M. Ridley and J. B. Burland. A pore pressure probe for the in situ measurement of soil suction. In *Proceedings of conference on advances in site investigation practice*, London., 1995. 23, 24

A. M. Ridley and J. B. Burland. Use of the tensile strength of water for the direct measurement of high soil suction. *Geotech. j.*, 36:178–180, 1999. 6, 22, 23

A. M. Ridley and W. K. Wray. Suction measurement: theory and practice, volume = 3, year = 1996. In *1st Int. Conf. Unsaturated Soils*, pages 1293–1322, Paris. 20, 21, 22

A. M. Ridley, K. Dineen, J. B. Burland, and Vaughan P. R. Soil matrix suction: some examples of its measurement and application in geotechnical engineering. *Geotechnique*, 53(2):241–253, 2003. 24

D. A. Robinson and S. P. Friedman. A method for measuring the solid particle permittivity or electrical conductivity of rocks, sediments, and granular materials. *Soil Science Society of America, Inc., Madison, WI.*, 108(2), 2003. 57, 59, 60

C. Rogers and S. Glendinning. Lime requirement for stabilization. *Transportation Research Board*, (0361-1981):9–18, 2000. 5, 42, 86, 102

P. L. Salter and J. B. Williams. The influence of texture on the moisture characteristics of soils. part 1: A critical comparison of techniques for determining the available water capacity and moisture characteristic curve of a soil. *Journal of Soil Science*, 16:1–15, 1965. 20

J. C. Santamarina and M. Fam. Changes in dielectric permittivity and shear wave velocity during concentration diffusion. *Can.Geotech. journal*, 32(4):647–659, 1995. 3, 7, 59, 117

A. Sawangsuriya, T.B. Edil, and P.J. Bosscher. Modulus-suction-moisture relationship for compacted soils. *anadian Geotechnical Journal*, 45(7):973–983, 2008. 53

P. Schultheiss. Simultaneous measurement of p & s wave velocities during conventional laboratory testing procedures. *Marine Geotechnology*, 4(4):343–367, 1981. 52

H. Seed, R.T. Wong, I.M. Idriss, and K. Tokimatsu. Moduli and damping factors for dynamic analyses of cohesionless soils. Technical report, 1984. 4, 47

E.T. Selig and S. Mansukhani. Relationship of soil moisture to the dielectric property. *Geotech. Eng. Div. Am. Soc*, 101(GT8):755, 1975. 59

A. Senol, E. Bin-shafique, and C.H. Benson. stabilization of soft subgrade. In *Fifth International Congress on Advances in Civil Engineering*. Istanbul Technical University, Istanbul, Turkey at 25-27 September 2002, 2002. 46

R. Shenbaga and G. Vasant. *Compressive strength of cement stabilized fly ash-soil mixtures*. PhD thesis, Department of Civil Engineering, Indian Institute of Technology Hauz Khas, New Delhi, 1999. 43

D. Shirley. An improved shear wave transducer. *Journal of Acoustical Society of America*, 63(5):1643–1645, 1978. 52

D. Shirley and L. Hampton. Shear wave measurements in laboratory sediments. *Journal of Acoustical Society of America*, 63(2):607–613, 1978. 52

W. S. Sillers. *The mathmetical representation of the soil-water characteristic curve*. PhD thesis, University of Saskatchewan, 1997. 19

A. Sreekrishnavilasam, S. Rahardja, R. Kmetz, and M. Santagata. Soil treatment using fresh and landfilled cement kiln dust. *Construction and Building Materials*, 21, 2007. 34

A. Suat and A. Seracettin. The variations of cation exchange capacity, ph, and zeta potential in expansive soils treated by additives. *INTERNATIONAL JOURNAL OF CIVIL AND STRUCTURAL ENGINEERING*, 1(2), 2010. 34

K. Suzuki, T. Nichikawa, J. Hayashi, and S. Ito. Approach by zeta potential on the surface change of hydration of C3S. *Cement and Concrete Res.*, 11:759–764, 1981. 116

P. Takkabutr. *Experimental Investigations on Small-Strain Stiffness Properties of Partially Saturated Soils via Resonant Column and Bender Element Testing*. PhD thesis, 2006. 53

A. Tarantino and L. Mongiovi. Calibration of tensiometer for direct measurement of matric suction. *Geotechnique*, 53(1):137–141, 2003. 23

F. Tatsuoka, G. Modoni, G. Jiang, L. Anh, A. Flora, M. Matsushita, and J. Koseki. *Stress-strain behaviour at small strains of unbound granular materials and its laboratory tests*. Lisbon, 1999. 51

K. Terzaghi. *Theoretical soil mechanics*. Wiley, New York, 1943. 24

S. Thevanayagam. Electrical response of two-phase soil: theory and applications. *J. Geotech. Eng.*, 119(8):12501275, 1993. 59

Z.G. Thomas and D.J. White. Engineering properties of self-cementing fly ash subgrade mixtures. *Proceedings of the International Ash Utilization Symposium*, pages 346–378, 2003. 46

T. Tika, P. Kallioglou, P. Papadopoulou, and K. Pitilakis. Shear modulus and damping of natural sands. In *3rd International Conference on Deformation Characteristics of Geomaterials*, volume 1, pages 401–407, London, 2003. 49

G.C. Topp, J.L. Davis, and A.P. Annan. Electromagnetic determination of soil water content: measurements in coaxial transmission lines. *Water Resources Research*, 16:574582, 1980. 59, 60

S.K. Vanapalli, D.G. Fredlund, and S.L. Barbour. A rationale for an extended soil-water characteristic curve. *49th Canadian Geotechnical Conference*, 1:457–464, 1996. 96

A. R. Victor, J. C. Santamarina, and R. E. Redolfi. Characterterization of collapsible soils with combined geophysical and penetration testing. pages 581–588, Atlanta, 1998. 2, 3, 6, 14, 15, 54, 55, 76, 82, 84

G. Viggiani and J. Atkinson. Interpretation of bender element tests. *Géotechnique*, 45 (1):149–154, 1995. 53

M. Vucetic. Cyclic threshold shear strains in soils. *Journal of Geotechnical Engineering, ASCE*, 120(12):2208–2228, 1995. 48

N. Wagner and K. Lauer. Simultaneous determination of the dielectric relaxation behaviour and soil water characteristic curve of undisturbed soil samples. *In Proceedings of the IEEE International Remote Sensing Symposium IGARSS 2012*, pages 3202–3205, 2012. 59, 60, 69, 70, 105, 137

N. Wagner and A. Scheuermann. On the relationship between matric potential and dielectric. *Canadian Geotechnical Journal*, 46:12021215, 2009. 58

N. Wagner, K. Emmerich, F. Bonitz, and K. Kupfer. Experimental investigations on the frequency and temperature dependent dielectric material properties of soil. *IEEE Transactions on Geoscience and Remote Sensing*, 47(7):25182530, 2011. 3, 4, 6, 57, 58, 59, 60, 69, 71, 72, 105, 107, 137

K. Waltham. Hydrocompaction of Collapsing Soils. *Ground subsidence, Blackie, Glasgow*, page 202, 1988. 2

S. J. Wheeler and D. Karube. *Unsaturated Soils*. 1996. 25

S. J. Wheeler and V. Sivakumar. An elasto-plastic critical state framework for unsaturated soils. *Géotechnique*, 45(1):35–53, 1995. 26

T. Wichtmann and T. Triantafyllidis. On the influence of the grain size distribution curve of quartz sand on the small strain shear modulus G_{max}. *Journal of Geotechnical and Geoenvironmental Engineering, ASCE*, 135(10):1404–1418, 2009. 53

F. Wuttke, M. Asslan, and T. Schanz. Time-lapse monitoring of fabric changes in granular materials by coda wave interferometry. *ASTM Geotechnical Testing Journal*, 35 (2), 2012. 53, 74

N. Yesiller, J.L. Hanson, A.T. Rener, and M.A. Usmen. Ultrasonic testing for evaluation of stabilized mixtures. pages 32–39. 2001. 74

E. J. Yoder and M. W. Witczak. Principles of pavement design. 1975. 31, 36

S. Yucel, G.and Dursun, C. Murat, and T. Mustafa. Impact of cyclic wettingdrying on swelling behavior of lime-stabilized soil. *Building and Environment*, 42:681–688, 2007. 38

Ji-ru. Zhang and CAO. Xing. Stabilization of expansive soil by lime and fly ash. *Journal of Wuhan University of Technology*, 17(4), 2002. 37

Appendix A

A.1 Physical properties of soils studied

The investigation of the physical properties of soils studied included the determination of specific gravity, grain-size distribution and Atterberg limits. These tests were performed based on ASTM standards [ASTMD6913, 1978].

For specific gravity determination, the method proposed in [ASTMD6913, 1978] for high plastic clay was performed for comparison. In order to release entrapped air in the specimen, the picnometer with the saturated specimen was placed on a sand bath and stirred carefully. The specific gravity was obtained from the tests based on ASTM standards, respectively.

The grain size distribution of undisturbed soil was investigated using the sedimentation method. The sample was dispersed using a dispersing solution (i.e. sodium pyrophosphate) during experiment. The results of grain size distribution for undisturbed soil are presented in Figure A.1.

The Atterberg limits were performed according to [ASTMD6913, 1978]. The tests included the liquid limit using Casagrande and the plastic limit determination. The samples were mixed with distilled water to reach different values of water content and remixed every day for a minimum of one week before investigation.

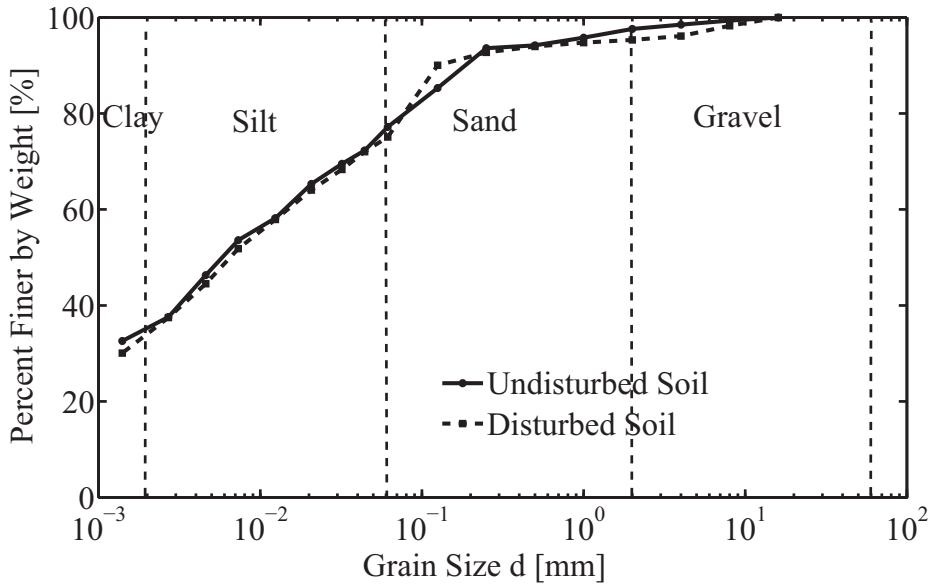

Figure A.1: Grain size distribution test

A.2 Chemical properties

In this study, chemical, pH-value and mineralogical properties tests are carried out on the soils used, since soil behavior such as compressibility, collapse, swelling, permeability, etc., are controlled by its chemical, and mineralogical properties. The chemical and mineralogical characterization of soil used in this study includes the determination of specific surface area (SSA), cation exchange capacity (CEC), and mineralogical and chemical compositions.

A.2.1 Cation Exchange Capacity (CEC)

The amount of basic exchangeable cations (i.e., Na^{+1},K^{+1},Ca^{+2}, and Mg^{+2}) was determined inductively using coupled plasma atomic emission (ICP) according to the European Standard EN ISO 11885. The amount of cations (i.e., Na^{+1}, Ca^{+2}, Mg^{+2}, and K^{+1}) are 2, 50, 13, and 1 meq/100g, respectively. Therefore, the total quantity of basic exchangeable cations is 66 meq/100g.

A.2.2 Mineralogy and Chemical Compositions

The mineralogy of soils was investigated using the X-ray diffraction (XRD) method. The result shows that the predominant clay minerals of soil used in this study are montmorillonite, muscovite which is known as common mica, quartz, chlorite which is one of the plagioclase feldspars and Dolomite which is the sedimentary carbonate rock and composed of gypsum material in crystals.

A.3 Oedometer test

A.3.1 Preparation of samples

To prepare the specimens for the oedometer test, two types of soil samples were used:

A.3.1.1 Undisturbed soil sample

Two undisturbed samples with different initial conditions were taken from situ: natural uncompacted sample (NUS) and natural compacted sample (NCS). A ring with a diameter of 5 cm and height of 2 cm was used to cut the specimen from the undisturbed sample by using a hydraulic machine as shown in Figure A.2 (top). The ring weights before and after sampling, as well as the initial water content, were recorded to calculate all the properties of specimens used. The initial conditions of NUS and NCS samples were (w = 7% and e_o = 0.83) and (w=10% and e_o = 0.43), respectively.

A.3.1.2 Disturbed soil sample

To study the effect of fly ash stabilization on collapse potential, three different types of soils in three boxes were mixed with optimum moisture content based on the proctor test. Box (1) consists of (disturbed soil mixed with 5% fly ash), box (2) consists of (disturbed soil mixed with 15% fly ash) and box (3) consists of (disturbed soil mixed with 25% fly ash). From each box, nine samples in an oedometer ring were compacted statistically by using a hydraulic machine with three layers and the weight of each specimen was divided into three weights. After compacting each layer in the ring as shown in Figure A.2 (bottom), the height of the ring was recorded to achieve the target wet density, void ratio as well as the weight of the sample with ring and the water

Figure A.2: The sampling of undisturbed specimens (Top) and the sampling of disturbed specimens (bottom)

content of the sample was recorded to calculate the actual initial condition. To study the effect of the curing period, the nine samples were divided into three sample series (three samples were tested after a 1 day curing period, three samples after 3 days curing and three samples after 7 days curing). At each test step, three samples were chosen because one sample was used in single oedometer tests and the other two samples were used in double oedometer tests.

A.3.2 Techniques used for Oedometer test

Two techniques were used with the oedometer tests to determine the collapse potential value as follows:

A.3.2.1 Single Collapse Test (SCT)

Collapse potential is determined by single collapse tests using the oedometer cell (see Figure A.3 (top)) and the procedure stated by [Jennings and Knight, 1957]. In this test, the sample was loaded according to the procedure in the standard consolidation tests but at dry state (no water was used). After the application of a stress of (200 kPa) and waiting for (24 hrs), water was added to the cell and left for (24 hrs). The additional thickness changes (Δh) were recorded. Then the test was continued as in the conventional consolidation test.
Collapse potential (C_p [%]) is determined by equation A.1 using a predetermined applied vertical stress and fluids applied to a soil specimen taken from the soil layer.

$$C_p = \frac{\Delta e}{1+e_o} * 100\% = \frac{\Delta h}{h_o} * 100\% \tag{A.1}$$

Where:

Δe = Change in void ratio in an oedometer test on inundation at a given stress.
e_o = Initial void ratio of the oedometer test specimen before inundation.
Δh = Change in thickness due to inundation at the given stress.
h_o = Initial height of the sample before inundation.

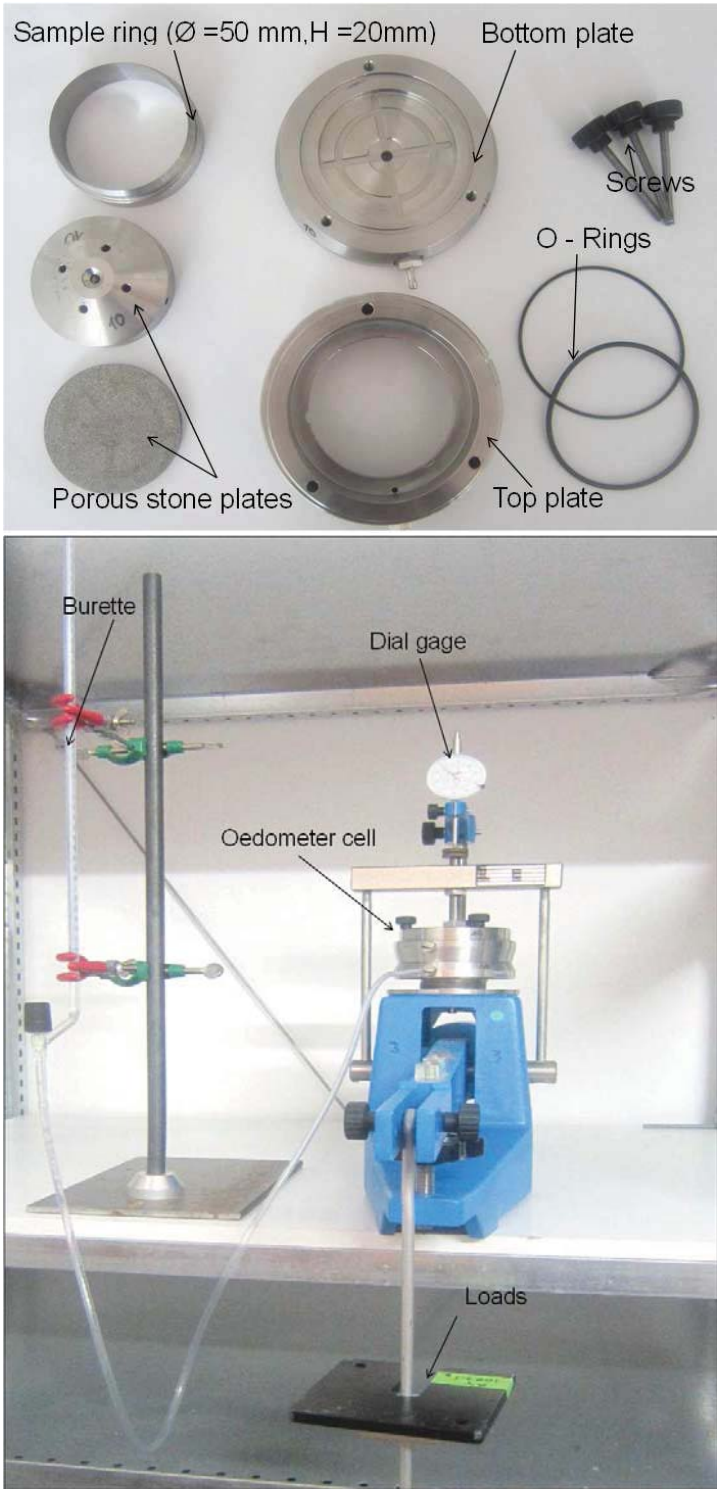

Figure A.3: Oedometer cell used (Top) and Oedometer devices used (bottom)

A.3.2.2 Double Oedometer Test (DOT)

This method was proposed by [Jennings and Knight, 1975] to determine the collapse potential. The procedure of this test is summarized as follows: Two identical specimens are loaded in two oedometer devices (see Figure A.3 (bottom)) one in dry natural state and the second in wet state (water is added in the beginning of the test), thickness changes are recorded for each. The difference between the two curves of $(\varepsilon - log\sigma)$ represents the soil collapse at any given pressure.

A.4 Soil water characteristic curve (SWCC) test

A.4.1 Preparation of sample

The preparation of the SWCC samples were carried out by using three boxes consist soil with difference properties: (box1) consist (natural undisturbed soil +23% water content) , (box2) consist (natural undisturbed soil +17% water content) and (box 3) consist (natural undisturbed soil +15% fly ash+ 31% water content). These water content in each box were calculated according to the basic soil equations to get each soil in box a full saturation (S_r =100%) based to the void ratio which it used to prepare the sample from the each box. The ceramic disc of the pressure plat device put in water for one week to achieve fully saturated conditions.
Soil samples for pressure plate testing were compacted in a ring of 5cm diameter and 2cm thickness. Two samples form each box were compacted to reach the target void ratio and dry density weight (see Figure A.4). Then the saturated ceramic plates along with the saturated soil specimen were placed inside the pressure chamber and closed tightly using clamping bolts.

A.4.2 Techniques used for SWCC test

A.4.3 Axis translation technique (ATT)

For unconfined drying and wetting paths the pressure plate apparatus from soil moisture was used (see Figure A.5). The main part of the pressure plate apparatus is the high-air-entry ceramic plate. Three ceramic plates with different air-entry values;

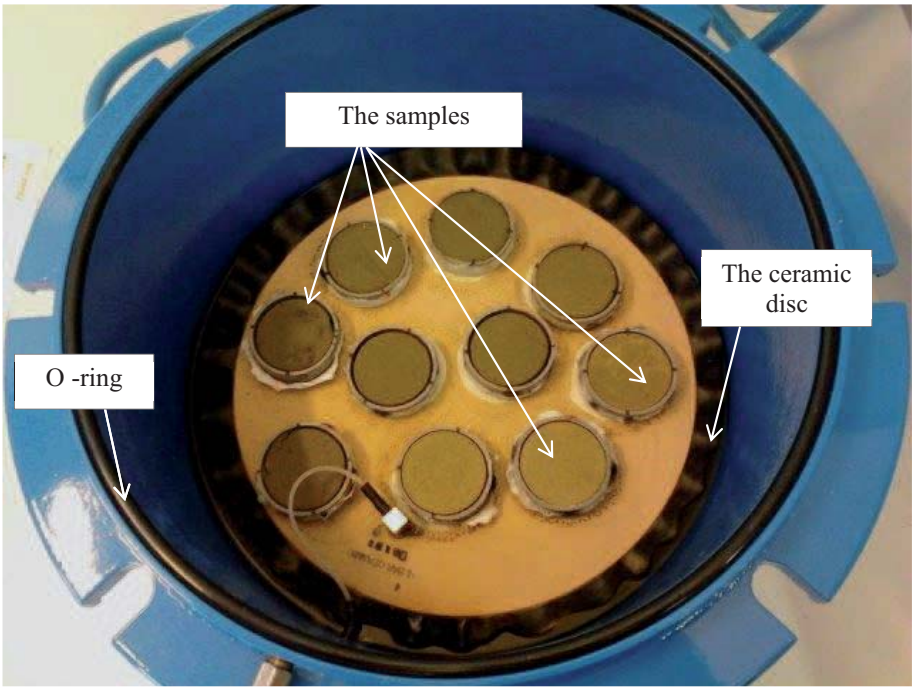

Figure A.4: The samples of pressure plate test

namely, 100 kPa, 500 kPa and 1500 kPa were used in the investigation depending on the applied matric suction. The use of ceramic plate with a high air-entry value is not desirable when lower matric suction value is to be applied [Agus, 2005]. This is due to the fact that the coefficient of permeability of the ceramic plate with a higher air-entry value is lower than that of the ceramic plate with a lower air-entry value. Therefore, the test can run for long time duration. Specimens with different densities and cementation material of compacted collapsible- specimens were placed on the ceramic plate. A dead weight of about 50 g was placed on the specimen to maintain a good contact between the specimen and the ceramic plate.

An air pressure was slowly and carefully applied to reach the target matric suction by also considering the water column in the burette. The flushing of the water compartment was performed regularly to remove the diffused air bubbles collected beneath the ceramic disk. It is important to note that the existence of diffused air bubbles in the water compartment results in discontinuity between the water phase in the specimen

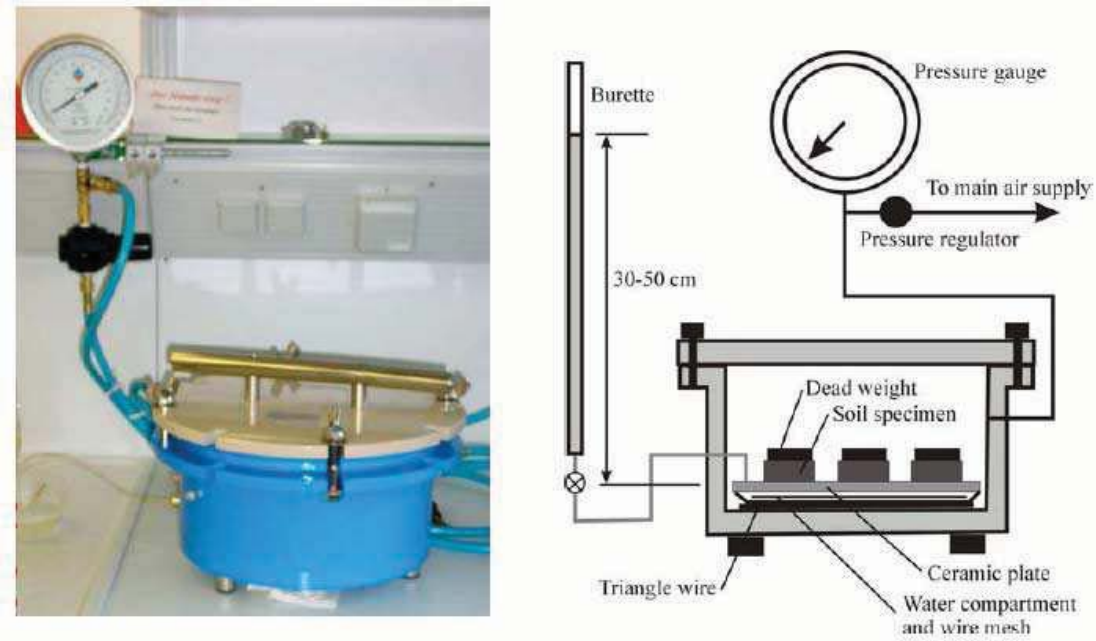

Figure A.5: Pressure plate apparatus setup used in study

and the source of water. The water phase continuity has to be established through out the experiment as to warrant liquid transfer of water into and out of the specimen. The water outlet in the pressure plate apparatus was connected to a burette for flushing purpose. The test started with saturating the ceramic plate with distilled deaired water. The water compartment located between the ceramic plate and the rubber membrane was filled with distilled deaired water. Low value of air pressure of (about 1half value of its air-entry value) was applied to pressure water on the ceramic plate for several hours. The pressure was stopped when no air bubbles were observed to come out of the compartment and flowed towards the burette. Diffused air bubbles collected beneath the ceramic plate was flushed using sufficient amount of water in the burette. The above flushing process repeated at least two times until no air bubbles were observed. The water left on the ceramic plate was wiped off and an air pressure as high as the air-entry value of the ceramic plate was applied. The water level in the burette was monitored. Initially, there was a small increase in burette water level. The water level in the burette stopped increasing indicating that there was no air flowed across the ceramic plate.

The change in mass and dimensions (i.e., the diameter and height) of the specimen

were monitored. A precision weighing balance with an accuracy of 0.0001 g was used to weigh the specimen. The dimensions of the specimen were monitored using a digital vernier caliper that could measure to the nearest 0.01 mm. At low matric suction (i.e., below 80 kPa), the measurement of dimensions of the soil specimen was only performed after the specimen had reached equilibrium based on the water content versus time plot. At matric suction below 80 kPa, the specimen was soft enough such that the dimension measurement using the digital calliper could introduce disturbance along the circumference of the specimen. After each suction equilibration, the ceramic disk was resaturated. Both water content and void ratio of the specimen were used to judge the equilibrium conditions before applying the next matric suction increment or decrement.

A.4.4 Vapor equilibrium technique (VET)

The experiment was conducted in a temperature-controlled room that could maintain a constant temperature of $22^oC \pm 0.5^oC$. In this study a large desiccators for testing up to eight specimens simultaneously (Figure A.6) were used. Several aqueous and molal salt solutions were used to induce total suction to the specimen by changing the relative humidity of the vapour space in the desiccator. Procedures similar to those used in the pressure plate apparatus (ATT) to determine the changes in water content and void ratio was adopted. At the end of the test, the relative humidity of the solution was measured using chilled mirror technique to compute the actual total suction applied to the specimens.

A.5 Suction control-oedometer tests

A.5.1 Preparation of sample

To study the collapse behavior during the changing in suction and water content, suction control-oedometer tests were done for this purpose. Three different types of soils in three boxes were mixed, (box1) consist (natural undisturbed soil+7% water content), (box2) consist (natural undisturbed soil +10% water content) and (box3) consist (natural undisturbed soil +15% fly ash+7% water content). From each box, three samples

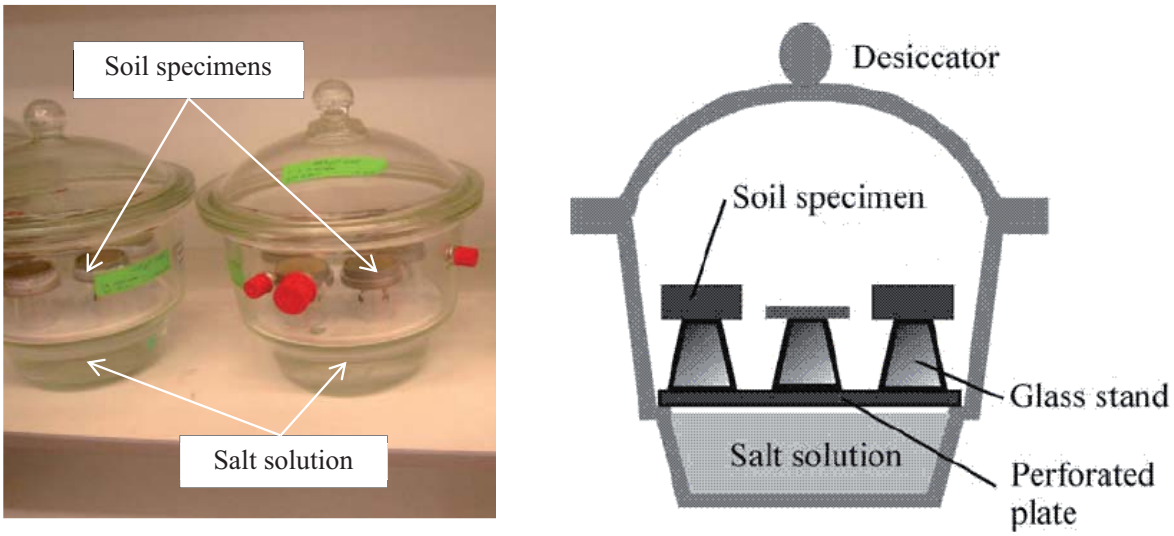

Figure A.6: Large desiccator test setup used in study

in oedometer ring were compacted statistically by using Hydraulic machine with three layers and the weight of each specimen was divided in three weights. The procedure of the suction control-Oedometer test will explain in the following section

A.5.2 UPC-Barcelona cell techniques for suction control-oedometer test

The cell was made by the workshop at Universitat Politecnica de Catalunya (UPC), Barcelona, Spain (see Figure A.7). The cell is controlled-suction oedometer and the suction can be controlled using either axis-translation technique or vapour equilibrium technique. The vertical or net stress is applied by air pressure using flexible membrane. Similar to the modified controlled-suction oedometer cells, the UPC-Barcelona cell was used for determination of the one dimensional volume change under 1D strain condition (i) one and multi-step drying or wetting paths under constant net stress and (ii) increase net stress (loading) under constant suction. The axis-translation technique is used only to control the suction.

The UPC Barcelona cell is connected with high accuracy burette, one air-pressure sys-

tem for application of matric suction as well as one air-pressure system for application of vertical net stress. The diameter of the specimen is 50 mm and the high is 20 mm. The pressure-deformability of UPC-Barcelona cell during loading and unloading was verified using dummy stainless steel specimen [Agus, 2005]. The stainless steel specimen was placed in the oedometer cells with two dry filter papers (i.e., each on the top and bottom of the dummy specimen). When a real soil specimen is saturated, the filter papers used will be wet and therefore dummy tests were also performed with wet filter papers. The dummy stainless steel specimen with the filter papers was subjected to increasing and decreasing vertical pressure in the oedometer test system. Figure A.8 (bottom) shows the deformation characteristic of the UPC-Barcelona cell. The deformation characteristic of the systems was used to give correction to the one-dimensional unsaturated volume change tests. Soil specimens were consolidated to a total stress used for each test for each sample and a pore-air pressure u_a of 0 kPa under undrained conditions. A specific air pressure greater than the absolute initial pore-water pressure was applied to the specimens at a constant vertical total stress which is used. The drainage valve connected to the ceramic disk was then opened to achieve a pore-water pressure of u_w = 0. The specimen was loaded to a specific stress under a constant air pressure u_a which is increased to = 400 kPa. The suction was then decreased from 400 to 200, 150, 50 and 0 kPa under a state of constant stress to perform a collapse test. Figure A.8 (top) shows the imposed stress paths for determining the collapse behavior of unsaturated soil. In these tests, the volumetric strain and the water change were measured. A negative value of water change means that water was absorbed into the specimens from the burette. Each of the soils used were loaded with three stresses (50, 200 and 400 kPa) with three paths: ABCDEFGH path, AB1C1D1E1F1G1H1 path and AB2C2D2E2F2G2H2 path. For more details of sample preparation and techniques used for the suction control-oedometer test.

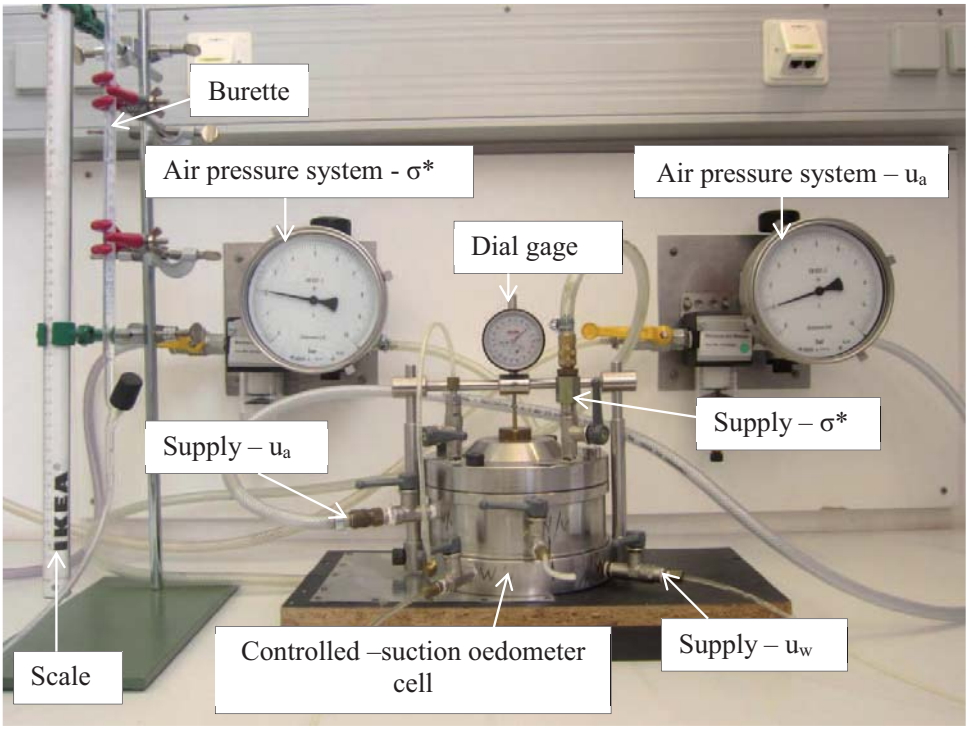

Figure A.7: UPC-Barcelona cell setup [Agus, 2005]

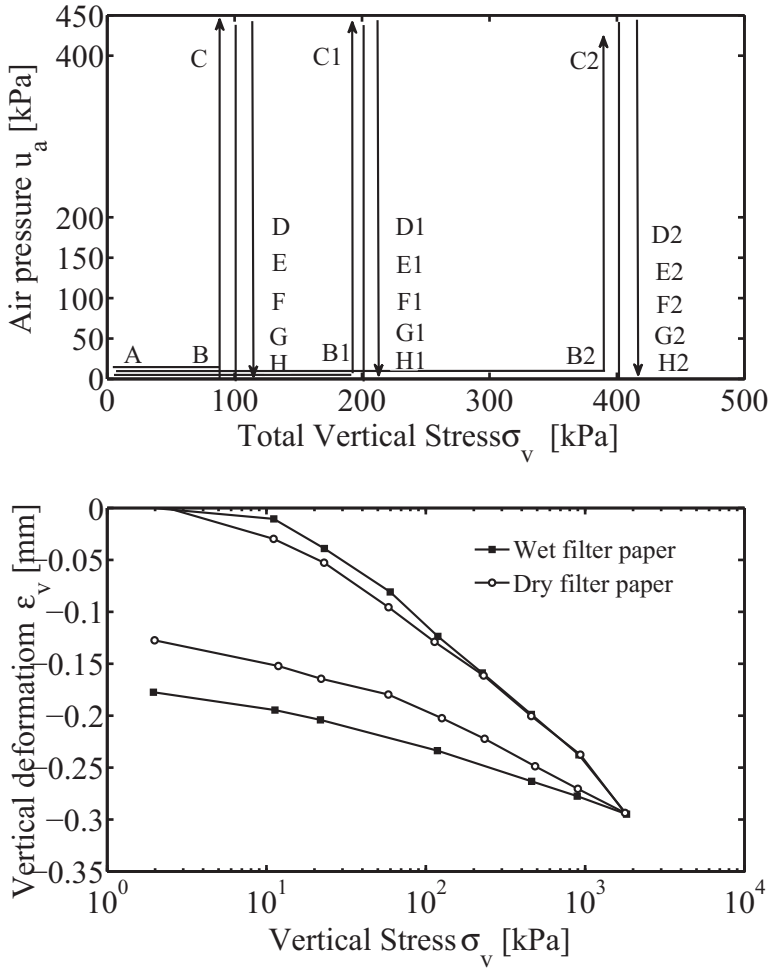

Figure A.8: (top) Stress paths of suction controlled oedometer tests (bottom) Pressure-deformation calibrations of UPC-Barcelona cell [Agus, 2005]

Appendix B

Table B.1: The initial conditions of specimens collapse potential test

Symbol	e_o [-]	w [%]	Dry density $[g/cm^3]$	Load at soaking [kPa]
UNS	0.825	6.4	1.471	No Soaking
UNS	0.832	5.43	1.428	12
UNS	0.813	6.55	1.465	200
UCS	0.471	10	1.836	No Soaking
UCS	0.52	9.9	1.777	12
UCS	0.462	8.8	1.792	200
D5FA	0.83	16.5	1.455	No Soaking
D5FA	0.825	16.3	1.46	12
D5FA	0.821	16.1	1.45	200
D15FA	0.83	18.85	1.456	No Soaking
D15FA	0.825	18.85	1.453	12
D15FA	0.821	18.9	1.458	200
D25FA	0.83	20.9	1.455	No Soaking
D25FA	0.825	20.5	1.453	12
D25FA	0.821	20.8	1.452	200

Table B.2: The initial conditions of SWCCs specimens

Symbol	Void ratio e_o [-]	Water content w [%]	Degree of saturation S_r [%]
DS	0.825	23.6	97.2
DS	0.83	22.6	97.3
DS	0.47	16.8	95.4
DS	0.48	16.9	96
D15FA	0.83	31.12	95.2
D15FA	0.832	30.5	95.2

Table B.3: The properties of salt solution desiccator

No.of desiccator	Relative humidity RH [%])	NaCl [g/l]	Suction value [kPa]
1	99.1	15.14	1200
2	96.4	62.25	5000
3	92.86	124.4	10000
4	86.24	248.22	20000

Table B.4: The initial conditions of UPCs specimens

Symbol	Void ratio e_o [-]	Water content w [%]	Vertical stress σ_v [kPa]
DS	0.825	6.4	50
DS	0.83	6.5	200
DS	0.835	6.8	400
DS	0.43	10	50
DS	0.432	10.5	200
DS	0.433	10.8	400

Table B.5: Results of Atterberg limits test for studied soils

Type of soil	Liquid Limit [%]	Plastic Limit [%]	Plasticity index [%]
N	36.3	17.8	18.5
N+%5 FA	35.2	18.5	16.7
N+%10 FA	34.4	19.2	15.2
N+%15 FA	32.2	21.0	11.2
N+%20 FA	31.5	22.1	9.4
N+%25 FA	NA	NA	NA
N = Natural soil			
FA = Fly Ash			

Table B.6: Results of unconfined compression tests of soils studies

Curing period days	0% FA		5% FA		10% FA		15% FA		20% FA		25% FA	
	σ_f [kPa]	ε_f [%]	σ_f [kPa]	ε_f [%]	σ_f [kPa]	ε_f [%]	σ_f [kPa]	ε_f [%]	σ_f [kPa]	ε_f [%]	σ_f [kPa]	ε_f [%]
0	132	2.34	-	-	-	-	-	-	-	-	-	-
1	-	-	173	1.62	205	1.3	245	1.45	257	1.58	274	1.38
3	-	-	242	1.18	295	1.08	343	1.15	365	1.16	385	0.97
7	-	-	302	0.98	383	0.91	443	0.95	470	0.8	460	0.6
14	-	-	312	0.73	393	0.9	480	0.45	495	0.58	502	0.8
20	-	-	325	0.72	403	0.85	520	0.82	510	0.69	500	0.58

σ_f = Failure strength
ε_f = Failure strain

Table B.7: The results of V_p and E_0 at different curing time for fly ash stabilization soils studied

Age	S+5% FA		S+10% FA		S+15% FA		S+20% FA		S+25% FA	
(days)	$V_{p,f}$	E_0	$V_{p,f}$	E_0	$V_{p,f}$	E_0	$V_{p,f}$	E_0	$V_{p,f}$	E_0
1	196.1	84.29	295.21	188.33	288.23	170.47	250.12	124.43	256.19	127.98
2	201.33	87.59	301.22	186.18	299.46	178.37	252.06	123.89	256.57	128.36
3	205.27	86.46	304.03	184.4	305.94	182.52	259.62	134.06	257.71	129.51
4	207.19	85.38	304.03	180.25	306.7	193.02	261.36	133.2	269.13	141.24
5	213.1	88.55	309.18	206.57	319.38	202.88	266.14	140.88	274.32	146.74
7	220.6	100.69	313.44	201.59	327.19	208.75	276.31	148.88	284.3	157.61
9	221.13	103.93	315.42	197.89	327.37	219.92	277.18	152.81	285.86	159.34
13	225.05	105.67	324.3	205.08	250.8	244.77	276.82	149.43	288.41	162.21
19	225	106.67	325	228.26	348.2	236.42	280.12	156.07	288	161.74

$V_{p,f}$ =P-wave velocity of fly ash-soil mixture [m/sec]
E_0 = Initial Shear stiffness [MPa]

Table B.8: The results of V_s and (G_{max}) at different curing time for fly ash stabilization soils studied

Age	S+5%FA		S+15%FA		S+25%FA	
[days]	Vs	G_{max}	$V_{s,f}$	G_{max}	$V_{s,f}$	G_{max}
1	80.42	14.17	170.415	59.6	161.45	20.82
2	141.55	43.92	170.94	60	204.20	81.31
3	158.39	54.99	188.92	73.24	218.24	92.87
6	192.3	81.05	230.63	109.15	237.5	109.98
7	182.19	72.75	234.09	112.45	238.08	110.53
8	180.19	71.17	240.57	118.766	240.10	112.42
10	191.1	80	256.47	134.977	238.41	110.84
13	191.5	80.4	268.72	14.178	244.57	116.63
14	198.63	86.5	274.70	154.85	249.99	121.86
15	211.34	97.9	306.38	192.62	250.91	122.76
16	195.53	83.80	311.53	199.15	253.54	125.35
20	208.64	95.42	315.35	204.06	262.86	134.73

$V_{s,f}$ = S-wave velocity of fly ash-soil mixture [m/sec]
G_{max} = Initial Shear stiffness [MPa]